arXiv:astro-ph/0610423v2 13 Oct 2006

Atomic Data for X-ray Astrophysics

T.R. Kallman

NASA Goddard Space Flight Center

P. Palmeri

Astrophysique et Spectroscopie, Université de Mons–Hainaut, Belgium

(Dated: February 5, 2008)

We review the available atomic data used for interpreting and modeling X-ray observations. The applications for these data can be divided into several levels of detail, ranging from compilations which can be used with direct inspection of raw data, such as line finding lists, to synthetic spectra which attempt to fit to an entire observed dataset simultaneously. This review covers cosmic sources driven by both electron ionization and photoionization and touches briefly on planetary surfaces and atmospheres. We review all of this, the applications to X-ray astronomy, the available data, recommendations for astronomical users, and attempt to point out the applications where the shortcomings are greatest.

PACS numbers: Valid PACS appear here

Contents

I. **Introduction** 1

II. **On the need for atomic data** 3
- A. Atomic Data Accuracy Requirements 7

III. **Theoretical Techniques** 8

IV. **Experimental Techniques** 12

V. **Line Finding Lists and Related Tabulations** 13
- A. Coronal Plasmas 13
- B. Photoionized Plasmas 14

VI. **Discrete Diagnostics** 15
- A. Coronal Plasmas 16
  - 1. He-like Diagnostics 16
  - 2. Dielectronic Satellite Lines 17
  - 3. Other Diagnostics 19
  - 4. Fe^{16+} 19
  - 5. Optical Depth Diagnostics 20
  - 6. Abundance Diagnostics 20
  - 7. Non-equilibrium Diagnostics 20
  - 8. Non-Maxwellian Diagnostics 20
- B. Photoionized 21

VII. **Spectrum Synthesis and Global Fitting** 21
- A. Coronal Plasmas 22
  - 1. Electron Impact Ionization (EII) 22
  - 2. Dielectronic Recombination (DR) 26
  - 3. Collisional Excitation 34
  - 4. Radiative Transition Probabilities 37
- B. Photoionized Plasmas 38
  - 1. Photoionization 39
  - 2. Radiative Recombination (RR) 41
  - 3. Dielectronic Recombination (DR) 42
  - 4. Charge Transfer 42
- C. Charge Transfer in Cometary and Planetary Atmospheres 43

VIII. **Discussion** 44

Acknowledgments 45

References 45

I. INTRODUCTION

Essentially every observation in astronomy which involves spectra requires some aspect of atomic data for its interpretation. This can range from stellar colors as probes of age or abundance to high resolution spectra of the Sun and the synthetic models which are used in their interpretation. The importance of atomic data to the field of X-ray astronomy comes from the fact that there are many atomic features in the X-ray band and the physical conditions in the sources are usually far from thermodynamic equilibrium, so that interpretation of line fluxes or ratios requires knowledge of collisional rate coefficients and radiative rates. Even the instruments with the greatest spectral resolving power are not capable of fully resolving many line blends, so that modeling is of particular importance. Furthermore, the field has evolved rapidly, and many of the needs for new or accurate atomic data have only recently become apparent. In this paper we point out the motivation for accumulation of atomic data, and review available atomic data used for interpreting and modeling X-ray observations.

A review of atomic data for an application such as astronomy spans an audience including specialists with tools capable of providing new data, astronomers seeking to understand the accuracy and range of available data, and those who can use the data to synthesize spectra or other observables for comparison with observations. The subject differs from some other review topics since it is unified more by the application to a common problem or challenge than by a single physical process. In this paper we try to balance the needs of these communities as best we can.

For the physicist reader, we attempt to describe the capabilities of current X-ray astronomy instruments, some of the astrophysical science challenges, and the scope of existing work on the measurement and calculation of relevant atomic constants. It appears that much of the recent calculation and experimental work which is most useful to X-ray astrophysics has been done when there is a clear understanding of the astrophysical application. We also attempt to draw attention to those who have made important or extensive contributions in the past, even in cases where their work has been superseded. In doing this, it is not feasible to be comprehensive. A great deal of work has been done in this area, and we refer the reader to the many extensive bibliographies which provide a more complete set of references. For some physical processes we do provide relatively long lists of references to work which spans the many ions or atomic species of interest. These are cases where we think such lists are both relevant and useful, since they convey the volume or comprehensiveness of past work and also are of current interest.

For the astronomer reader, we attempt to describe the technical challenges of calculating or measuring relevant quantities. The goal is to provide an appreciation of the uncertainties imposed on astrophysics by an incomplete knowledge of atomic quantities. In addition, in many cases, the data cited or described here can be directly applied to observations.

For the reader interested in the synthesis of atomic data into model spectra or diagnostics which can be directly fit to astronomical observations, we attempt to provide pointers to data which is appropriate for a given application, the limitations in accuracy and comprehensiveness of existing data, and the prospects for future measurements or calculations. We also hope to foster cooperation between modelers or astronomers and the atomic physics community. This has proven to be an effective way to stimulate work on problems which are relevant to astrophysics, while also educating astronomers and modelers about the limitations and applicability of atomic structure and cross section data.

We feel that the time is right for a review such as this, because the accuracy and quantity of atomic constants describing many processes has progressed significantly in the last 10-15 years. This is driven both by advances in observational data with the launch of the *Chandra* and $XMM-Newton$ X-ray astronomy satellites, both statistical quality and spectral resolution, and by advances in the tools available to the physics community. There now exist values for rate coefficients and cross sections which will be accurate enough to allow interpretation of much of the available observational data for the near future, and current techniques will continue to improve the situation. In principle, the project of calculating or measuring atomic cross sections for any specific application has finite scope, and can at some point be considered complete. Although this is not imminent, we can estimate the quantity and accuracy of atomic data that will be needed for most applications to X-ray astronomy in the near future.

In addition, the advent of on-line databases has revolutionized the dissemination of atomic data. There is no longer a need for publication of rate coefficients or cross sections in obscure laboratory internal publications or conference proceedings, and results based on proprietary or fee-based databases or computational tools are receiving limited attention. The use of the web, faster computers and essentially unlimited storage have made it practical to save and disseminate great quantities of data. So there is no technical limitation to the sharing of data. In this review we therefore intentionally omit reference to unpublished data, data which is part of a fee-based or proprietary database or code package, or which is published in obscure laboratory internal reports or conference proceedings which are not widely available. We feel strongly that scientific information of all types, to be truly useful, must be freely and easily available, and its provenance must be transparent to all.

Atomic data can be used in different ways according to the level of detail needed for a specific application. The levels of detail range from compilations used in direct inspection of raw data, such as line finding lists, to synthetic spectra which attempt to fit to an entire observed dataset simultaneously. The cosmic sources also differ, ranging from electron-ionized and photoionized plasmas to planetary surfaces and atmospheres. Although traditional X-ray astronomy is generally agreed to span the energy range 0.1 - 10 keV, modeling of X-ray data inevitably requires knowledge of cross sections which extend to the ionization potential of hydrogen. We adopt this broader definition, and include some discussion of cross sections and rate coefficients associated with photons emitted in the EUV and UV bands. X-ray spectra thus far are only capable of detecting the 15 or so most cosmically abundant elements, including C, N, O, Ne, Na, Mg, Si, Al, S, Ar, Ca, Fe, and Ni, and we generally restrict our consideration to calculations and experiments relevant to these elements.

Much of the information relevant to this topic has already been reviewed by others. Recent advances in astrophysical X-ray spectroscopy have been reviewed by Kahn et al. (2004), Paerels and Kahn (2003) and some experimental results in atomic data by Beiersdorfer (2003). The subject of atomic data for X-ray astronomy has been discussed in specialized conference proceedings, including Silver and Kahn (1993), Bautista, Kallman and Pradhan (2000), Ferland and Savin (2001) and Smith (2005). More specialized reviews pertaining to many of the subtopics discussed here will be mentioned in what follows.

This review is organized as follows: We begin with a discussion of some examples of the astronomical X-ray spectra, choosing from recent observations using *Chandra* and $XMM-Newton$, followed by a review of the techniques used to derive atomic data, both theoretical and experimental. We then discuss the atomic data currently available, classified according to the level of modeling needed in order to apply the data. These range from line finding lists which can be applied by inspection, to diagnostics of physical quantities involving a small number of measurable parameters such as line ratios or equivalent widths, to models which attempt to synthesize a large portion of the spectrum. These we divide into the likely excitation mechanism: coronal, for sources where the primary energy input is mechanical; photoionized, where photon excitation, heating and ionization plays a dominant role; and planetary, associated with neutral, molecular or solid material. Then we further subdivide according to physical process.

We divide the discussion of each physical process or subtopic into sections: In the first, denoted 'background', we provide an overview of the work on the topic, dating from the early suggestions of the importance of the process and simple approaches to estimating rate coefficients and cross sections. In the second section, denoted 'Recent Developments', we change tactics slightly, and provide an overview of the work which we consider to be the current state of the art, or which point the way to future developments or improvements in the state of the art. Inherent in this is the omission of some work in favor of that which we consider to be either of sufficient accuracy and comprehensiveness to be adequate for the needs of X-ray astronomy today, or which we think points the way toward such data.

The study of X-ray spectra associated with planets, comets, and other primarily neutral or solid objects is newer than the study of other emission mechanisms. As a result, there is less work so far on interpretive tools for such spectra, and we do not give a separate discussion of line finding lists or discrete diagnostics for them. We also include a glossary in order to help keep track of the many acronyms and terms describing computational techniques, physical effects, and approximations. Throughout this paper we adopt chemical notation for ionic charge states, i.e. with a superscript denoting the ionic charge. This is in contrast to the spectroscopic notation used in much of the astrophysics literature, in which the charge state is denoted with a roman numeral: I=neutral, II=charge +1, etc. In the final section of the paper we discuss remaining needs for atomic data and prospects for future work.

II. ON THE NEED FOR ATOMIC DATA

The recent impetus for atomic data applications to astronomy comes from developments in instrumentation. Evolution of instruments has been rapid in the field of space astronomy, which has arisen and grown to a level of sensitivity and spatial and spectral resolution which is comparable to that of ground-based optical instrumentation in approximately the last 40 years. The most recent developments are summarized in the review by Paerels and Kahn (2003) for the X-ray band. Much of the current work is motivated by the launch of the grating spectrographs on the *Chandra* and $XMM-Newton$ satellites in the year 1999. These are described in detail in Brinkman et al. (2000) for the Low Energy Transmission Grating (LETG), in Canizares et al. (2005) for the High Energy Transmission Grating (HETG) on the *Chandra* satellite, and by Rasmussen et al. (2001) for the reflection grating spectrograph (RGS) on $XMM-Newton$. The gratings provide spectra with resolving power $\varepsilon/\Delta\varepsilon$ ~300 – 1000 in the energy range between 0.2 keV and 8 keV, with effective areas $\sim 10-100$ cm^2. In terms of wavelength, the resolution is $\Delta\lambda = 0.01-0.05$Å depending on the instrument, and the wavelength range extends from ≃1.8 Å for the *Chandra* HETG to 170 Å for the *Chandra* LETGS. This is in contrast with the previous generation of instruments, exemplified by the *ASCA* satellite (Tanaka, 1986), which carried moderate resolution CCD (Charge Coupled Device) instruments and had a spectral resolving power ∼20. The grating instruments have discovered line features in spectra previously thought to be featureless, and require a significantly more comprehensive and accurate database of atomic constants than had previously been in use. However, both *Chandra* and $XMM-Newton$ also carry CCDs whose use is necessitated by cosmic sources which are too faint for adequate signal in the gratings, or which are spatially extended and hence cannot make use of the full grating spectral resolution.

The *Chandra* and $XMM-Newton$ gratings represent a tremendous advance in resolution, but are not capable of unambiguously resolving thermal or natural line shapes from many sources. The nominal resolution (σ) of the HETG at the energy of the O^{7+} Lyα line corresponds to a Doppler velocity of 170 km s^{-1} (Canizares et al., 2005). In a thermal plasma this would be obtained at a temperature of $10^{7.5}$ K, which is significantly greater than the temperature where this ion is predicted to be abundant under most plausible conditions. The natural width of the line corresponds to 0.008 eV or an equivalent Doppler velocity of 3.7 km s^{-1}. Natural widths increase rapidly with the nuclear charge, and so for iron the corresponding velocity is 550 km s^{-1}. A typical dielectronic recombination (DR) satellite line to a hydrogenic resonance line (these terms are described in detail later in this review) is shifted by $\Delta\varepsilon/\varepsilon \simeq 0.002$ (Boiko et al., 1977). This is at the nominal resolution of the *Chandra* HETG. With good statistics, parameters describing line centroids or widths can be determined to precision better than the nominal resolution by factors of several. Nonetheless, it is clear that the *Chandra* spectra are not capable of measuring thermal line shapes unambiguously, and the wavelength precision is not comparable to that obtainable in the laboratory or in solar observations with Bragg crystal spectrometers, for example. On the other hand, the HETG can resolve the important diagnostic lines discussed in this review, and it can detect the effects of supersonic turbulence or bulk motions at Mach numbers of $\sim 2-3$ or more. This is of great astrophysical interest, since many X-ray plasmas are located in regions of strong gravity, or near shocks or other energetic sources.

As an illustration of the capabilities and limitations of the data obtained with *Chandra* and $XMM-Newton$ we present spectra obtained using these instruments which test the available atomic data and synthetic spectra. These are not chosen because they are typical, but rather because they best show the capabilities of the instruments and the available atomic data. Figure 1 shows the spectrum of the Seyfert galaxy NGC 3783 obtained with the *Chandra* HETG. This object is an active galaxy, and the spectrum shows absorption from a large number of resonance lines from the K shells of highly ionized ions of medium-Z elements, O - S, and also from the L shell of partially ionized iron. The solid curve is a model fit, described by Krongold et al. (2003), showing general consistency but not perfect agreement for the majority of the strong lines. In this object the gas is likely to be photoionized, and all the lines are shifted to the blue from their rest wavelength by an amount corresponding to a velocity of $\sim$500 − 1000 km s^{-1}. This is interpreted as being a Doppler shift in an outflowing wind, and similar spectra have been observed from most of the other objects of this class. Discovery of such outflowing gas is surprising, since active galaxies are strong sources of continuum X-rays, and are thought to contain black holes which radiate as gas is pulled inward. This spectrum also illustrates the fact that the data from the gratings on *Chandra* and $XMM-Newton$ can be used to constrain observed line wavelengths to within $\sim$ 0.25%. This exceeds the precision of most *ab initio* calculations and therefore requires laboratory measurements to provide wavelengths precise enough to allow reliable line identifications and to infer line shifts.

Figure 2 shows the spectrum of the nearby active star Capella obtained with the *Chandra* HETG (Canizares et al., 2000). This shows rich line emission, similar to the Sun, and which is typical for a coronal source. For the most part the lines in the 10 − 18 Å range are due to emission from L-shell iron ions. The observed iron L spectrum can be reproduced almost entirely by assuming a single electron temperature of $kT_e =$ 600 eV (Behar et al., 2001b). This temperature is consistent with both the measured fractional ion abundances of iron and with the temperature derived from ratios of Fe^{16+} lines. However, there are some remaining discrepancies between single temperature models and the data for the lines of Fe^{17+} near 16 Å and also Fe^{16+} and Fe^{17+} at 15.015 and 14.206 Å which are all overestimated by current models. The statistical quality of this spectrum is comparable to that obtained from the Sun, illustrating the power of X-ray spectroscopy to study nearby objects outside the solar system.

An illustration of the power of high resolution X-ray spectroscopy to study distant objects is shown in Figure 3, which shows the spectrum of a composite of galaxy clusters taken with the RGS on $XMM-Newton$ (Peterson et al., 2003). The blue curve shows the data coadded for 13 clusters, which clearly exhibit coronal line emission from Fe^{22+}, Fe^{23+}, and O^{7+} Lyα. This is consistent with emission from gas at an electron kinetic temperature of $kT_e \simeq 1.5$ keV. This temperature has also been derived from lower resolution observations of these and similar clusters. The gas densities can also be derived from the X-ray luminosities and sizes. Based on these quantities, the time for the gas to cool radiatively is predicted to be short compared with the probable cluster age, hence the lines from lower ionization species are expected as the gas cools to $\sim$ 1 keV and below. The vertical dashed curves in the Figure denote the positions of the lines which are predicted from such cooling flow models, such as O^{6+} and Fe^{16+}. Their absence requires a major reexamination of the prevalent model for cluster X-ray gas. One possibility is that the gas, rather than cooling steadily over cosmological time, is reheated by active galaxies in the cluster. If so, it would provide an additional example of the influence of black holes on their environments and on their likely influence on the growth of cosmic structures (Ruszkowski et al., 2004).

Figure 4, shows the spectrum of a Seyfert galaxy NGC 1068 taken with the LETG on *Chandra* (Brinkman et al., 2002). The extended long wavelength coverage is a unique feature of this instrument. The black curve shows the data taken of the nuclear region of the galaxy, and the red curve shows a model. The model consists of emission due to gas which is emitting primarily as a result of photoionization, photoexcitation and scattering, as evidenced by the radiative recombination continuum (RRC) features due to O^{6+} near 16.5 Å and C^{4+} near 31.5 Å and their strengths relative to the resonance lines from these ions. This is interpreted as being due to the fact that the galaxy contains a strong source of EUV and X-ray continuum radiation, likely a black hole, but that this source is hidden from our direct view by cold obscuring gas. This appears to be typical of type 2 Seyfert galaxies, which are likely intrinsically similar to the type 1 Seyfert galaxy NGC 3783 (Figure 1). Both types contain a black hole partially surrounded by torus of nearly opaque cold gas, but their spectra reveal the fact that they are viewed at different orientations (Antonucci and Miller, 1985). Thus X-ray spectra such as these provide evidence for the presence of hidden black holes via their scattered radiation.

These examples illustrate the statistical quality of recent high resolution X-ray spectra, and, crudely, the extent to which current synthetic spectra are able to match the observations. They also provide a glimpse of the astrophysical issues which can be addressed using X-ray spectra and the potential importance of atomic data to address these issues. They also illustrate the unique nature of the information provided by X-ray spectra; the scientific insights provided by these observations are not accessible to any other waveband, or to observations using lower resolution X-ray instruments.

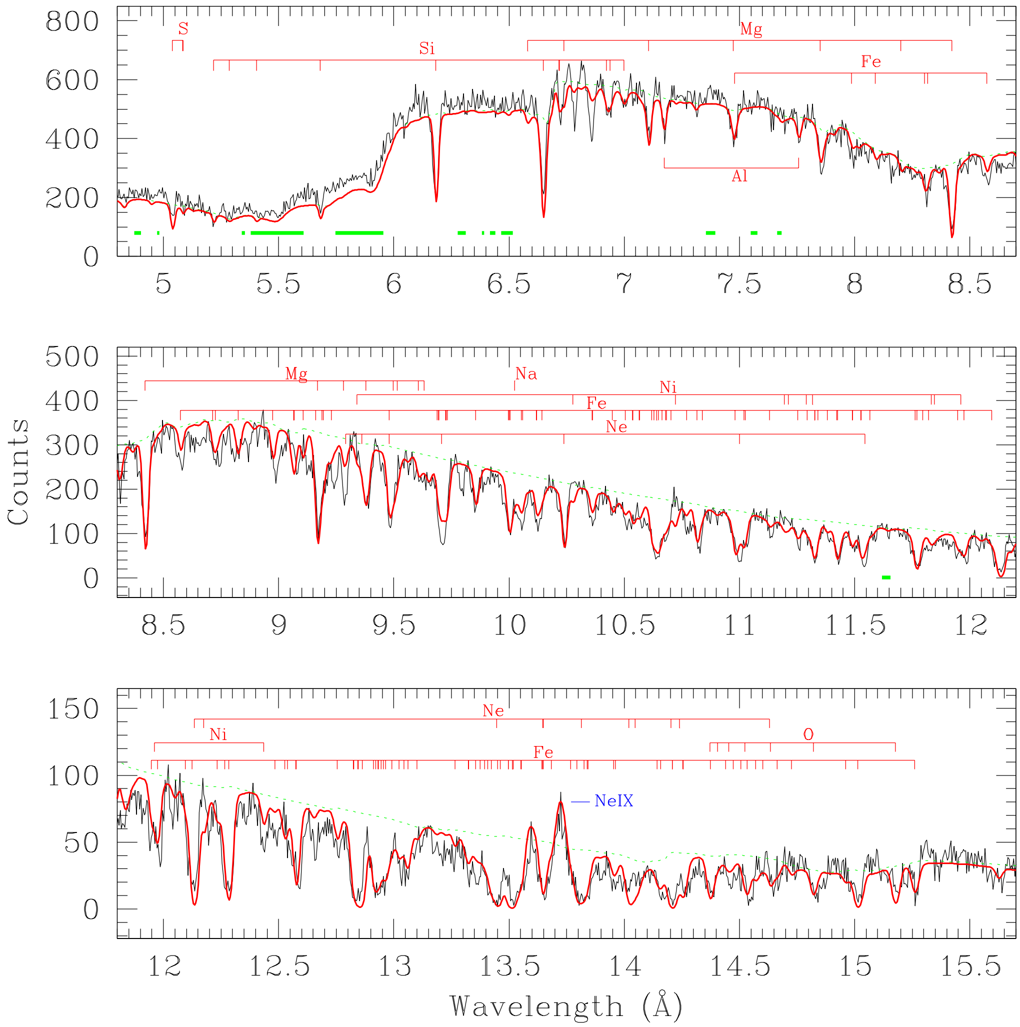

FIG. 1 *Chandra* HETG spectrum of NGC 3783, from Krongold et al. (2003)

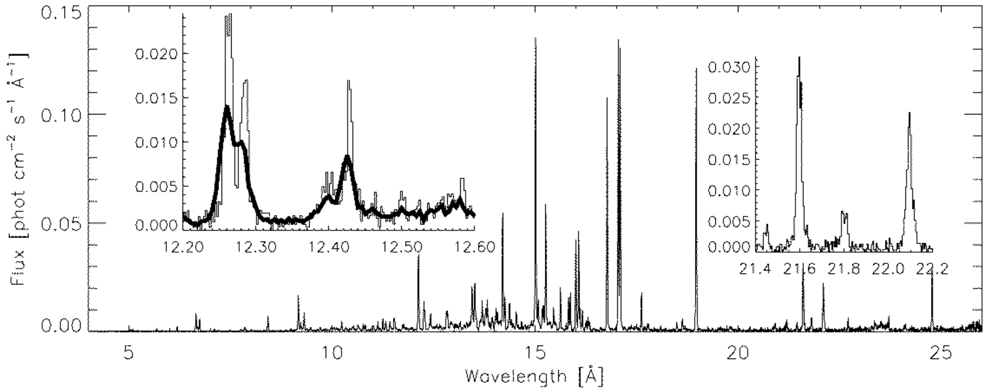

FIG. 2 HETG spectrum of Capella, from Canizares et al. (2000). Insets show the regions of the spectrum in the vicinity of the lines of He-like Ne^{8+} and O^{6+}. In the left inset panel the two curves are the data from the two arms of the dispersed image. The thin line is the data from the higher energy arm (HEG) and the thick line is the data from the medium energy arm (MEG).

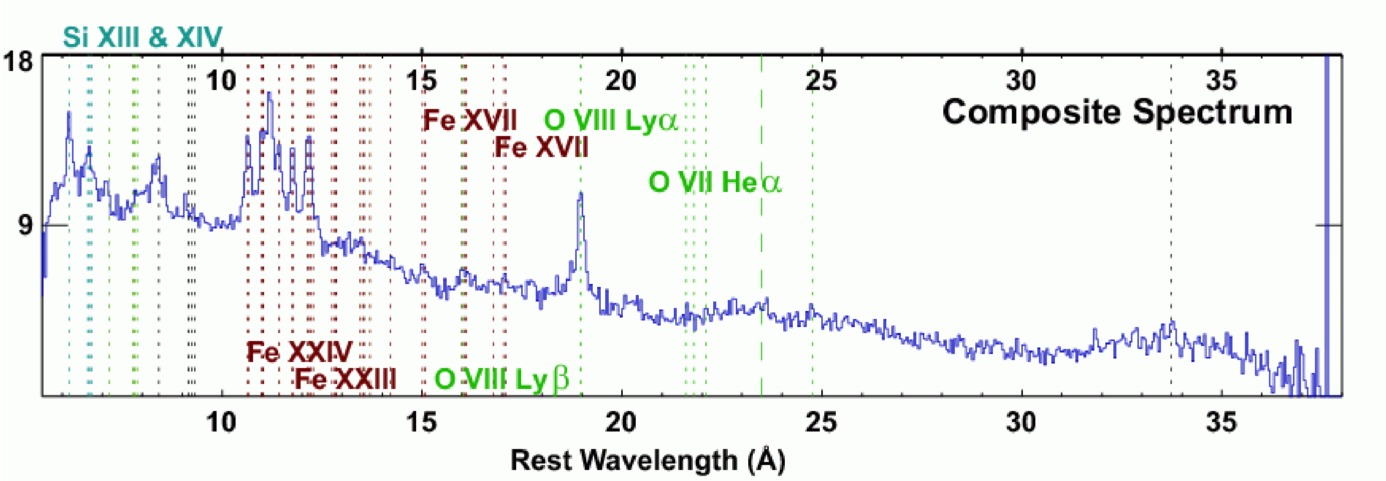

FIG. 3 Composite spectrum of galaxy clusters where cooling gas is expected, from Peterson et al. (2003). The solid curve shows data from the RGS on $XMM-Newton$ and dashed vertical lines show the predicted locations of various coronal emission lines.

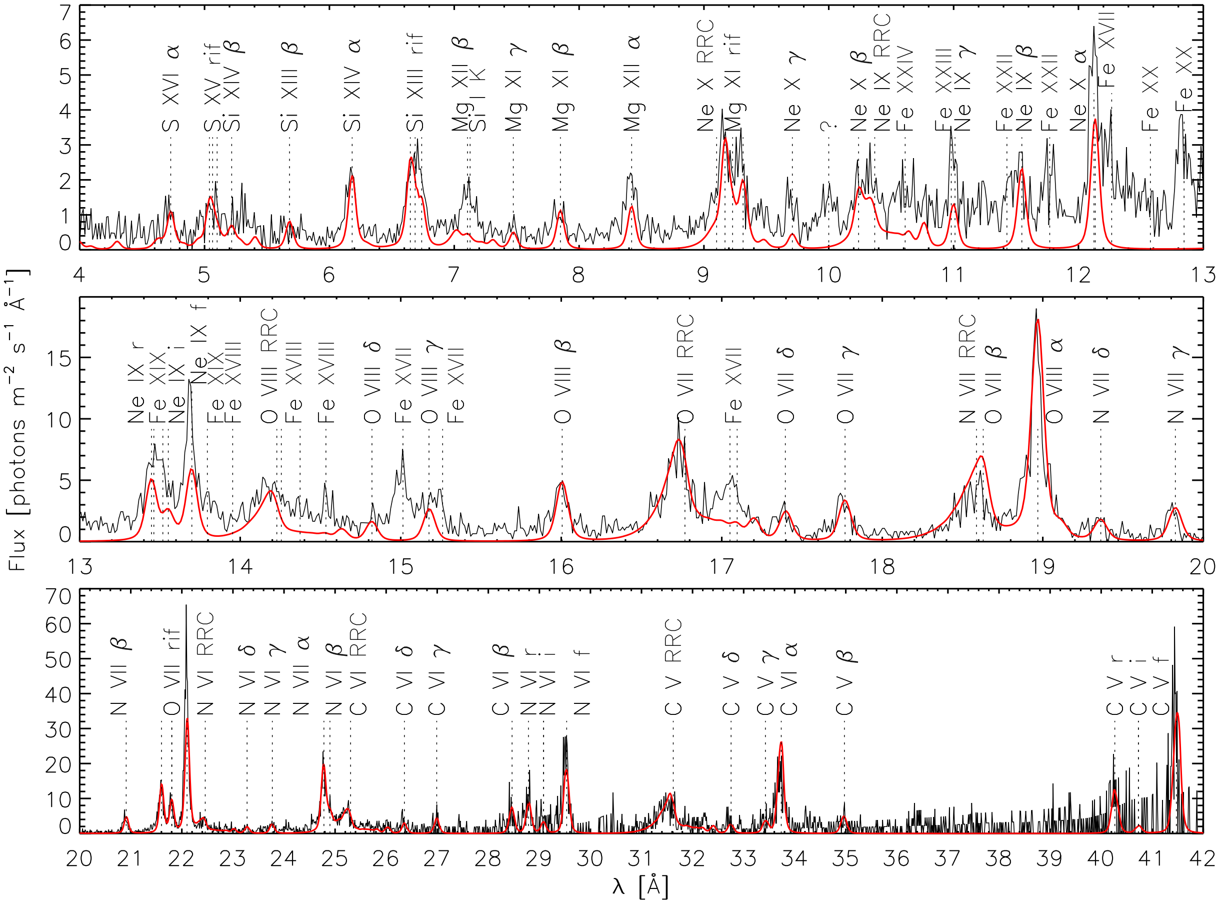

FIG. 4 Spectrum of the Seyfert 2 galaxy NGC 1068, taken with the LETG on the Chandra satellite, from Brinkman et al. (2002). Black curve shows the data and red curve shows a fit to a photoexcited and recombining model (Kinkhabwala et al., 2002).

A. Atomic Data Accuracy Requirements

Spectra such as the ones shown so far in this section can be used as a practical guide for X-ray atomic data accuracy requirements. Simple estimates can be obtained by examination of the spectra. The strongest emission line (the Lyα line of O^{7+}) in the spectrum of Capella, as shown in Figure 2 for example, has flux 0.02 photons cm^{-2} s^{-1}, corresponding to a total of $\simeq$1300 counts in a 3×10^4 s observation. The dominant error for such an observation is counting statistics, and assuming Gaussian errors this corresponds to a statistical error on the line intensity of $\simeq$3%. This may be viewed as the implied accuracy requirement for a single atomic rate coefficient which affects the line flux linearly, if all other quantities which can affect the line flux are known or not of interest. Such rate coefficients, when they describe collisional processes, are derived by averaging the energy dependent cross section for the process over the Maxwellian distribution of electron velocities. So an accuracy requirement on a rate coefficient translates approximately linearly into the requirement on the energy dependent cross section if interpreted as applying uniformly over all energies. On the other hand, a greater uncertainty in the cross section can be tolerated if it applies over a narrow energy range. An observed line flux can be used to infer the total number of emitting ions if the excitation rate for the line is known. The accuracy of such a determination will be limited by the atomic data if the uncertainty in the excitation rate exceeds the statistical error in the observed spectrum.

On the other hand, inferring physical quantities such as gas temperature, density or elemental abundance from a line or a spectrum in many cases requires comparison with models. Model results depend on various atomic rate coefficients: those affecting the ionization balance, those affecting excitation and those affecting photon emission. The dependence of observables such as line strengths on rate coefficients affecting ionization balance or excitation can be non-linear, and are not well suited to analytic estimates for atomic data accuracy requirements. Numerical experiments can illustrate the sensitivity of line strengths to the rate coefficients affecting ionization and excitation. As an illustration, Figure 5 shows the ionization balance in coronal equilibrium for iron. Ion fractions are plotted as a function of temperature T in the range $4\leq\log(T)\leq8$ and the dominant ionization stage ranges from Fe^{+} at low temperature to Fe^{26+} at the highest temperature. The left panel shows these quantities calculated using rate coefficients from Arnaud and Raymond (1992) for iron. We denote these as our baseline ionization balance (but note that the work by Bryans et al. (2006) represents a significant update). The right panel has been calculated using the baseline rate coefficients, except that the rate coefficients for recombination for each ion have been perturbed, i.e. multiplied by a randomly chosen factor ranging between 0.79 and 1.28 (i.e. $\Delta\log[\mathrm{ratecoefficient}] = \pm0.1$). This range is only slightly greater than the magnitude of the effect which is likely to be associated with plasma microfields, cf., Section VII.A.2 and Badnell et al. (2003), and so reflects a realistic limit to the level of accuracy needed from zero-external-field rate coefficients for this process. Within this range, the multiplicative factor affecting recombination is randomly chosen and evenly distributed. The recombination rate coefficients are stored as analytic functions of temperature and, for each ion, the same multiplicative factor is applied at all temperatures. Comparison of the two panels of Figure 5 indicates the sensitivity of the ionization distribution to changes in the recombination rate of this magnitude: at a given temperature ion fractions can differ by factors ∼2–4, although closed shell ions such as Ne-like and He-like ions are relatively unaffected. The temperature where the maximum fraction occurs can also change by $\sim0.1 - 0.2$ in log(T).

The effects of the ionization balance change on the synthetic spectrum, and on the inferred distribution of gas temperatures in a real astrophysical source, are illustrated in Figures 6 and 7. Figure 6 shows an observed spectrum from the active star Capella taken with the HETG grating on the *Chandra* satellite, the same source shown in Figure 2. The observed spectrum is shown as the data points with error bars. The solid (red) curve in Figure 6 is a synthetic spectrum calculated using the baseline ionization balance shown in the left panel of Figure 5. This spectrum is calculated using the ionization balance at two temperatures, log(T)=6.9 and log(T)=7.1. The element abundances and the relative normalizations of the two components were allowed to vary in order to achieve a fit which has χ^2=3267 for the 1602 independent energy channels shown in this figure. This is not in a range of χ^2 which permits application of traditional statistical measures of probability of random occurrence (Bevington, 1969), and is primarily of illustrative value. Similar values of χ^2 are found when these data are fit to two temperature component models calculated with other modeling packages which are in widespread use, such as APEC (Smith et al., 2001) and MEKAL (Mewe et al., 1995b).

In the region of the spectrum shown most of the features are due to iron, the exception being the Lyman lines of Ne^{9+}. We find a best fit value of [Ne/Fe], the abundance ratio relative to solar (Grevesse et al., 1996), of 0.66. The strongest lines in this spectrum are indicated in Figure 6: Fe^{16+} between 12 and 17 Å, and the Lyα line of Ne^{9+} at 12.13 Å, which is blended with the corresponding Fe^{16+} line. Higher ionization lines include lines from Fe^{18+} at 10.5 – 10.8 Å, Fe^{17+} between 11 and 16 Å, Fe^{18+} at 13.5 – 13.8 Å and Fe^{19+} at 12.85 Å. Lower ionization lines include O^{7+} at 16.00 Å, Fe^{17+} blended with Ne^{9+} Lβ at 10.24 Å and Ne^{8+} at 11.03 Å . The baseline model accounts for the strengths of many of the strongest lines, but under predicts the Fe^{16+} 15 and 17 Å lines; this is a manifestation of problems with rate coefficients affecting this ion which are in widespread use and which are discussed in section VI.A.4.

The emission line spectrum radiated by the plasma is calculated using rate coefficients for electron impact collisional excitation culled from the references discussed later in this paper. These are enumerated in Bautista and Kallman (2001), with the addition of rate coefficients from the recent CHIANTI version 5 compilation (Landi et al., 2005). It is well known that a source such as Capella is best fit using a broad distribution of temperatures, ranging from log(T)$\simeq$6 – 7.4 (Canizares et al., 2000), but we adopt the two component model shown here for illustrative purposes.

The effects of perturbing the ionization balance on the fit to the spectrum can be seen in Figure 7, in which the analogous procedure is carried out using the ionization balance shown in the right panel of Figure 5. In making this fit we have not attempted to reoptimize any of the parameters describing the fit, i.e. the normalization, temperatures or elemental abundances in the two temperature components. Rather, we have left them the same as in Figure 6 in order to illustrate the sensitivity to the ionization balance. Comparison with the fit shown in Figure 6 shows that the fits to the strongest lines, i.e. those of Fe^{16+} and Ne^{9+}, are essentially identical. This is a reflection of the fact that the ionization balance of the closed-shell Fe^{16+} is little affected by the perturbation in recombination rate coefficients. However, significant differences are apparent in the fit to the ions in adjacent ionization stages, notably Fe^{17+} and Fe^{19+}. These show up in the lines near 14.2-14.5 Å for Fe^{17+} and 12.8 Å for Fe^{19+}, which are under predicted by the model shown in Figure 7. The lines of Fe^{18+} are not strongly affected by the perturbation in the recombination rate coefficients. The fit between data and model in Figure 5 has χ^2=3610 for 1602 energy channels and is clearly worse than for the baseline model. However, when the perturbed model is iteratively fitted to the *Chandra* data a better fit is found when the high temperature component increases to log(T)=7.2. The resulting fit is improved, although still inferior to the baseline model: χ^2=3522 for 1602 energy channels as compared with χ^2=3267 for 1602 energy channels for the baseline model.

These experiments illustrate some of the effects of changes in the rate coefficients affecting ionization balance on fitting to observed astrophysical X-ray spectra and on the inferred temperature distribution. They indicate that changes of $\sim$25% in these rate coefficients can affect the model strengths of the lines of the more delicate ions by factors $\sim$3 – 10, while the strong lines from stable ions are more robust. Such changes in model line strengths lead to changes in the inferred physical conditions derived by iterative model fitting which are significant. In this case we find changes of 0.1 in log(T) from such a procedure, which is at the resolution of the grid of models used to calculate the spectra.

In a coronal plasma there is an exact symmetry between recombination and electron impact collisional ionization, so that perturbations to recombination rate coefficients can be interpreted as corresponding inverse perturbations to the ionization rate coefficients. The inferences from these numerical experiments are reciprocal between the two types of rates. At the same time, it is clear that the above model fits have been applied to only one spectrum, and only one numerical experiment at perturbing the rate coefficients has been performed. In order to adequately characterize the effects of perturbing various rate coefficients, this experiment should be repeated in order to truly randomize the perturbations, and experiments should be carried out with different amplitudes and with fits to other astrophysical X-ray spectra. More extensive experimentation of this type has been carried out with application to solar EUV and X-ray line emission by Savin and Laming (2002) and Gianetti, Landi and Landini (2000). Masai (1997) examined the effects of uncertainties in rates affecting ionization balance on the results of fitting to moderate resolution X-ray spectra obtained using CCD instruments.

III. THEORETICAL TECHNIQUES

Theoretical calculation of atomic processes begins with the solution to the multi-electronic Schrödinger or Dirac equation,

$$\left\{\sum_i h_i + \sum_{i<j} V_{ij}^{e-e}\right\}\Psi = E\Psi. \tag{1}$$

where h_i are the one-electron Hamiltonians and V_{ij}^{e-e} the electron-electron interaction potentials. In the fully relativistic case, h_i are Dirac Hamiltonians, V_{ij}^{e-e} include the direct and exchange part of the electrostatic interaction (the interaction energy due to the positional correlation of parallel-spin electrons according to the Pauli exclusion principle) and the Breit interaction (the two-body magnetic interaction), and Ψ is a four-component wave function. In the non-relativistic case, h_i are Schrödinger Hamiltonians and V_{ij}^{e-e} include only the electrostatic interaction. In the Breit–Pauli (BP) relativistic approximation, the non-relativistic multi-electronic Hamiltonian is corrected by adding terms resulting from the reduction of the one-electron Dirac Hamiltonian and the Breit interaction to the Pauli form (Bethe and Salpeter, 1972). The relativistic correction terms are then the mass-correction, Darwin, and spin-orbit terms that are added to h_i, and the spin-other-orbit, spin-spin, orbit-orbit, spin-contact, and two-body Darwin terms that are added to V_{ij}^{e-e}. Higher-order relativistic interactions like QED have also to be treated in the case of highly-ionized heavy atoms. The angular part of the solution of the Schrödinger equation is known exactly and is found using the Racah algebra (Edmonds, 1960; Fano and Racah, 1959; Racah, 1942, 1943). With regards to the radial part, the exact solution cannot be found due to the V_{ij}^{e-e} terms. One of the simplest approximation is the

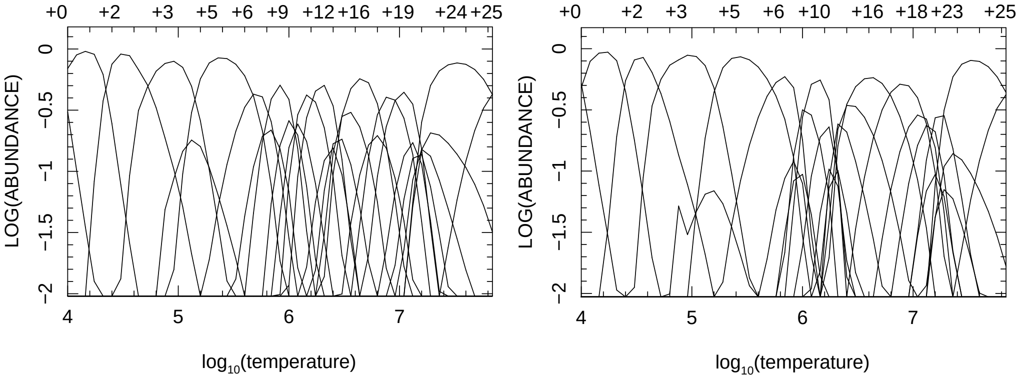

FIG. 5 Left Panel: Ionization balance for iron in a coronal gas, calculated using rate coefficients described in the text. Right panel: Ionization balance calculated using perturbed rate coefficients as described in the text. Curves correspond to various ions of iron: in the left panel Fe^{+} dominates at log(T)=4, Fe^{+5} dominates at log(T)=5.2, Fe^{+8} dominates at log(T)=5.9, Fe^{+12} dominates at log(T)=6.3, Fe^{+16} dominates at log(T)=6.6, Fe^{+24} dominates at log(T)=7.5. In the right panel, the temperature of maximum abundance of Fe^{+8} – Fe^{+23} is displaced to lower temperature by ≃0.1 in log(T).

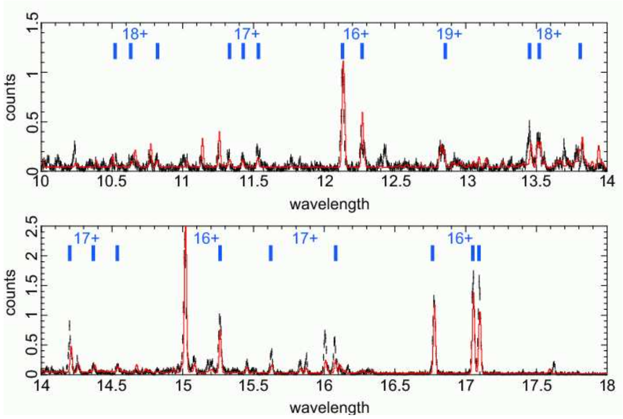

FIG. 6 Fit to a 3×10^4 s *Chandra* HETG observation of the active star Capella in the 10 – 18 Å region using the baseline ionization balance shown in the left panel of figure 5.

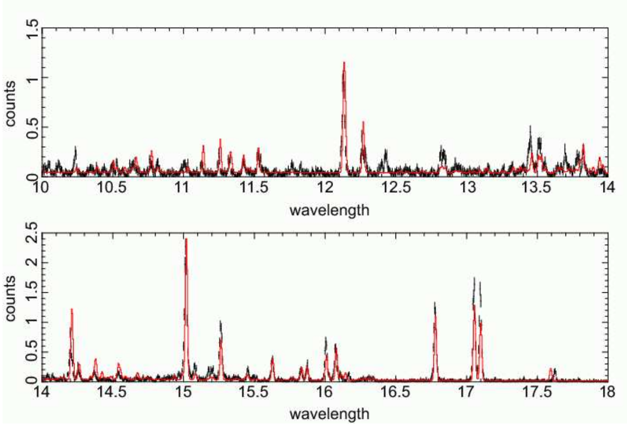

FIG. 7 Same as figure 6 except using ionization balance shown in figure 5 derived from perturbed rate coefficients as described in the text and displayed in the right panel of figure 5.

independent-particle or central-field model where

$$\sum_{j\neq i} V_{ij}^{e-e} \sim V_i(r) \tag{2}$$

where $V_i(r)$ are local central potentials in which each electron moves independently. The atomic state function Ψ is then a product of the atomic orbitals ϕ_i which are eigenstates of the mono-electronic Hamiltonians,

$$\{h_i + V_i(r)\}\,\phi_i = \epsilon_i\phi_i,\ i = 1, ..., N \tag{3}$$

where N is the number of electrons. Different forms of the functions $V_i(r)$ can be considered (Cowan, 1981). Forms that depend upon the orbitals themselves lead to the use of the self-consistent-field (SCF) iterative procedure (Cowan, 1981).

A more elaborate solution of Eq. (1) comes from the application of the variational principle. Using the trial atomic state function defined by

$$\Psi = (N!)^{-1/2} det\ \phi_i(x_j) \tag{4}$$

where x_j are the electron space and spin coordinates and the determinant insures the Pauli exclusion principle, the ϕ_i are obtained by requiring that the expectation value of the multi-electronic Hamiltonian is minimum

$$\langle\delta\Psi|\sum_i h_i + \sum_{i<j} V_{ij}^{e-e}|\Psi\rangle = 0 \tag{5}$$

where the variation is taken with respect to the radial parts of the orbitals ϕ_i. This leads to the Hartree–Fock equations (Hartree, 1957)

$$h_i\phi_i(x) + \sum_j \int dr'\phi_j(x')\frac{1}{|r-r'|}\phi_j(x')\phi_i(x) = \epsilon_i\phi_i(x)$$

$$+\sum_j \int dr'\phi_j(x')\frac{1}{|r-r'|}\phi_i(x')\phi_j(x),\ i = 1, ..., N. \tag{6}$$

These non-homogeneous coupled integro-differential equations are solved iteratively in a SCF procedure. An important property of the Hartree–Fock approximation follows from the Brillouin's theorem which implies that the diagonal matrix elements of single-particle operators are given correctly to first order by Hartree–Fock atomic state functions. This approach essentially takes into account the part of the electron correlations within an electronic configuration.

Further improvement can be made using trial atomic state functions Ψ that are expansions of configuration state functions Φ,

$$\Psi = \sum_k c_k \Phi_k \tag{7}$$

where Φ_k are themselves expansions of Slater determinants (Eq. (4)) and c_k are the mixing coefficients. The summation in Eq. (7) can be systematically extended in principle to yield results of arbitrarily high accuracy or to achieve convergence. This approach is referred to as the configuration interaction (CI) approximation. When the variational principle (Eq. (5)) is applied to Eq. (7) varying the c_k and the orbitals ϕ_i, one talks about the multi-configuration approach such as in the multi-configuration Hartree-Fock (MCHF) (Fischer, 1996) and multi-configuration Dirac-Fock (MCDF) (Parpia et al., 1996) methods. Otherwise one talks rather about the superposition of configurations approach where Eq. (3) or Eq. (6) is used to determine the orbitals ϕ_i and the multi-electronic Hamiltonian matrix is diagonalized afterward to obtain the c_k and the eigenvalue E as, for example, in Cowan's code (Cowan, 1981). In practice, the CI expansion in Eq. (7) is limited and in order to include more correlation in Ψ, the multi-electronic Hamiltonian matrix elements are corrected to reproduce the few available experimental energy levels. The approximation becomes then a semi-empirical one.

A different approximation which is also capable of systematic improvement of the atomic state function is based on the many-body perturbation theory (MBPT) of Brueckner (1955) and Goldstone (1957). In this method, the multi-electronic Hamiltonian is written as a sum of a zero-order Hamiltonian and a perturbation term

$$H = H_0 + H_{pert} \tag{8}$$

where

$$H_0 = \sum_i \{h_i + V_i(r)\} \tag{9}$$

and

$$H_{pert} = \sum_{i<j} V_{ij}^{e-e} - \sum_i V_i(r). \tag{10}$$

A complete set of orbitals ϕ_i are then obtained by solving Eq. (3) and used in the order-by-order Rayleigh–Schrödinger perturbation expansion of the atomic state energies E and other properties such as oscillator strengths. An example of the reduction of the perturbation expansion to MBPT formulas using Feynman diagrams and second-quantization method is given in Avgoustoglou et al. (1992) for closed-shell atoms.

For processes involving the continuum, the continuum atomic state function $\Psi(\varepsilon)$ for the $(N+1)$-electron system has to be evaluated,

$$\Psi(\varepsilon) = \sum_\alpha \chi_\alpha \phi_\alpha(\varepsilon) \tag{11}$$

where ε is the energy of the free electron, ϕ_α are free-electron orbitals and χ_α are atomic state function of the N-electron target Hamiltonian. The free-electron orbitals are solutions of the following Schrödinger equations

$$\left\{h_\alpha^K + \varepsilon\right\} \phi_\alpha = \sum_{\alpha'} U_{\alpha\alpha'} \phi_{\alpha'} \tag{12}$$

where h_α^K are one-electron kinetic Hamiltonians and the matrix potential $U_{\alpha\alpha'}$ is defined by

$$\begin{aligned} U_{\alpha\alpha'} = \textstyle\int dx_1 ... dx_N \; \chi_\alpha(x_1 ... x_N) \\ \times \; U(x_1 ... x_N x_{N+1}) \; \chi_{\alpha'}(x_1 ... x_N) \end{aligned} \tag{13}$$

where U is the sum of the nuclear and electron-electron interaction potentials acting on all the $(N+1)$ electrons of the target-plus-free-electron system.

The widely used distorted wave (DW) approximation consists in neglecting the coupling between the different channels or the interaction between continuum states, i.e.

$$U_{\alpha\alpha'} = 0, \alpha \neq \alpha', \tag{14}$$

by using the central-field model defined in Eq. (3). It becomes a good approximation for both the non-resonant background and resonance contribution. However, many DW excitation rate coefficients omit the resonance contribution entirely.

At sufficiently large ionization or free-electron energies, DW orbitals approximate closely to Coulomb orbitals calculated using

$$U_{\alpha\alpha} \sim -\frac{(Z-N)}{r} \tag{15}$$

where Z is the atomic number. It is then called the Coulomb–Born (CB) approximation. The exchange part of the electrostatic interaction is neglected in CB approximation but included in the Coulomb–Born–Oppenheimer (CBO) and Coulomb–Born–Exchange (CBE) approximations.

The simplest approximation consists in considering plane waves to describe the continuum orbitals. It is equivalent to switching off the matrix potential, i.e. $U_{\alpha\alpha} \sim 0$. This technique called the Born approximation is most likely to be accurate for energies far above threshold, and for an electron colliding a neutral atom. It is a good approximation for the background cross section over a wide range of energies for positive ions, because the infinite energy limit for scattering of a positive ion is exactly the Born cross section and this limit controls the finite energy cross section over a wide range of energies due to the slowly varying behavior of the cross section with energy.

The three above-mentioned approximations make assumptions about the wave function of the continuum electrons which are only appropriate when the energy of the projectile electron (or free electron) is much greater than the binding energy of the target electrons (or bound electrons) of interest. In contrast, approximations such as the more elaborate and widely used R-matrix method (Burke and Berrington, 1993) can be invoked for free electrons at low energies and for low ionization charges up to negative ions where the coupling between channels is generally strong.

Moreover, the importance of resonant enhancement of rate coefficients for collisional excitation (see e.g. Section VI.A.1) means that the R-matrix method is widely used for highly-charged ions as well, as it is a very efficient way of determining the resonance contribution. Distorted-wave cross sections are traditionally non-resonant. There are two ways in which resonances can be taken account of subsequently. Firstly, (as exemplified by HULLAC) autoionizing states can be included in the collisional-radiative equations when calculating level populations and effective recombination and ionization rate coefficients. This can become very demanding computationally but it does allow for collisional redistribution of autoionizing states in dense plasmas. Secondly, the low-to-medium density approach, appropriate to the solar atmosphere, magnetic fusion plasmas, is to include the resonances in the excitation calculation, either via R-matrix (always present), or perturbatively (as has been done for some ions using FAC) and so omit autoionizing states from the collisional-radiative population rate equations (otherwise they would be double-counted). This hugely simplifies the collisional-radiative problem but means there is a density range below that for collisional equilibrium, where partial collisional redistribution of autoionizing states takes place, and where non-autoionizing level populations are not well described [1].

The R-matrix method consists of dividing the space into an internal and external regions. In the internal region where the interaction between the free electron and the target electrons is strong, the $(N+1)$-system atomic state function $\Psi(\varepsilon)$ is expanded in terms of target eigenfunctions χ,

$$\Psi(\varepsilon) = \mathcal{A} \sum_{\alpha} \bar{\chi}_{\alpha} \frac{u_{\varepsilon,\alpha}(r)}{r} + \sum_{i} c_i \Phi_i \tag{16}$$

where $\mathcal{A}$ is the anti symmetrization operator insuring the Pauli exclusion principle, the bar sign over χ indicates the coupling with the angular and spin parts of the free-electron orbital $\phi(\varepsilon)$, $u_\varepsilon(r)/r$ represents the radial part of the latter, and Φ_i are bound states of the $(N+1)$-system that are constructed with target orbitals to ensure completeness of $\Psi(\varepsilon)$ and improve short-range correlations. The functions $u_\varepsilon(r)$ and the coefficients c_i are obtained applying the Kohn variational principle to Eq. (16) giving rise to a set of coupled integro-differential equations.

These are solved by determining the R-matrix which is a real, symmetric matrix whose rows and columns are labeled according to the possible channels of the scattering problem. At this point, one should notice by looking at Eq. (16) that resonances (quasi-bound states) are automatically included either in terms of closed channels in the first expansion or as linear combinations of bound states in the second expansion. In the external region, $\Psi(\varepsilon)$ is represented by Eq. (11) and Eq. (12) is solved with the following long-range matrix potential,

$$U_{\alpha\alpha'}(r) = \sum_{\lambda} C^{(\lambda)}_{\alpha\alpha'}/r^{\lambda+1}. \tag{17}$$

The MBPT method described above is also a powerful technique to compute continuum processes. Here, the perturbation expansion is reduced using Feynman diagrams involving, for instance, the photoelectron of the photoionization process.

We now describe some specific codes for computations of atomic structure and scattering. Codes employing similar assumptions and computational algorithms are grouped together.

-HULLAC:

The Hebrew University Lawrence Livermore Atomic Code (Bar-Shalom, Klapisch and Oreg, 2001) is a full package for structure and scattering calculations. It solves the multi-electronic Dirac equations and includes QED corrections. An analytical parameterized central-field potential is used to obtain the analytical Slater-type spin-orbitals. The atomic states Ψ are constructed using CI expansions. The parameters appearing in both the central-field potential and the spin-orbitals are varied in a MC approach in order to minimize the energies of any set of levels or, in its semi-empirical mode, to minimize the rms deviation between a set of experimental energy levels and their corresponding theoretical values. The continuum is treated in a DW approximation. Using interpolation techniques for the radial part of collision strengths, it can calculate large quantities of data.

-FAC:

The Flexible Atomic Code (Gu, 2003a) is also a fully relativistic program computing both structure and scattering data. It uses a modified Dirac–Fock–Slater central-field potential which includes an approximate treatment of the exchange interaction. The orbitals are optimized in a SCF iterative procedure during which the average energy of a fictitious mean configuration with fractional orbital occupation numbers is minimized. This mean configuration represents the average electron cloud of the configurations retained in the CI expansion. This is an intermediate approach between MC and SC. The DW method is used to calculate continuum atomic state functions $\Psi(\varepsilon)$.

---

[1] The authors thank Dr. N. Badnell for pointing this out and providing the text for this paragraph.

-MCDF/GRASP/GRASP92:

The Multi-Configuration Dirac–Fock structure code (Grant et al., 1980) and its more recent versions, GRASP (Dyall et al., 1989) and GRASP92 (Parpia et al., 1996), use the elaborated fully relativistic Hartree–Fock MC variational principle to obtain the c_i and four-component ϕ_i in the CI expansion defined by Eq. (7). One energy level or the average of a group or all energy levels is minimized in the orbital optimization. The QED interaction is treated as corrections to the energy levels.

-SUPERSTRUCTURE/AUTOSTRUCTURE/AUTOLSJ:

SUPERSTRUCTURE (Eissner et al., 1974) solves the Breit–Pauli Schrödinger equation. CI atomic state functions are built using orbitals generated from the scaled Thomas–Fermi–Dirac central-field potential that is based on the free-electron gas with exchange approximation. The scaling factors for each orbital are optimized in a MC variational procedure minimizing a LS term energy or weighted average of LS term energies. Semi-empirical corrections can be applied to the multi-electronic Hamiltonian in which theoretical LS term energies are corrected in order to reproduce the centers of gravity of the available experimental multiplets. Other versions are AUTOSTRUCTURE (Badnell, 1986a, 1997) and AUTOLSJ (Dubau et al., 1981). These include the treatment of the continuum in a DW approach. In AUTOSTRUCTURE, analytical Slater-type orbitals can be also used, and non-orthogonal orbital basis sets can be considered for the calculations of inner-shell processes.

-CIV3:

The Configuration Interaction Version 3 code of Hibbert (1975) uses analytical Slater-type orbitals in CI expansions to represent atomic state functions and solves either the non-relativistic or the Breit–Pauli Schrödinger equations. The orbital parameters are varied in a MC optimization procedure to minimize one or several energy levels using an analytical central-field potential. The atomic state function can be improved in a semi-empirical procedure called fine tuning in which the multi-electronic Hamiltonian matrix elements are corrected in order to reproduce the available experimental energy levels.

-R-MATRIX/BPRM/DARC:

The BPRM scattering package described in Burke and Berrington (1993) implements the elaborated R-matrix method in the Breit–Pauli relativistic approximation. In the latter, only the one-body Darwin, mass-correction and spin-orbit terms are considered. The scattering package can use either SUPERSTRUCTURE, AUTOSTRUCTURE or CIV3 target orbitals. The radiation and Auger dampings which are important in processes involving inner-shells have been included using an optical potential (Gorczyca and Badnell, 1996, 2000). A fully relativistic implementation of the R-matrix approach using GRASP target spin-orbitals is also available (DARC; Ait-Tahar et al. (1996)).

-MCHF:

In the Multi-Configuration Hartree–Fock structure code (Fischer et al., 1997), the non-relativistic multi-electronic Schrödinger equation is solved using the elaborated Hartree–Fock MC variational principle to obtain the orbitals and the mixing coefficients utilized in the CI expansion of the atomic state function. The relativistic corrections are included by diagonalizing afterward the Breit–Pauli multi-electronic Hamiltonian.

-HFR:

The pseudo-relativistic Hartree–Fock code of Cowan (1981) solves the Hartree–Fock equations for the spherically averaged atom for each electronic configurations. These equations are the result of the application of the variational principle to the configuration average energy. Relativistic corrections are also included in this set of equations, i.e., the Blume–Watson spin–orbit, mass-variation and one-body Darwin terms. The Blume–Watson spin–orbit term comprises the part of the Breit interaction that can be reduced to a one-body operator. CI is taken into account in an SC approach. The radial parts of the multi-electronic Hamiltonian can be adjusted to reproduce the available energy levels in a least-squares fit procedure. These semi-empirical corrections are used to allow the inclusion of higher-order correlations in the atomic state functions. Continuum orbitals are calculated in a DW approach using HXR central–field potential which uses an approximate exchange part of the Hartree–Fock non-local potential.

-MZ:

This code is base on the Z expansion technique (Safronova and Urnov, 1980) in which a MBPT is applied using screened hydrogenic orbitals. The perturbation expansion then contains powers of Z, the atomic number. The Breit interaction and QED are also treated in this expansion. Convergence is best with this method for highly ionized ions, and all members of an isoelectronic sequence are treated simultaneously.

IV. EXPERIMENTAL TECHNIQUES

Experiments have the potential to directly simulate in the laboratory the same processes observed remotely using telescopes, and so can provide the most accurate and appropriate data for use in interpreting astronomical observations. This cannot always be achieved, owing to practical challenges of achieving the densities or radiation environments occurring in some sources, and also because the scope of the data needs exceeds the available experimental resources. So in many cases we rely on experimental results as crucial checks on computations, while for many other quantities of interest experiments represent the only means to determine atomic quantities with sufficient accuracy for comparison with observations. This accuracy is needed in the case of line wavelengths or energy levels, where inaccurate values can lead to line misidentification or misleading redshifts or radial velocities. Experiments are also crucial for checks of the accuracy of DR rate coefficients at low temperature ($\sim 10^4$ K), owing to the fact that this process requires energy levels which are accurate to $\simeq$1 eV.

Experimental techniques have progressed at a rate comparable with the development of theoretical tools and computer platforms. Notable in their application to X-ray processes are the electron beam ion trap (EBIT), which has been described in detail by Beiersdorfer et al. (1990), and the storage rings described by Abrahamsson et al. (1993), Schippers et al. (1998), and Gwinner et al. (2001). These developments have been reviewed recently by Beiersdorfer (2003) and we will not repeat them here. In what follows we will describe, for each process, which experiments have contributed to the available database and what future developments might include.

V. LINE FINDING LISTS AND RELATED TABULATIONS

In order to organize the many different types and applications for atomic data, we divide them according to the level of computation required for their use. Atomic data which is simplest to use, in principle, includes things like line finding lists, which can be utilized with a minimum of detailed fitting or model calculation. Such tabulations are crucial to interpretation of datasets taken at high resolution. They allow a crude determination of the likely conditions in the gas under study, and may be able to address simple questions about element abundances and the likely range of plasma conditions. In addition, they are needed for successful application of the tools described in the later sections. These differ according to the physical excitation mechanism, and we discuss them separately.

A. Coronal Plasmas

Background

Coronal plasmas are those in which the ionization balance is determined primarily by collisions between ions and thermal electrons. They are common to situations involving mechanical heating, such as supernova remnants, stellar coronae and clusters of galaxies. For our purposes this includes objects such as supernova remnants which may not be in ionization equilibrium (Shklovsky, 1968). A feature of coronal plasmas which are in or near equilibrium is that the ionization balance adjusts so that the ionization potentials of the most abundant ions are comparable to the gas temperature. As a result, the electrons have sufficient energy to excite many atomic bound states, and so the spectra are generally rich in line emission. For coronal plasmas, the most useful low level tools are likely to be finding lists for emission lines. This typically includes resonance lines, lines which have the ionic ground term as the lowest level, since these are often the strongest and therefore most easily measured. It also includes satellite lines, which resemble resonance lines but with the addition of a spectator electron, since these can be used to infer temperature. Finally, it includes electric-dipole forbidden lines and lines connecting excited levels (subordinate lines) which are potential diagnostics of various plasma parameters such as electron density and the effects of cascades.

Prior to the launch of $Chandra$ and $XMM-Newton$ the need for accurate X-ray line wavelengths in astronomy was driven by the study of solar X-rays. This led to the development of line lists in close cooperation with laboratory spectroscopists. Early work originated from data taken by rocket flights and the OSO satellites. These include rocket observations of first solar detection of O^{6+} lines and others in the 14 – 22 Å range by Freeman and Jones (1970). Walker and Rugge (1970) presented observation of the forbidden lines in the He isosequence. Meekins et al. (1968) presented flare spectra from crystal spectrographs on OSO-4 in the wavelength ranges 0.5 – 3.9 Å and 1.0 – 8.5 Å. An analysis of the solar spectrum in the range 33 – 110 Å was presented by Widing and Sandlin (1968), and a rocket UV spectrum of the Sun from 60 to 385 Å was presented by Behring et al. (1972). These and other solar X-ray observations were reviewed by Culhane and Acton (1974). The launch of the second generation of solar instruments, the NRL spectroheliograph on Skylab and SMM led to lists by Widing et al. (1982) of solar flare lines in the 170-345 Å range, and by Phillips et al. (1982) of the flare lines in the 5.7 – 19 Å range. Lemen et al. (1984) published a compilation of observations of the iron K line from solar flares. A compilation of solar spectra of the K line of $Fe^{17+} - Fe^{23+}$ was performed by Seely et al. (1986), along with a comparison theoretical values calculated with the Z expansion technique. Doschek and Cowan (1984) compiled a line list based on observations of the Sun for the 10-200 Å range.

Motivated at least in part by solar observations, laboratory measurements of spectra using plasma machines or sparks provide spectra in the EUV and X-ray for many ions. Examples include study of S, Ar and Ca ions by Deutschman and House (1966, 1967). Feldman and Cohen (1968) published a list of lines from iron in the 10-18 Å range from both laboratory and solar flare spectra. Kunze et al. (1968) measured He-like line intensities from a theta pinch machine for C^{4+} and O^{6+} ions. Connerade et al. (1970) compared laboratory plasma measurements with Hartree-Fock structure calculations for Fe between 10 and 17 Å. Fawcett (1970) classified lines between 240 – 750 Å produced in a laser plasma, and Fawcett (1971) classified lines of Fe^{10+} –

Fe^{14+} from a theta pinch machine. Goldsmith et al. (1972) classified Li-like spectra of K - Mn in the EUV. Fawcett and Hayes (1972) identified Ni^{10+} – Ni^{16+} and Co^{9+} – Co^{16+} $3s-3p$ and $3p-3d$ lines from laboratory spectra. Fawcett et al. (1974) made *ab initio* calculations of $2p-3d$ line wavelengths and oscillator strengths in Fe^{18+} - Fe^{23+}, and compared the results with experimental values. Goldsmith et al. (1973) classified $2s-2p$ transitions in laboratory spectra of Ca^{16+} and Ti^{18+}. Feldman et al. (1973) classified transitions of Fe^{17+} and Fe^{18+} observed in laser produced plasmas. Fawcett and Hayes (1973) classified n=2 – 3 transitions from S^{9+} – S^{13+} and Ar^{11+} – Ar^{15+}. Other examples include study of Fe by Fawcett et al. (1972) and by Boiko et al. (1978). Comparison of theoretical and experimental n=2 energy levels for the C, N, Li Be, O and F isoelectronic sequences was carried out by Edlen (1983, 1984, 1985). Identifications of EUV lines of Fe^{9+} – Fe^{23+} based on solar and laboratory data were performed by Jupen (1993).

Recent Developments

A commonly accepted standard set of line lists for all applications have been compiled from laboratory spectra and energy levels for various elements by NIST. These include compilations for: Mg (Kaufman and Martin, 1991a) Al (Kaufman and Martin, 1991b; Martin and Zalubas, 1979), Si (Martin and Zalubas, 1983), and S (Kaufman and Martin, 1993; Martin et al., 1990). Collections of energy levels and transition probabilities for iron were made by Sugar and Corliss (1979), Corliss and Sugar (1982), Sugar and Corliss (1985) and by Shirai et al. (1990). The data are defined as NIST Standard Reference Data, implying known or estimated accuracy. An exception is the energy level data compiled by Kelly (1987) for some ions, which also includes some inner shell energies. Together with older data on spectra of light ions (Wiese et al., 1966, 1996) this has been incorporated into the NIST spectroscopic database (Fuhr et al., 1999) at: http://physics.nist.gov/PhysRefData/ASD/index.html. The accuracies of the transition strengths are evaluated according to the NIST convention: A=3%, B=10%, C=25%,D=50%,E= 50%. Many of the lines in the X-ray band have ratings of C or below. A consequence of the restriction to critically evaluated data is that the data included in this database lag behind the production of data available for such a compilation. This does not greatly affect the selection or accuracy of data for strong lines in well studied wavelength bands, but it does result in incompleteness of some line lists for use in X-ray astronomy.

Recent work using the EBIT instrument at Lawrence Livermore National Laboratory (LLNL) represent the beginning of an effort to fill the need for line wavelengths which are both comprehensive and sufficiently accurate to be used in fitting high resolution space astronomy data. Brown et al. (2001a) have measured the spectrum of ions of Fe^{16+} – Fe^{23+} in the 10 – 20 Å wavelength range. Lepson et al. (2003) have measured the spectra of ions of Ar in the range 20 – 50 Å, and Lepson et al. (2005a,b) summarize measurements for Ne-like through Li-like Ar, S and Si.

Using many-body perturbation theory approaches, Gu (2005) has calculated the level energies of excited L shell complexes in iron and nickel ions. Comparison with experimental results shows that the line wavelengths are generally in agreement to within ≤10 mÅ. Energy levels with comparable accuracy have been obtained by Kotochigova et al. (2005) also using a many-body perturbation method. This is a significant improvement over that obtainable with *ab initio* calculations using standard configuration interaction methods, and is adequate for many purposes for fitting to observed spectra using *Chandra* and $XMM-Newton$.

Attempts to update and extend the NIST database for use in analyzing *Chandra* data include the lists for Ne, Mg, Si, S in the 10 – 30 Å wavelength range by Podobedova et al. (2002). Lists specific to the X-ray band are given as part of the CHIANTI database (Dere et al., 1997; Landi and Bhatia, 2005a; Landi et al., 1999). Other compilations widely used in analyzing X-ray and EUV spectra are APEC (Smith et al., 2001) and MEKAL (Mewe et al., 1995b). These generally represent compilations from diverse sources, including both experimental and theoretical work, in order to be sufficiently comprehensive to be used in analyzing *Chandra* and $XMM-Newton$ data. Effort has been devoted to updating these to the accuracy required for interpreting high resolution observations, since most of these compilations were begun before the launch of these instruments. These updates are available as part of the corresponding data analysis packages in widespread use for analyzing X-ray spectral data (cf. http://heasarc.gsfc.nasa.gov/docs/software/lheasoft/, http://cxc.harvard.edu/ciao/).

B. Photoionized Plasmas

Background

In astrophysical sources containing a strong source of ionizing continuum radiation and where mechanical heating is negligible, the ionization balance in the gas will be determined by photoionization. Electron-ion collisions play a role in recombination and cooling the gas, and in equilibrium the temperature is determined by balancing the heating by photoelectrons with collisional cooling (Tarter et al., 1969). A key distinction between photoionized and coronal plasmas is that the electron temperature in a photoionized plasma is $\sim 5-10\%$ of the ionization potential of the dominant ions. Line emission is due to recombination, inner shell fluorescence, or collisional excitation of low-lying levels. Emission line equivalent widths are defined as the ratio of the line flux to the average continuum level in the vicinity of the line. These are generally smaller in photoionized plasmas than for coronal plasmas, owing partly to the contribution from the continuum source and also because of the reduced energy available from electron collisions.

The interpretation of photoionized plasmas shares with coronal plasmas the need for line lists. Photoionization by a radiation field which is non-thermal can lead to a situation where there is a substantial flux of ionizing photons with energies far above the first ionization potential of the abundant ions. This is in contrast to the typical situation in coronal plasmas. It greatly increases the importance of inner shells in opacity and ionization. As a result, spectra can have strong fluorescence line emission and inner shell lines seen in absorption as the source of photoionization is viewed through the transmitted spectrum of intervening gas. Fluorescence emission and inner shell absorption are unique X-ray signatures which can be observed from gas under a wide range of conditions, including neutral or near-neutral gas. Few inner shell transitions, other than satellite lines excited by DR, are included in the compilations of lines for coronal plasmas. Theoretical wavelengths for K lines were calculated by House (1969) using a single configuration Hartree-Fock method. Kaastra and Mewe (1993) compiled wavelengths and branching ratios for many inner shell lines based on energy levels of Lotz (1967). A compilation of solar spectra of the K lines of Fe^{17+} – Fe^{23+} was performed by Seely et al. (1986), along with a comparison with theoretical values calculated with the Z expansion technique. Shirai et al. (2000) compiled experimental energy levels for Fe ions.

Recent Developments

Wavelengths and oscillator strengths of inner shell n=2 to n=3 transitions in iron ions (Fe^{0} – Fe^{15+}) have been calculated by Behar et al. (2001a) using HULLAC. These features form a broad unresolved transition array (UTA) near 16 – 17 Å. Calculations of transition probabilities for a subset of these lines, using CIV3 and an extensive selection of configurations in the CI expansion was carried out by Kisielius et al. (2003). Extensive calculations of the UTA transitions, including transitions to n=4 states, have been carried out by Dubau et al. (2003) using AUTOLSJ. Wavelengths, A-values and Auger rate coefficients for K lines of all the ions of iron have been published by Palmeri et al. (2002), Palmeri et al. (2003a), Palmeri et al. (2003b) and Bautista et al. (2003). These represent a compilation of experimental results where available, supplemented by calculations using AUTOSTRUCTURE and HFR for the lower ionization states.

An additional observable which is associated primarily with photoionized gases is the photon spectrum due to radiative recombination (RR). The continuum radiation associated with radiative recombination (RRC) is emitted as a feature at the threshold energy which has an exponential shape, i.e. $j(\varepsilon) \propto \exp(-(\varepsilon - \varepsilon_{Th})/kT_e)$, above threshold ε_{th}, with a width proportional to the electron temperature T_e. RRC features in coronal plasmas are broadened by the higher characteristic temperature and therefore are not easily observable. There is no published database of experimental RRC threshold energies as such, although energy level databases such as the NIST database can be used to derive them.

Lists of resonance lines, which can be applied to spectra seen in absorption in front of a strong continuum source, were compiled by Verner, Barthel and Tytler (1994). This includes lines from all wavelengths longward of the He^{+} Lyman limit at 227.838 Å and all the ion states of all elements from hydrogen to Bismuth (Z=83) and includes experimental and critically evaluated wavelengths. At shorter wavelengths, Verner, Verner and Ferland (1996) compiled experimental and critically evaluated energy level and derived wavelengths for lines originating from ground-term multiplets in the spectral region 1–200 Å.

Ab initio wavelengths for some K lines of medium-Z elements have been calculated by Behar and Netzer (2002) using HULLAC. Comparison with *Chandra* spectra suggests a likely accuracy of $\geq$ 20 mÅ. Wavelengths for the K lines of oxygen have been calculated by Pradhan (2000) and Pradhan et al. (2003) using BPRM. Using a multi-platform approach (AUTOSTRUCTURE, HFR and BPRM), Garcia et al. (2005) calculated the atomic data relevant to the photoabsorption near the K-edge of all the oxygen ions. The accuracy of the K line wavelengths was estimated to be better than 20 mÅ by comparison to the available experimental data. Experimental measurements of inner shell lines include K lines of Fe^{16+} – Fe^{23+} measured from tokamak plasmas by Beiersdorfer et al. (1993), measurements of K lines of Fe^{9+} –Fe^{15+} by Decaux et al. (1997) using EBIT, and the EBIT measurements of the K lines from O^{4+} and O^{5+} by Schmidt et al. (2004). Gu et al. (2005) combined EBIT measurements of the K lines of oxygen ions with FAC calculations of population kinetics to provide line wavelengths and identifications with accuracies ranging from 5 to 20 mÅ . Wavelengths of $n = 1 - 2$ inner-shell transitions in the Be-like up to F-like ions of magnesium, aluminum, silicon, phosphorus and sulfur were measured in a laser-produced plasma and were interpreted using the Z expansion technique (Faenov et al., 1994). Biemont et al. (2000) observed the Kα lines of Ar^{9+}–Ar^{16+} in a plasma focus discharge and modeled the spectra using HFR and MCDF. K shell binding energies and line wavelengths can also be derived from Auger electron spectroscopy. Examples of this are given by Bruch et al. (1979, 1987, 1992) and Lin et al. (2001a,b). Experimental techniques and results have been reviewed by Stolterfoht (1987).

VI. DISCRETE DIAGNOSTICS

Beyond the detection and identification of spectral features, physical parameters of the gas can be derived from the shapes and strengths of the features. Line ratios can be used to infer density or temperature. These require the accurate measurement of a subset of lines or spectral features, and can only be applied in situations where the measurement is clean enough to make these features unambiguous. If so, they serve to allow accurate determination of some physical quantities describing the gas under study often without requiring extensive numerical calculation or use of spectral deconvolution.

A. Coronal Plasmas

Use of line ratios has been extensively applied to coronal plasmas, where they have been used to infer density, temperature, elemental abundance, departures from ionization equilibrium, and non-Maxwellian electron velocity distribution. Density diagnostics rely on the competition between collisions and radiative transitions for two or more lines with greatly differing radiative decay rates. Ratios of lines with differing excitation energies provide temperature diagnostics. Examples of the use of these diagnostics in the context of classical nebulae such as H II regions and planetary nebulae are discussed in detail by Osterbrock and Ferland (2006). In the Sun the conditions in X-ray gas vary both in time and with position, and the use of discrete diagnostics provides a means to study a limited spatial region, corresponding to the atmospheric zone where a given set of lines is emitted most efficiently. This may provide insight which is easier to interpret for objects which are clearly inhomogeneous, than global modeling, which involves modeling the entire atmosphere at once (Mariska, 1993; Zirin, 1988). Use of such diagnostics must be applied with care, however, since there may be neighboring regions which may have lower emissivity but larger emission measure and which can thereby contaminate the diagnostic line measurements.

1. He-like Diagnostics

Background

He-like ions are stable against ionization over a comparatively wide range of conditions, and they emit strong n=1 – 2 lines which are relatively free from confusion with other lines. The three characteristic lines are the resonance r ($1s^2\ ^1S_0 - 1s2p\ ^1P_1$), intercombination i ($1s^2\ ^1S_0 - 1s2p\ ^3P_{2,1}$), and forbidden f ($1s^2\ ^1S_0 - 1s2s\ ^3S_1$), forming the “triplet” lines. The i line actually consists of two components corresponding to the two different total angular momentum states in the upper level, but these are blended at the resolution of all available astronomical X-ray observations. The relative strengths of these lines are studied through conventional line ratios R=f/i and G=(f+i)/r. The ratio R is sensitive to gas density via collisions or the effects of a strong UV radiation field driving the transition $1s2s\ ^3S_1 - 1s2p\ ^3P_{2,1}$. The ratio G is sensitive to temperature owing to the fact that the excitation energies for the ^3P and ^3S levels are lower that for the ^1P levels. The G ratio is also affected strongly by recombination, which increases the populations of the ^3S and ^3P upper levels relative to the ^1P level. Radiative excitation of the ^1P from ground can have the opposite effect on G.

The importance of the He-like lines as diagnostics was pointed out by Gabriel and Jordan (1969), who discussed the density dependence of R and made a density determination for the solar corona. Blumenthal et al. (1972) discussed the processes populating the upper levels of these lines and showed that R is also temperature dependent. The dependence of G and R on temperature and density for many elements, including the effects of satellite lines from DR into the Li-like ion, resonances and inner shell ionization for coronal equilibrium conditions were calculated by Pradhan and Shull (1981). Mewe and Schrijver (1975) calculated population densities of all levels with principal quantum number $n = 2$ in several He-like ions with Z ranging from 6 to 20. Calculation of level populations including the effects of photoexcitation within the $n = 2$ manifold were performed by Mewe and Schrijver (1978a). Mewe and Schrijver (1978b) examined the effects of time-dependent ionization appropriate to solar flares. Pradhan (1985) showed that recombination drives up the value of G in a plasma which is recombination dominated, i.e. photoionized, owing to the fact that RR preferentially populates the triplet states.

Recent Developments

Diagnostic use of He-like line ratios depends on rate coefficients and cross sections populating the n=2 levels, and on the line wavelengths needed for accurate identifications. Other rate coefficients needed for complete modeling of He-like diagnostics include radiative rate coefficients for the non-dipole allowed transitions, which have been calculated by Lin et al. (1977), and DR satellite line intensities, which have been calculated by Safronova, Vasilyev and Smith (2001) and others as discussed in section VII.A.2. Theoretical wavelengths for He-like ions up to $Z = 100$ using non-relativistic variational calculations were calculated by Drake (1988). Rate coefficients for 2 photon decay of metastable He-like ions were calculated by Derevianko and Johnson (1997). R-matrix calculations of transition probabilities for He-like ions were presented by Fernley, Taylor and Seaton (1987) and have been incorporated into TOPbase (Cunto and Mendoza, 1992). Wavelengths for the He-like lines in solar flares have been measured for the $1s2s\ ^3S_1 - 1s2p\ ^3P_{0,2}$ lines in He-like Ne, Mg, Na and Si to within 20-30 mÅ using the *SOHO* SUMER instrument (Curdt et al., 2000). Lifetime measurements have been carried out for the excited states of many ions, not just for the He-like isosequence, and many of these are reviewed by Träbert (2002). Experiments using ion traps can measure lifetimes for forbidden and intercombination transitions, and these provide an important check on transition probabilities for use in modeling He-like lines.

The rate coefficients for collisional excitation of

He-like ions were reviewed by Dubau (1994) and Kato and Nakazaki (1989), who showed the importance of resonances in the $1s2s$ manifold for high Z elements, i.e., Ca and Fe. These have been taken into account in the modified relativistic DW calculations of Zhang and Sampson (1987). Adoption of these rate coefficients is recommended for high Z elements, and R-matrix calculations for low Z elements. These rate coefficients, together with radiative recombination coefficients from Pequignot et al. (1991), calculations of f-values and energy levels from Fernley, Taylor and Seaton (1987) and DR satellite calculations of Bely-Dubau et al. (1982a,b) were used by Porquet and Dubau (2000) to model He-like line ratios, including a discussion of recombining plasma compared with coronal plasma. Bautista and Kallman (2000) calculated the line emissivities and level populations using similar collisional rate coefficients plus a recombination cascade treatment, including the effects of 3-body recombination and suppression of DR at high density. The calculations by Porquet and Dubau (2000) and Bautista and Kallman (2000) provide consistent physically reasonable values for density when applied to *Chandra* spectra from both recombination and collision-dominated objects. Harra-Murnion et al. (1996) calculated rate coefficients for the emission of the lines from S^{14+}, bench marked these against observations of tokamaks, and then used them to set limits on the density in solar flares.

2. Dielectronic Satellite Lines

Lines emitted during dielectronic recombination (DR) are in principle sensitive temperature diagnostics because the emission process involves collisional excitation of a recombining ion, so the rate depends on the fraction of electrons capable of surmounting the core excitation energy barrier. DR is a two-step recombination process that begins when a free electron approaches an ion, collisionally excites a bound electron of the ion, and is simultaneously captured. This process is discussed in more detail in Section VII.A.2; here we limit ourselves to discussion of satellite emission. Satellite lines are emitted during the stabilization of the doubly excited state, when the core electrons relax to their ground level in the presence of the additional recombined electron. This spectator electron is responsible for shifting the line wavelength away from the wavelength of the resonance line in the parent ion. Detection of satellite lines requires spectral resolution $\varepsilon/\Delta\varepsilon \geq 500$. Interpretation of satellite intensities is simplified by the lack of ambiguity about the excitation mechanism, although satellites can also be emitted following inner shell collisional or radiative excitation. Even if they are not resolved, satellites can contribute significantly to the intensity of the adjacent resonance line. Thus they can affect the use of discrete diagnostics, such as the H-like diagnostics, and must be taken into account for accurate treatment of discrete diagnostics.

A basic description of the calculation of intensities of DR satellites and their diagnostic value was first presented by Gabriel (1972) and by Gabriel and Paget (1972). Most DR proceeds through high n ($n > 50$) for ions in isoelectronic sequences beyond H and He, and satellites from this are indistinguishable from resonance lines. For satellites, only states with $n < 4$ produce lines which can be resolved from the adjacent resonance line. The low n satellites require different assumptions to calculate compared with the high-n states, and the importance of low-n states increases with Z. Gabriel (1972) showed that satellites are temperature diagnostics, largely independent of ionization balance. The satellite intensity depends on Z^4, and so they are relatively unimportant for $Z< 10$. The formalism for treating satellite intensities makes the assumption of LTE between satellite upper level and the relevant autoionizing continuum. The satellite intensity then depends on energy separation and branching ratio for line emission. The resonance line intensity must also be corrected for unresolved satellites, and satellite intensities must include the effects of direct excitation of inner shells in the adjacent ion. Enhancement of resonance line intensities by unresolved satellites has been treated by Ansari and Alam (1975). Gabriel and Phillips (1979) showed that satellites can be a diagnostic of non-Maxwellian electron energy distributions. This is because of the relative importance of inner shell excitation to DR. The resonance line can be excited by all electrons with energies greater than threshold, while DR is a resonant process, selectively excited by electrons at an energy corresponding to the particular resonance. Thus, with 2 or more measured satellites plus the resonance line it is possible to determine if the excitation rate is consistent with a Maxwellian electron velocity distribution, and to constrain the form of the distribution if not.

Calculations of satellite intensities using non-relativistic Hartree-Fock orbitals were reported in a series of papers by Karim and Bhalla. Bhalla et al. (1975) calculated intensity factors for DR satellite spectra for highly charged He-like ions. This includes more accurate calculations of autoionization rate coefficients and more accurate calculations of inner shell collisional excitation rate coefficients than the previous work by Gabriel (1972). This results in smaller emissivities for lines arising from $1s2p(^1P)2s^2P$ levels. These calculations used non-relativistic Hartree-Fock-Slater orbitals in LS coupling with CI and exchange. Karim and Bhalla (1986) and Bhalla et al. (1986b) used this technique to calculate intensity factors for the satellite to the Lyα line of Ne^{9+}. Karim and Bhalla (1988b) calculated DR for selected hydrogen like ions (Z=10, 14, 18, 20, 22, 26, and 28) using the Hartree-Fock-Slater orbitals. The effects of configuration interaction and spin-orbit coupling were included for $n \leq 4$. Configuration average rate coefficients were used to calculate DR rate coefficients for $n = 5$, and $1/n^3$ scaling was assumed for all higher states. This shows that the maximum DR rate decreases with Z and the position of maximum shifts to higher temperature with increasing Z. At lower temperatures DR rate coefficients for light elements are greater than those for heavy elements while at higher temperature the trend is reversed. Satellite line intensities were compared with calculations using Thomas-Fermi (Dubau et al., 1981) and Z-expansion (Bitter et al., 1984), and ∼10% difference is found. Karim and Bhalla (1988b) found an ∼40% difference in the maximum DR rate for Fe compared with Dubau et al. (1981), possibly due to neglect of some high nl states ($2lnl'$, $n>4$). Karim and Bhalla (1988c) calculated X-ray and Auger transition rate coefficients from doubly excited states of He-like ions for Z=10, 14, 18, 20, 22, 24, 26, and 28, along with intensity factors of satellites originating from DR of ground-state hydrogenic ions via the autoionizing states. Bhalla et al. (1988) calculated satellite intensity factors for H-like Fe^{25+}, showing good agreement with Thomas-Fermi calculations for $n=2$, but discrepancies for $n>2$. DR satellite spectra for high-lying resonance states of H-like Fe and Ni were calculated by Karim and Bhalla (1995), and for H-like Si, Ca, and Fe (Karim et al., 1992). DR rate coefficient for some selected ions in the He isoelectronic sequence were calculated by Karim and Bhalla (1989b) and Karim and Bhalla (1989a). These authors presented a comparison with other calculations, including that of Nilsen (1986) which employs relativistic wave functions but which uses rate coefficients which are extrapolated for levels above $n=4$. They argued that accurate treatment of the high-n levels is important for ions with Z<20. Effects of radiative cascades on H-like DR satellite spectra were studied by Karim and Bhalla (1988a), in an attempt to address conflicting claims by Gau et al. (1980) and Dubau et al. (1981). Possible systematic discrepancies are discussed between results obtained using Hartree-Slater, Thomas-Fermi and Z-expansion techniques. Calculations of DR satellites arising from levels with $n>4$ for He-like Cr and Ni were presented by Karim and Bhalla (1990). The validity of the commonly used $1/n^3$ scaling for high-n satellites was discussed, and it was pointed out that high-n satellites are likely to be unresolvable, but can appreciably affect total line intensity and should be taken into account. The dependence of DR satellite intensity factors on n for $1s\epsilon l \rightarrow 2l'nl" \rightarrow 1snl"$ in selected hydrogen-like ions was studied by (Karim et al., 1991), and for $1s^2\epsilon l \rightarrow 1s2pnl \rightarrow 1s^2nl$ in He-like ions by Karim and Bhalla (1991).

Calculations of satellite intensities using wave functions based on a Thomas-Fermi potential were carried out by Dubau and coworkers. Dubau et al. (1980) calculated the emission from DR satellites to the Mg^{11+} resonance lines including CI, intermediate coupling and wave functions calculated with SUPERSTRUCTURE. This showed that the relative importance of satellites increases up to $n=4$, and decreases for higher n. Also included were the cascade contribution to the lower n satellites. The results are consistent with previous work of Vainshtein and Safranova (1978) for wavelengths and radiative transition probabilities, but differ systematically for the autoionization probabilities. Dubau and Volonte (1980) reviewed calculations and solar observations of satellite line intensities. Volonte et al. (1987) calculated DR satellites to Ca^{19+} Lyα. This resolved a problem dating from the work of Dubau et al. (1981) and Blanchet et al. (1985) in which the extrapolation of the contribution of the low-n satellites does not properly converge to the resonance line for $n>4$, and may explain why the calculated intensity for Lyα was lower than observed from solar flares in Dubau et al. (1981). Bely-Dubau et al. (1982a) calculated rate coefficients for production of satellite lines by DR and inner-shell excitation in Ca, as well as the production of He-like spectra by excitation, radiative and DR and through cascades. Bely-Dubau et al. (1982b) calculated n=$1-2$ spectra of Fe^{23+} and Fe^{24+} due to inner shell direct excitation, cascade, RR and DR. The results were compared with solar spectra. Bely-Dubau et al. (1983) compared results of these calculations with spectra from the PLT tokamak. The Fe^{24+} DR rate coefficient associated with the $1s-2p$ core excitation was measured for temperatures in the range $0.9-3$ keV and good agreement was obtained with contemporaneous calculations.

The use of DR satellites as temperature diagnostics in the solar corona was discussed for iron by Bely-Dubau et al. (1979a), Bely-Dubau et al. (1979b) and for Ca by Bely-Dubau et al. (1982a). Doschek and Feldman (1987) discussed temperature determinations from solar flares. These authors presented model temperature distributions and studied their effect on the satellite line strengths and on the temperatures which would be inferred from them based on available calculations. A review of the X-ray emission from solar flares was provided by Doschek (1972), who also discussed temperature determinations using H/He like ratios for S, Si, Mg and satellites due to DR onto He-like ions. The He-like rate coefficients for Mg^{10+} were calculated by Keenan et al. (1986), who showed that the $1s-3p$ line, when compared with the n=1–2 lines, can be used as a temperature diagnostic in solar flares and active regions.

Phillips et al. (1983) used HFR to calculate inner shell spectra of Fe^{18+} - Fe^{21+} under conditions of solar flares. The excitation was found to be primarily due to DR rather than direct excitation. Chen (1986a), Nilsen (1987) and Nilsen (1988) also carried out calculations of satellite spectra of H- and He-like ions using relativistic multi-configuration wave functions. Calculations of DR coefficients and satellite spectra for He-like ions was carried out by Vainshtein and Safranova (1978) and by Safranova et al. (2000), using the Z-expansion technique and including Breit-Pauli operators. The systematic dependence with Z is examined and compared with previous work. An extensive discussion and comparison of different computational methods for satellite spectra for iron was presented by Kato et al. (1997).

Calculations of satellite line wavelengths and of the cross section for satellite emission by DR have been benchmarked by the EBIT experiment. Beiersdorfer et al. (1992) measured the satellite spectrum of Fe^{24+} and Fe^{23+} in order to measure the cross section for DR capture and stabilization. They find reasonably close agreement with the theoretical calculations of Vainshtein and Safranova (1978), Bely-Dubau et al. (1979a), and Bely-Dubau et al. (1982a). Gu et al. (2001) measured the EBIT spectra for the other ions of iron Fe^{20+} – Fe^{23+} over a wide range of incident electron energies, and showed that unresolved DR satellites can contribute as much as 15% to the intensities of strong resonance lines. Satellite spectra of He-like Fe and Ni obtained from a tokamak plasma were studied by Smith et al. (1993). Experimental measurements of satellite lines from He-like ions of Ne and heavier elements using EBIT were carried out by Wargelin et al. (2001), Smith et al. (1996) and Smith et al. (2000b).

3. Other Diagnostics

Ions in the Be – Ne isoelectronic sequences have ground terms with many levels which can be mixed collisionally at high density. When this occurs it opens channels for emission in X-ray lines whose strength is therefore a density diagnostic. This occurs for densities greater than $\sim 10^{13}$ cm^{-3} for lines in the $2s^22p^k - 2s2p^{k+1}$ transition array of the ions of iron Fe^{17+} – Fe^{20+} in the in the 80 – 140 Å range (Stratton et al., 1984). Mauche (2005) has modeled the effect of the ground term mixing on lines in the 10 – 20 Å wavelength range from these ions. The lines from the ions Fe^{15+}, Fe^{16+} and Fe^{17+} in the 14 – 19 Å range have been modeled by Cornille et al. (1994b). They calculated the structure, radiative and collisional rate coefficients using AUTOLSJ. These can be used to identify lines in the spectrum of solar active regions. The intensities of the Fe^{15+} DR satellites to Fe^{16+} at 15 Å and of the lines of Fe^{17+} at 14.2 and 16 Å are shown to be sensitive to temperature.

Calculations of level populations affecting emission in strong UV, EUV and X-ray lines demonstrating density dependence due to the collisional mixing of levels in the ground configuration, have been carried out in a series of papers by Bhatia and coworkers: Si^{6+}(Bhatia and Landi, 2003a), Si^{7+}(Bhatia and Landi, 2003d), S^{8+}(Bhatia and Landi, 2003c), S^{9+}(Bhatia and Landi, 2003b), S^{10+}(Bhatia et al., 1987), Ca^{14+}(Bhatia and Mason, 1986b), Ca^{16+}(Bhatia and Mason, 1983) , Fe^{9+}(Bhatia and Doschek, 1995b), Fe^{10+}(Bhatia and Doschek, 1996; Bhatia et al., 2002), Fe^{13+}(Bhatia and Doschek, 1993a; Bhatia et al., 1994), Fe^{14+}(Bhatia and Kastner, 1980; Bhatia and Mason, 1997), Fe^{16+}(Bhatia and Doschek, 2003), Fe^{18+}(Bhatia et al., 1989b), Fe^{19+}(Bhatia and Mason, 1980a; Mason and Bhatia, 1983), Fe^{20+}(Mason et al., 1979), Fe^{21+}(Mason and Storey, 1980), Fe^{22+}(Bhatia and Mason, 1981, 1986a), Ni^{12+}(Bhatia and Doschek, 1998), Ni^{15+}(Bhatia and Doschek, 1999), Ni^{16+}(Bhatia and Kastner, 1980), and Ni^{20+}(Bhatia et al., 2003). These include energy levels based on CI calculations using SUPERSTRUCTURE, transition probabilities and collision strengths in the DW approximation with the addition of a correction calculated in the Coulomb-Bethe approximation (Burgess and Sheorey, 1974) to take into account high partial waves. These references are only a representative sample of available work on such density diagnostics. Other references can be found in the extensive bibliographic tabulations contained in the AMBDAS (http://www-amdis.iaea.org/AMBDAS/) and ORNL (http://www-cfadc.phy.ornl.gov/bibliography/search.html) databases. Other relevant data for application to fusion plasmas is collected in the ALADDIN (http://www-amdis.iaea.org/ALADDIN/) database.

4. Fe^{16+}

The strong lines of Fe^{16+} near 15 and 17 Å are among the most prominent in the X-ray spectra of many coronal sources. The relative strengths of the $2p^6 - 2p^53s$ lines near 17 Å the $2p^6 - 2p^53d$ lines near 15 Å and the $2p^6 - 2p^54d$ lines near 12 Å are temperature sensitive owing to the differing rate coefficients for electron impact ionization (EII) (Raymond and Smith, 1986). The ratio of the lines $2p^6 - 2p^53d$ lines near 15 Å and the $2p^6 - 2p^53s$ lines at 17 Å can also be an indicator of recombination (Liedahl et al., 1995).

Calculation of transition probabilities in intermediate coupling with CI have been carried out by Loulergue (1971). The wavelengths of the 3s-3p subordinate lines for several Ne-like ions have been calculated by Kastner (1983). Bhatia and Kastner (1985) discussed the use of the the $2p^6\ ^1S_0 - 2p^53s\ ^3P_2$ forbidden line as a density diagnostic. They also presented observability diagrams which serve as a convenient overview of the known and unobserved lines, both for Fe^{16+} and for other ions in the neon isoelectronic sequence. Cross sections for excitation of the Fe^{16+} lines have been calculated by Mann (1983), Hagelstein and Jung (1987), Zhang and Sampson (1989) and for Fe^{15+} by Zhang et al. (1989). The lines have been modeled by Loulergue and Nussbaumer (1973, 1975), Smith et al. (1985), Bhatia and Doschek (1992), Cornille et al. (1992, 1994a) and Phillips et al. (1997). Calculations of excitation for Fe^{14+} – Fe^{16+} were reviewed by Badnell (1994). Cross sections for excitation of the Fe^{16+} lines have been calculated by Gupta, Deb and Msezane (2000) and Chen, Pradhan and Eissner (2003)

It has long been known that the ratios of the $2p^6 - 2p^53d$ components observed from the sun (Parkinson, 1973, 1975) differ from calculations. This was emphasized by Beiersdorfer et al. (2004), who pointed out that calculations of Fe^{16+} excitation cross sections differ systematically from the ensemble of laboratory and astrophysical data. Earlier suggested explanations for this discrepancy include the effects of cascades (Goldstein et al., 1989), inner shell ionization of Fe^{15+} (Bautista, 2000) and optical depth effects (Bhatia and Kastner, 1985). The effects of cascades were further explored by Loch et al. (2006), who point out the importance of correcting experimental measurements for polarization. Smith et al. (1985) have shown that the Fe^{15+} DR satellites, such as the 15.226 Å satellite to the Fe^{16+} $2p^6\ ^1S_0 - 2p^5 3d\ ^3D_1$ line at 15.261 Å can be comparable to the intensity of the Fe^{16+} λ 15.01 Å lines.

The strongest lines from Fe^{16+} under coronal conditions are the $2p^6\ ^1S_0 - 2p^5 3d ^1P_1$ resonance and $2p^6\ ^1S_0 - 2p^5 3d\ ^3D_1$ intercombination lines at 15.01 and 15.26 Å. The relative strengths are not highly sensitive to temperature or density (Loulergue and Nussbaumer, 1973), and they have been observed and modeled extensively (Fawcett et al., 1979). The ratio of the strengths of these two features, as measured in the laboratory (Brown et al., 1998) is found to be independent of conditions and excitation process, including radiative cascades, resonance excitation, and blends with unresolved DR satellites. The laboratory ratio is measured to be 3.04, and is greater than that measured in many astrophysical sources. EBIT measurements and modeling of the lines of Ni^{19+} (Gu et al., 2004) confirm the results for Fe^{17+}.

5. Optical Depth Diagnostics

Multiple resonance scatterings will affect conveniently measured ratios of lines with differing thermalization properties. Thermalization depends on the line optical depth and on the probabilities of destruction or conversion per scattering. Such ratios, whose excitation is relatively insensitive to other conditions, include the relative strengths of the Fe^{16+} 15 Å lines. The effects of optical depth on the ratios of X-Ray and EUV lines of this ion have been studied by Bhatia and Kastner (1999). Although optical depths have been suggested as the origin of ratios of the 15 Å lines which are discrepant with calculations, the discrepancy now appears to be affected by blending and possibly with omission of important physical effects in the calculations (Beiersdorfer et al., 2004). Other line ratios which are affected by optical depth include the Lyman series of hydrogenic ions, and the G ratio of He-like $n = 1-2$ lines. In both of these cases the ratio in question also depends on other factors such as density or temperature, and this complicates diagnostic measurement of optical depth using these lines.

6. Abundance Diagnostics

Elemental abundances cannot be directly derived from line intensity ratios, owing to the dependence of emissivities on temperature and density. Line equivalent widths have been used to derive abundances in coronal plasmas, since the continuum in many spectral regions is dominated by electron-proton bremsstrahlung, and so is only weakly dependent on abundances of metals (Sylwester et al., 1998). This requires that the temperature be derived from measurement of the continuum shape, for example, since both the line and continuum emissivities depend on temperature. Abundances can also be derived through full spectral fitting, as described in the next section.

7. Non-equilibrium Diagnostics

Departure from ionization equilibrium shifts the ionization balance, at a given electron temperature, away from the equilibrium value. This has the effect of increasing the importance of processes associated with adjacent ions in emitting lines from a given species, such as inner shell ionization (excitation-autoionization or direct ionization) when the ionization balance shifts to the low side, or recombination (DR or RR) when the balance shifts to the high side. An example was studied by Mewe and Schrijver (1978b) for He-like lines, who showed that non-equilibrium effects can enhance the inner shell contribution from ionization of the Li-like species, if the temperature is high and the ionization is low, or the recombination from the H-like species if the temperature is low and the ionization is high. Oelgoetz and Pradhan (2004) studied time-dependent recombination dominated plasmas. Oelgoetz and Pradhan (2001) showed that the DR satellites dominate the emission of the Fe^{24+} at temperatures below that of maximum abundance in collisional ionization equilibrium. Owing to their extreme temperature sensitivity, the satellites are excellent spectral diagnostics for such temperatures in photoionized, collisional or hybrid plasmas, whereas the forbidden, intercombination and resonance lines of Fe^{24+} are not. Similar effects occur with Fe^{16+} (Bautista, 2000), and other ions. The importance of iron K lines as diagnostics of non-equilibrium, and detailed modeling of the excitation and emission of these lines, was discussed by Decaux et al. (2003).

8. Non-Maxwellian Diagnostics

Gabriel and Phillips (1979) first suggested the use of DR satellites as indicators of non-thermal electron velocities. They showed that the intensities of two satellite lines $1s^2nl - 1s2pnl$ with $n=$ 2,3 relative to the Fe^{24+} resonance line $1s^2 - 1s2p$ can be described by a single temperature only if the emitting plasma has a

Maxwellian distribution of electrons. This effect was detected in the laboratory by Bartiromo et al. (1985) and in solar flares by Seely et al. (1987). The effects of non-Maxwellian velocity distributions on the coronal ionization balance have been examined by Dzifcakova (1992) and by Dzifcakova (1998), following on work by Owocki and Scudder (1983), who showed that the oxygen ionization balance in the solar corona is more sensitive to non-thermal effects than is iron, and that these effects can cause apparent differences in temperatures inferred from the two elements. The effects of non-Maxwellian velocity distributions on the He-like line ratios have been examined by Dzifcakova and Kulinova (2002). They parameterize the electron velocity distribution according to the formulation of Owocki and Scudder (1983), and show that at large departures from Maxwellian the value of G can greatly exceed that of an equilibrium coronal plasma at the same value of R. This corresponds to the appearance of greater temperature in the G ratio, for a given value of R.

B. Photoionized

RRCs have an exponential shape with characteristic width equal to the electron temperature, and only in photoionized plasmas are they likely to be narrow enough to be clearly detected. This was pointed out by Liedahl et al. (1995), and has been used to infer the temperature in X-ray binaries (Wojdowski et al., 2001), and in Seyfert 2 galaxies (Brinkman et al., 2002; Kinkhabwala et al., 2002; Sako et al., 2000). This procedure relies on the determination of the background continuum level, and so is subject in principle to blending and confusion with other features. The influence of bremsstrahlung continuum emission cannot be ignored (Mewe et al., 1986). Blending with lines of iron complicates use of the features from Ne, for example, but is less important for the RRCs from Si and S. Use of relative strengths of RRCs to determine abundances requires atomic data for the photoionization cross section. The atomic data needed for this is discussed in the next section.

Metastable levels in ions of the Be isoelectronic sequence can provide diagnostics of the combined effects of gas density and UV photoexcitation. These can be applied to gases which are photoionized via their effect on the absorption spectrum. As shown by Kaastra et al. (2004), the absorption from metastable $2s2p^3P$ in the ion O^{4+} provides a constraint on density in the range 10^8 – 10^{13} cm^{-3}. They show a marginal detection of lines arising from this level from an active galaxy observed with the LETG on *Chandra*.

Owing to the presence of a strong continuum source, spectra of photoionized sources in the X-ray band can be viewed in transmission, and if so exhibit primarily absorption due to bound-free continuum and resonance lines. Line strengths, as measured by the line equivalent width, are therefore diagnostic of the gas column density and the line intrinsic width. Curve of growth analysis, familiar from the analysis of stellar spectra (Mihalas, 1978), has been applied to analysis of *Chandra* spectra of active galaxies by, e. g. Lee et al. (2001). An important difference between the optical/UV and X-ray case is that the damping parameter a, which is typically $\leq 10^{-8}$ for a line such as Lyα of hydrogen, can be as great as ~ 1 for X-ray lines such as Fe Kα lines owing to the typically very short lifetimes of line upper levels (Liedahl, 2003; Masai and Ishida, 2004).

Broadening of bound-free absorption features is dominated by the intrinsic properties of the transition, i.e., level or resonance structure near the threshold and the phase space above the threshold. So such features serve as diagnostics of the presence of certain ions or atomic species. Examples include the resonance structure and edge position in ions of oxygen. These have been calculated for O^{5+} (Pradhan, 2000), neutral oxygen, O^{+} and O^{2+} (Pradhan et al., 2003) and for all ions of oxygen by Garcia et al. (2005). The position and shape of the neutral oxygen edge, and the resonance structure have been calculated by Gorczyca et al. (2003) using the R-matrix code package. Comparison with experimental measurements (Schmidt et al., 2004) using the EBIT device at Lawrence Livermore National Lab shows that the calculations of Garcia et al. (2005) are accurate to within $\simeq$ 10 mÅ for O^{4+} and O^{5+}. O^{2+} – O^{5+} K line wavelengths were measured with an accuracy ranging from 5 to 20 mÅ in an EBIT experiment and were interpreted in a collisional-radiative model using the FAC code (Gu et al., 2005). These lines were observed by Paerels et al. (2001), and have been used by Juett et al. (2004) to infer the mean ionization balance in the interstellar gas along the lines of sight to several X-ray binaries.

VII. SPECTRUM SYNTHESIS AND GLOBAL FITTING

In many situations the most detailed information about the conditions in astrophysical plasmas can be gained by modeling the microphysical processes affecting the excitation/decay, and ionization/recombination in sufficient detail to synthesize the effects on the spectrum from many ions and elements simultaneously. This entails calculating the ion fractions and level populations and also the emitted spectrum or opacity or both. This procedure, sometimes described as spectrum synthesis or global modeling, is necessary in cases where the observed spectral resolution or signal-to-noise is not sufficient to cleanly resolve individual spectral features to be used as discrete diagnostics. This is the realm of data analysis in X-ray astronomy prior to the gratings on *Chandra* and $XMM-Newton$, when the instrumental resolution was capable of resolving only the strongest lines in uncrowded spectral regions, such as the Lyman-α line from O^{7+} in coronal sources. Much of the data obtained by *Chandra* and $XMM-Newton$ still is obtained with the CCD instruments alone, for sources which are too faint for gratings or which are spatially extended, and even grating spectra or bright sources are unable to resolve or unambiguously detect weak lines in crowded spectral regions. Global modeling is also useful when there is strong coupling expected between the ions responsible for spectral formation. An example is in a photoionized gas, where in equilibrium the temperature will couple the emission and absorption properties of all the ions in the gas.

A. Coronal Plasmas

Early work on coronal ionization balance was carried out by Jordan (1969, 1970), who first included a treatment of DR and autoionization and the suppression of these processes at high densities. Early work on the cooling function of coronal plasma was presented by Cox and Tucker (1969) and Cox and Daltabuit (1971). Other calculations of coronal ionization and emission include Landini and Fossi (1972), Jain and Narain (1978), Allen and Dupree (1969) and Tucker and Koren (1971). The work of Mewe and coworkers served to better characterize many of the rate coefficients needed for coronal emissivity calculations. These began with calculations of X-ray (Mewe, 1972a,b; Mewe et al., 1985) and EUV (Mewe, 1975) lines from the solar corona, He-like lines (Mewe and Schrijver, 1978a), exploration of abundance dependences on lines (Mewe and Gronenschild, 1981) and continuum (Gronenschild and Mewe, 1978), and non-equilibrium ionization (Gronenschild and Mewe, 1982). Many of these rate coefficients and cross sections were incorporated into the MEKAL code (Kaastra, 1992; Mewe et al., 1985, 1986, 1995a,b), and updated to the SPEX code (Kaastra, Mewe and Nieuwenhuijzen, 1996), a unified plasma model/analysis environment.

Current ionization balance calculations in widespread use are those of Arnaud and Rothenflug (1985) who calculated the ionization balance for most elements of interest to X-ray astrophysics, and Arnaud and Raymond (1992) who evaluated and compiled recombination and collisional ionization rate coefficients for all ions of iron, and the ionization balance of Mazzotta et al. (1998). Both Arnaud and Rothenflug (1985) and Mazzotta et al. (1998) make use of many of the rate coefficients of Shull and van Steenberg (1982a,b), which in turn use the DR rate coefficients of Jacobs et al. (1977a). As pointed out in Section VII.A.2, the rate coefficients of Jacobs et al. (1977a) have been shown to overestimate the effect of cascades to autoionizing levels. Bryans et al. (2006) have published ionization balance calculations which make use of the most recent rate coefficients (summarized later in this section) and which have now been extensively bench marked and fitted to experiments. The CHIANTI database (Dere et al., 1997, 2001) contains evaluated collisional excitation and radiative data, augmented to include wavelengths shorter than 50 Å (Landi et al., 1999) and excitation by protons (Young et al., 2003), and including much of the data appropriate to coronal plasmas reported in this review. The most recent update to CHIANTI, version 5 (Landi and Bhatia, 2005a) also includes transitions to the $n \geq 4$ levels of iron ions based on calculations using FAC, and new UV lines from C-, N-, and O-like isosequences, and updated level energies from Landi and Phillips (2005).

Other calculations of coronal ionization balance and spectra include studies of time-dependent ionization (Shapiro and Moore, 1976; Sutherland and Dopita, 1993), exploration of the effects of ionization balance on plasma diagnostics (Gianetti, Landi and Landini, 2000), calculation of non-equilibrium ionization in supernova remnants (Hamilton, Chevalier and Sarazin, 1983), and spectra of supernova remnants in the adiabatic phase (Itoh, 1979). Comprehensive calculations of coronal emission spectra for the X-ray band, including both ionization balance and spectrum synthesis by Raymond and Smith (1977) remain in widespread use. These have recently been updated and greatly expanded by Brickhouse, Raymond and Smith (1995) and Smith et al. (2001) to form the core of the APEC code, which is in use in analyzing high resolution astrophysical X-ray spectra.

1. Electron Impact Ionization (EII)

Background

Electron impact ionization (EII) is of fundamental importance to coronal plasmas, in which electrons are energized by some mechanical agent such as shocks, acoustic waves or MHD dissipation. It can be divided into direct ionization (denoted DI), which we discuss in this subsection, and other processes involving an intermediate state which are addressed in the succeeding subsections. It is challenging to compute owing to the fact that it requires a treatment of two continuum electrons in the final state. Therefore experimental cross sections play a key role in the determination of accurate rates. Measurement techniques include crossed beams, merged beams, traps, plasmas, or indirect methods. Of these, crossed beam measurements have been most widely applied. Storage ring methods have the potential to eliminate the greatest systematic uncertainty, namely the metastable states in the target beam.

A convenient point for comparison comes from the classical treatment of electron scattering (Seaton, 1962). In a collision between two free electrons, one initially at rest, the energy transferred is $\epsilon = E/(1+(RE/e^2)^2)$, where E is the kinetic energy of the incident electron and R is the impact parameter. If this energy transfer is instead interpreted as the energy available for ionization of a bound electron, then the cross section is determined by the maximum impact parameter such that the transferred energy is the ionization potential, I:

$$\sigma_{classical}(E) = 4\left(\frac{I_H}{I}\right)^2\left(\frac{I}{E}\right)\left(1-\frac{I}{E}\right)\pi a_0^2 \qquad (18)$$

This formula is not accurate enough for quantitative work; at low energies it overestimates the cross section and at large energies measured cross sections decrease $\propto \log(E)/E$. The functional behavior derived from this formula, with modifications, has been used to parameterize the cross section in many tabulations of cross sections and collision strengths derived from both experiment and theory.

The semi-empirical formula of Lotz (1967) was developed at a time when few accurate experimental measurements were available. Selected experimental rate coefficients and isoelectronic interpolation, based on the compilation of experimental rate coefficients by Kieffer and Dunn (1966), were fitted by hand for each subshell to a formula

$$\sigma(E) = \zeta\frac{a\ \ln(E/\chi)}{\chi E} \qquad (19)$$

where χ is the ionization potential of the subshell. This formula captures the correct behavior in the asymptotic (Born) limit, while allowing semi-empirical adjustment of the cross section near threshold. It was found that a good fit to the available experimental data was obtained if a is approximately constant and ζ is the average number of electrons per subshell. This was done for the lowest two charge states of H, He, Li, N, Ne, Na, K and for neutral Ar, Kr, Rb, Xe, Cs and Hg. Based on this, Lotz (1968) derived the energy dependent cross section and ionization rate coefficients for all ions of elements up to Ca, estimated to be accurate to $^{+40}_{-30}\%$.

Summers (1974) developed calculations for direct ionization using the semi-classical Exchange Classical Impact Parameter (ECIP) method. This combines a classical binary treatment of close collisions, which gives accurate cross sections at low energies, with a treatment which has the proper asymptotic behavior (Burgess and Summers, 1976). This method was applied by Summers (1972, 1974) to calculations of ionization rate coefficients. Burgess et al. (1977) evaluated these rates by comparison with experiment, and found better agreement than other calculations available at the time for most ions. Calculations using the CBO approximation, were carried out by Golden and Sampson (1977), Golden et al. (1978), Golden and Sampson (1980) and Moores et al. (1980). Born approximation cross sections were computed for ions of Al and Na (McGuire, 1977, 1982). The importance of excitation-autoionization and direct ionization of Na-like ions was pointed out by Sampson (1982). Shevelko et al. (1983) used the CBE approximation to calculate the rate coefficients for EII for ions belonging to the isoelectronic sequences from H to Ca. DW calculations in LS coupling were carried out for the isosequences: H and Li (Younger, 1980a), He (Younger, 1980b), Ne (Younger, 1981a), Na (Younger, 1981b), Cl (Younger, 1982a), and Ar (Younger, 1982b). These remain in widespread use for astrophysical modeling.

DW calculations are likely to be accurate for ions with charge greater than a few, but in order to provide calculations for less ionized species techniques such close-coupling must be used. Close-coupling calculations for the electron-impact ionization include the time-dependent close-coupling method, which was applied by Pindzola and Robicheaux (2000), and Pindzola et al. (2000) to calculations of ionization of He, C and Ne. In this technique the time-dependent Schrodinger equation is solved for the radial wave functions. These calculations used a configuration-averaged potential due to the core electrons and resulted in poor agreement with experiment for Ne, suggesting the need for a full Hartree-Fock treatment of the interaction with the core electrons. Comparison of time-independent and time-dependent close-coupling methods was carried out by Badnell et al. (1998) for Na-like Mg, Al, and Si. The time-independent methods were R-matrix and convergent close-coupling solutions, based on a total wavefunction constructed using antisymmetrized products of Laguerre pseudo-orbitals and physical bound orbitals. General agreement was found between the results of the methods and with the experiment of Peart et al. (1991) at the 10% level. Calculation of ionization from metastable Ne was carried out by Ballance et al. (2004), and for C^{2+} by Loch et al. (2005), using the R-matrix with pseudostates method. Relativistic methods have not been extensively applied to calculations of collisional ionization. The use of MCDF methods has been demonstrated by Moores and Pindzola (1990) and by Pindzola et al. (1989).

Experimental Measurements

Experimental measurements of collisional ionization have been carried out for many ions of interest to astrophysics, and these are summarized in Table I. Measurements using crossed beams include those of Brook et al. (1978) for He, C, N and O, Crandall et al. (1982) for Na-like ions of Mg, Al, and Si, Diserens et al. (1984) for Ne^+ , Gregory et al. (1983) for Ne^{3+} and Ar^{3+}, Gregory et al. (1986) for Fe^{5+}, Fe^{6+}, Fe^{9+}, Gregory et al. (1987) for Fe^{11+}, Fe^{13+}, and Fe^{15+}, Montague et al. (1984) for Fe^+. Measurements of single and multiple ionization of sulfur atoms by EII were made by Ziegler et al. (1982).

Experiments by Stenke (1999) and by Linkemann et al. (1995) illustrate the complications inherent in the measurement of collisional ionization. These include the effects of metastable levels in the initial state ions, which can have greater cross section for collisional ionization than the ground state, and excitation-autoionization (EA) in which an ion is collisionally excited to a level which autoionizes. Stenke (1999) made crossed beam measurements of ionization of iron ions, Fe^+ – Fe^{9+}, showing the influence of metastables as evidenced by the ionization at energies below the ground state threshold, and also excitation-autoionization on the total cross section. Metastables are not likely to be present in the lowest density astrophysical plasmas, and so must be separated from the total cross section for use in astrophysics. However, their inclusion in a self-consistent way is a goal for the realistic simulation of finite-density astrophysical plasmas. Falk et al. (1983a) used crossed beams to measure the influence of metastables on the EII for Be-like ions of B, C, N, and O by varying the metastable fraction in the target beam, demonstrating that metastable levels can dominate the collisional ionization in this isoelectronic sequence.

Experimental and theoretical data have been reviewed by several groups. Early reviews include those of Kieffer and Dunn (1966) and Bely and van Regemorter (1970). A review by the Belfast group includes Bell et al. (1983) for elements lighter than fluorine, and Lennon et al. (1988) for elements from fluorine to Ni. These result in a set of recommended data utilizing the scaling formula of Lotz (1968), normalized to the distorted wave calculations of Younger (1980a,b, 1981a,b, 1982a,b) and, where available, experimental measurements. These rate coefficients have been further evaluated by Kato, Masai and Arnaud (1991), who find the rate coefficients too low for neutral and near-neutral species, and also for Na-like ions due to neglect of excitation-autoionization. Voronov (1997) has compiled rate coefficients based on the Belfast compilation, but which attempts to correct these problems by adopting the rate coefficients of Lotz (1968) for many of the species in question. An extensive review of the physical principles and many experimental and theoretical results is by Müller (1991). In addition, rate coefficients for collisional ionization have been reviewed as part of all the previously mentioned ionization balance calculations: Arnaud and Raymond (1992); Arnaud and Rothenflug (1985) and Mazzotta et al. (1998). Sources include Kato, Masai and Arnaud (1991) and corrections to errors in the Belfast collections in http://dpc.nifs.ac.jp/aladdin/. Bibliographies of measurements and calculations of collisional ionization are given by Burgess and Chidichimo (1983) and by Itikawa et al. (1984), Itikawa (1991), and Itikawa (1996). Both theoretical cross sections and extensive bibliographic data have been collected at the ORNL collisional database website, http://cfadc.phy.ornl.gov/astro/ps/data/home.html.

TABLE I Experimental measurements of collisional ionization cross sections.

Ion	Reference	Compilation
H^0	McGowan and Clarke (1968)	Bely
H^0	Rothe et al. (1962)	Bely
H^0	Fite and Brackmann (1959)	Bely
H$^-$	McDowell and Williamson (1963)	Bely
H$^-$	Inokuti and Kim (1968)	Bely
H$^-$	Dance et al. (1967)	Bely
H$^-$	Tisone and Branscomb (1968)	Bely
He^0	Montague et al. (1984)	Belfast
He^0	Dolder et al. (1961)	Bely
He^0	Brook et al. (1978)	Belfast
C^0	Brook et al. (1978)	Belfast
C$^+$	Hamdan et al. (1978)	Belfast
C$^+$	Aitken et al. (1971)	Burgess
C^{2+}	Falk et al. (1983a)	ORNL
C^{2+}	Woodruff et al. (1978)	Burgess
C^{3+}	Gregory et al. (1985)	ORNL
C^{3+}	Crandall et al. (1979b)	ORNL
C^{4+}	Crandall et al. (1979b)	ORNL
C^{5+}	Aichele et al. (1998)	
N^0	Brook et al. (1978)	Belfast
N^{2+}	Gregory et al. (1985)	ORNL
N^{2+}	Aitken et al. (1971)	Burgess
N^{3+}	Falk et al. (1983a)	ORNL
N^{3+}	Gregory et al. (1985)	ORNL
N^{4+}	Crandall et al. (1979b)	ORNL
N^{4+}	Defrance et al. (1990)	
N^{5+}	Crandall et al. (1979a)	ORNL
N^{6+}	Aichele et al. (1998)	
O$^-$	Tisone and Branscomb (1968)	Bely
O^0	Rothe et al. (1962)	Bely
O^0	Brook et al. (1978)	Belfast
O^0	Fite et al. (1968)	Bely
O$^+$	Aitken and Harrison (1971)	Burgess
O$^+$	Loch et al. (2003)	
O^{2+}	Gregory et al. (1985)	ORNL
O^{2+}	Aitken and Harrison (1971)	Burgess
O^{2+}	Loch et al. (2003)	
O^{3+}	Crandall et al. (1979a)	ORNL
O^{3+}	Loch et al. (2003)	
O^{4+}	Falk et al. (1983a)	ORNL
O^{4+}	Loch et al. (2003)	
O^{5+}	Defrance et al. (1990)	
O^{5+}	Trefftz (1963)	Bely
O^{5+}	Crandall et al. (1986)	ORNL
O^{5+}	Crandall et al. (1979a)	ORNL
O^{5+}	Crandall et al. (1979b)	ORNL
O^{5+}	Rinn et al. (1987)	ORNL
O^{7+}	Aichele et al. (1998)	
Ne^0	Nagy et al. (1980)	Belfast
Ne^0	Bannister (1996)	ORNL
Ne$^+$	Dolder et al. (1963)	Bely
Ne$^+$	Diserens et al. (1984)	Belfast
Ne^{2+}	Matsumoto et al. (1990)	
Ne^{2+}	Danjo et al. (1984)	Belfast
Ne^{2+}	Bannister (1996)	ORNL
Ne^{3+}	Gregory et al. (1983)	ORNL
Ne^{4+}	Bannister (1996)	ORNL
Ne^{4+}	Duponchelle et al. (1997)	
Ne^{5+}	Duponchelle et al. (1997)	
Ne^{6+}	Bannister (1996)	ORNL

The extent of the available experimental data is illustrated in Table I, which list the ion stage and reference for various experimental papers appropriate to astrophysically abundant elements, along with the referring compilation in cases where these have been adopted by a compilation such as Belfast, ORNL (http://cfadc.phy.ornl.gov/astro/ps/data/home.html) or Bely and van Regemorter (1970). It is apparent that there are multiple measurements for many ionic species, and that there is little overlap between the adopted datasets used by various compilations. This is a manifestation of the fact that the ionization database needs to be thoroughly reexamined because different data bases give different rate coefficients (Savin, 2005). There is no consensus among the widely used calculations of ionization balance as to which is most accurate. In

TABLE I continued: Experimental measurements of collisional ionization cross sections.

Ion	Reference	Compilation
Ne^{6+}	Duponchelle et al. (1997)	
Ne^{7+}	Defrance et al. (1990)	
Ne^{7+}	Duponchelle et al. (1997)	
Ne^{8+}	Duponchelle et al. (1997)	
Mg^{0}	Karstensen and Schneider (1978)	Belfast
Mg^{+}	Becker et al. (2004)	
Mg^{+}	Peart et al. (1991)	
Mg^{+}	Martin et al. (1968)	Bely
Al^{+}	Hayton et al. (1994)	
Al^{2+}	Crandall et al. (1982)	ORNL
Al^{3+}	Aichele et al. (2001a)	
Al^{4+}	Aichele et al. (2001a)	
Al^{5+}	Aichele et al. (2001a)	
Al^{6+}	Aichele et al. (2001a)	
Al^{7+}	Aichele et al. (2001a)	
Si^{+}	Djuric et al. (1993)	ORNL
Si^{2+}	Djuric et al. (1993)	ORNL
Si^{3+}	Crandall et al. (1982)	ORNL
Si^{4+}	Thompson et al. (1994)	ORNL
Si^{5+}	Thompson et al. (1994)	ORNL
Si^{6+}	Zeijlmans et al. (1993)	ORNL
Si^{7+}	Zeijlmans et al. (1993)	ORNL
S^{4+}	Howald et al. (1986)	ORNL
Ar^{0}	Wetzel et al. (1987)	Belfast
Ar^{0}	Stephen et al. (1980)	Belfast
Ar^{+}	Woodruff et al. (1978)	Burgess
Ar^{+}	Diserens et al. (1988)	Belfast
Ar^{+}	Man et al. (1987)	Belfast
Ar^{+}	Müller et al. (1985c)	
Ar^{2+}	Man et al. (1993)	
Ar^{2+}	Matsumoto et al. (1990)	
Ar^{2+}	Mueller et al. (1985a)	ORNL
Ar^{3+}	Gregory et al. (1983)	ORNL
Ar^{4+}	Crandall et al. (1979a)	ORNL
Ar^{4+}	Pindzola et al. (1984)	ORNL
Ar^{5+}	Gregory et al. (1985)	ORNL
Ar^{6+}	Howald et al. (1986)	ORNL
Ar^{7+}	Zhang and Sampson (1992)	ORNL
Ar^{7+}	Rachafi et al. (1991)	
Ar^{8+}	Zhang et al. (1991)	ORNL
Fe^{2+}	Mueller et al. (1985a)	ORNL
Fe^{5+}	Gregory et al. (1986)	ORNL
Fe^{6+}	Gregory et al. (1986)	ORNL
Fe^{9+}	Gregory et al. (1986)	ORNL
Fe^{9+}	Stenke et al. (1995b)	
Fe^{11+}	Gregory et al. (1987)	ORNL
Fe^{13+}	Gregory et al. (1987)	ORNL
Fe^{15+}	Gregory et al. (1987)	ORNL
Fe^{15+}	Linkemann et al. (1995)	
Fe^{23+}	Wong et al. (1993)	
Ni^{2+}	Stenke et al. (1995a)	
Ni^{3+}	Stenke et al. (1995a)	
Ni^{3+}	Gregory and Howald (1986)	ORNL
Ni^{4+}	Stenke et al. (1995a)	
Ni^{5+}	Wang et al. (1988)	ORNL
Ni^{5+}	Stenke et al. (1995a)	
Ni^{6+}	Wang et al. (1988)	ORNL
Ni^{7+}	Wang et al. (1988)	ORNL
Ni^{8+}	Wang et al. (1988)	ORNL
Ni^{12+}	Wang et al. (1988)	ORNL
Ni^{14+}	Wang et al. (1988)	ORNL

fact, Arnaud and Rothenflug (1985) and Mazzotta et al. (1998) primarily make use of distorted wave calculations, such as those by Younger (1980a), rather than experimental results directly. This is due to the remaining uncertainties with regard to the applicability of experimental results to low density environments, as well as convenience. Experimental results such as those of Stenke (1999) and Bannister (1996), in which the beam composition can be thoroughly characterized provide a hopeful step in this direction.

Excitation Autoionization

Excitation-autoionization (EA) is a process in which an ion is collisionally excited to a multiply excited level which then autoionizes. This process can dominate the total collisional ionization cross section for many ions at energies above the threshold for direct ionization. Its importance was pointed out by Goldberg et al. (1965) and by Bely (1968). An experimental demonstration of the importance of EA was performed by Martin et al. (1968).

Calculations of the effect in Fe^{15+} were carried out by Cowan and Mann (1979). Burgess and Chidichimo (1983) performed functional fitting similar to that of Lotz for EA. DW calculations include rate coefficients from ground and excited levels of Ar L shell ions by Cohen et al. (1998), and by Griffin, Bottcher and Pindzola (1982a) and Griffin, Pindzola and Bottcher (1987). Also in this category are the calculations for Na-like and Mg-like ions and $\mathrm{Fe}^{5+} - \mathrm{Fe}^{13+}$ by Pindzola et al. (1986a,b, 1998), and Mitnik et al. (1998), for Fe^{0+} by Pindzola et al. (1995) and for all ions of Ni by Griffin and Pindzola (1988) and Pindzola et al. (1991). CBE calculations of EII with inclusion of EA in the H – C isoelectronic sequences were performed by Sampson and Golden (1979, 1981), and Sampson (1982) made similar calculations for Na-like ions

Close-coupling calculations including inner shell excitation and EA were made for Li-like ions of C, N, and O (Henry, 1979), Na-like ions of Al and Si (Henry and Msezane, 1982), and for Fe^{23+} using R-matrix (Butler and Moores, 1985). R-matrix with pseudostates calculations include pseudo-orbitals in order to allow for an accurate treatment of the bound and continuum wavefunctions. Ions which have been treated in this way include H (Bartschat and Bray, 1996), He (Hudson et al., 1996), Li^{+} (Brown et al., 1999), Be^{+} (Bartschat and Bray, 1997; Pindzola et al., 1997), B (Marchalant and Bray, 1997), B^{2+} (Marchalant et al., 1997; Woitke et al., 1998), C^{3+} (Mitnik et al., 1999) and Na-like Mg, Al and Si (Badnell et al., 1998), Al^{2+} (Teng, 2000).

An additional process which affects EII is resonance excitation double autoionization (REDA), which is the first stage of dielectronic recombination, dielectronic capture (cf. Section VII.A.2), followed by double autoionization. A related process is resonant excitation auto-double-ionization (READI), in which the autoionization occurs as a single event resulting in the ejection of two Auger electrons. The net result is an effective ionization event. Linkemann et al. (1995) have studied the effects of EA and REDA in Fe^{15+} using the Heidelberg storage ring, and compared their results with distorted wave calculations by Badnell et al. (1993) and Chen et al. (1990).

EA dominates the cross section by a factor ∼5 above 800 eV for this ion, and REDA can contribute ∼20–30% to the total ionization rate. Theoretical cross sections reproduce the magnitude of the experimental cross section, but they do not accurately reproduce the complex resonance structure. Possible reasons for this are the isolated resonance approximation which omits interacting resonance effects. Experimental measurements of multiple ionization have been carried out by Müller et al. (1985b) for Ar^{+} and Ar^{4+}, Teng et al. (2000) and Knopp et al. (2001) for C^{3+}, and Aichele et al. (2001b) for Ne^{7+}. Semiempirical formulae for electron impact double ionization cross sections were presented by Shevelko et al. (2005, 2006). R-matrix calculations can reproduce the fine structure in the EA/REDA/READI cross section for some ions, as evidenced by the comparison shown in Figure 8. This shows the R-matrix calculation and crossed-beam measurements of excitation-autoionization for the K shell of O^{5+} (Müller et al., 2000).

2. Dielectronic Recombination (DR)

Background

In coronal equilibrium ionization balance is determined by the relative rates of collisional ionization and recombination, where the most important recombination processes at low density are radiative recombination (RR), discussed in the next section, and dielectronic recombination (DR), which we discuss in this section. We offer first a note about terminology. It is most common to refer to recombination of ion j when discussing recombination from ion with charge state j to charge state $(j-1)$, and we will adopt this convention in most of our discussion of DR. In the less common case where DR is discussed in terms of the final state ion, $(j-1)$, we will refer to it as recombination *into* ion $(j-1)$.

DR dominates over RR in coronal equilibrium for many ions and at a wide range of temperature, but not universally. The H- and He-like ions are an exception, in which RR dominates at the temperatures characteristic of equilibrium. Accurate ionization balance calculations require that both processes be included. A description of the process is provided by Savin et al. (2003), which we quote with minor modification: “ DR is a two-step recombination process that begins when a free electron approaches an ion, collisionally excites a bound electron of the ion, and is simultaneously captured. The electron excitation can be labeled $nl_j \to n'l'_{j'}$, where n is the principal quantum number of the core electron, l is its orbital angular momentum, and j is its total angular momentum. This intermediate state, formed by the simultaneous excitation and capture, may autoionize. The DR process is complete when the intermediate state emits a photon which reduces the total energy of the recombined ion to below its ionization limit. Conservation of energy requires that for DR to go forward $E_k = \Delta E - E_b$. Here E_k is the kinetic energy of the incident electron, ΔE is the excitation energy of the initially bound electron, and E_b is the binding energy released when the incident electron is captured onto the excited ion. Because ΔE and E_b are quantized, DR is a resonant process..”

For the purposes of computation, DR is generally treated as an independent process from RR (although a unified approach is discussed later in this section). The calculation of rate coefficients divides into two basic parts: determination of the energy structure of the doubly excited levels which mediate the process, and the rate coefficients or branching ratios for the stabilizing decays. The first discussion of the importance of this process is that of Massey and Bates (1942). A more detailed summary of the history of the importance of DR is given by Seaton and Storey (1976). Historically, the understanding of this process has progressed at a rate determined primarily by the atomic structure calculations and measurements. This is particularly true for DR at low temperatures, where the excitation energy of the initially bound core electron in the presence of the captured electron (i.e. the quantity ΔE defined above) is very small for each of the resonances which contribute to the rate coefficient. This increases the need for accurate calculations of these resonance energies, since the Maxwellian distribution of the recombining electron kinetic energies will be sharply peaked at low energy if the temperature is low. An accurate calculation of the extent to which a given resonance overlaps with this distribution requires values for ΔE which are accurate to $\ll kT_e$, or $\ll$1 eV at $T_e \sim 10^4$ K.

An outline of the rate calculation was provided by Bates and Dalgarno (1962), which we reproduce here. If the autoionization of the capture state is much more probable than stabilization, then the capture state can be regarded as being in LTE with the continuum to a good approximation. Then the DR rate is simply the equilibrium abundance of the capture state, given by the Saha-Boltzmann equation, times a (small) branching ratio expressing the fraction of ions which stabilize. That is, the capture and autoionization reactions will maintain a quasi-equilibrium between the forward and reverse reactions of

$$\mathrm{X}_i^{q+} + e \to \mathrm{X}_d^{(q-1)+}. \tag{20}$$

State d is an excited state of the recombined ion $\mathrm{X}^{(q-1)+}$ that lies above the ionization potential of ion $\mathrm{X}^{(q-1)+}$, and i is the ground state of the recombining ion X^{q+}. The population of state d can be derived from the local balance between dielectronic capture and autoionization. The DR rate coefficient is then the density of the capture state times the stabilization rate:

$$\alpha_i^{dr}(T) = \frac{n(\mathrm{X}_d^{(q-1)+})}{n_e n(\mathrm{X}_i^{q+}) b(\mathrm{X}_d^{(q-1)+})}\Gamma_s \tag{21}$$

where $n(\mathrm{X}_d^{(q-1)+})$, $n(\mathrm{X}_i^{q+})$ are respectively the number

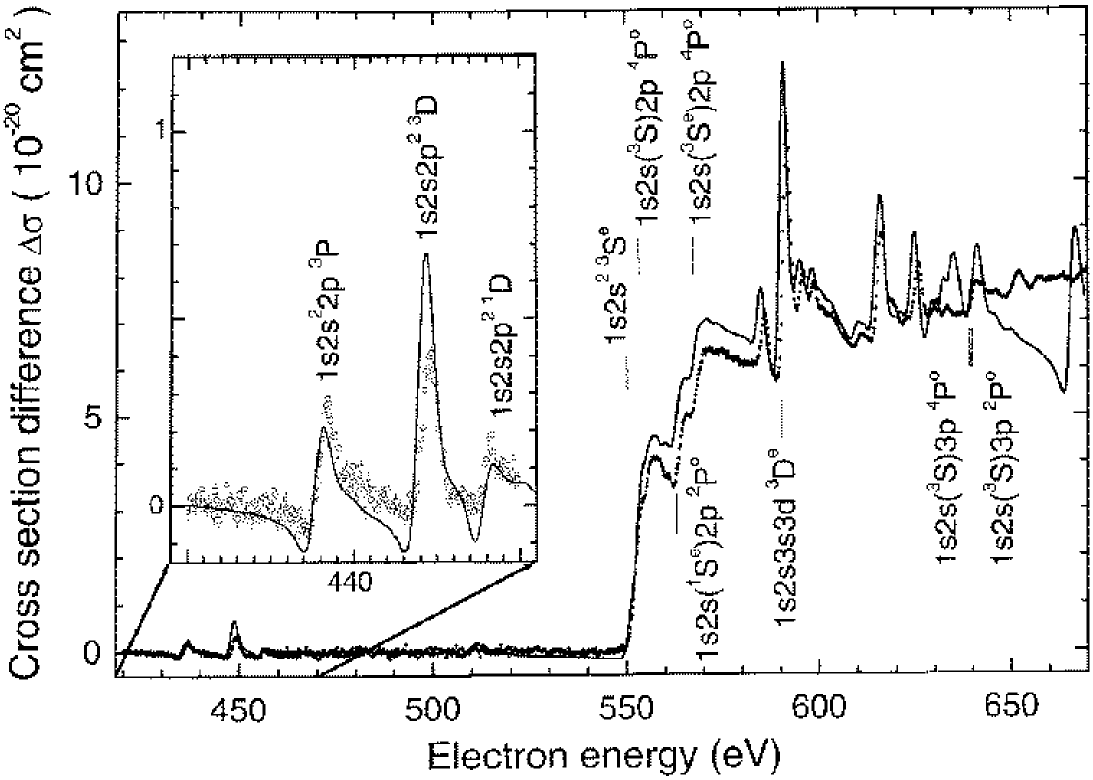

FIG. 8 Cross section for electron-impact ionization of O^{5+} in the vicinity of the $1s2s^2\ {}^3S^o$ EA threshold. The DI contribution has been subtracted off. Data points are crossed beam measurements (Müller et al., 2000), solid curve is R-matrix calculation.

densities of state d and state i, n_e is the electronic density, and Γ_s is the damping constant for radiative stabilization. The factor $b(\mathrm{X}_d^{(q-1)+})$ is a departure coefficient which reflects the fact that the true number in state d will be reduced from the Saha value by the branching ratio for autoionization, which is very close to unity:

$$b(\mathrm{X}_d^{(q-1)+}) = \frac{\Gamma_a}{\Gamma_a + \Gamma_s}. \tag{22}$$

In this equation Γ_a is the damping constant for the autoionizing transition and $n(\mathrm{X}_d^{(q-1)+})$ is given by the Saha equation:

$$\frac{n(\mathrm{X}_d^{(q-1)+})}{n_e n(\mathrm{X}_i^{q+})} = \frac{\omega_d}{2\omega_i}\frac{h^3}{(2\pi mkT)^{3/2}}\mathrm{e}^{-\varepsilon_i/kT} \tag{23}$$

where ω_d and ω_i are respectively the statistical weights of states d and i, and ε_i is the energy difference between states d and i. So the rate coefficient may be written

$$\alpha_i^{dr}(T) = \frac{\Gamma_a\Gamma_s}{\Gamma_a + \Gamma_s}\frac{\omega_d}{2\omega_i}\frac{h^3}{(2\pi mkT)^{3/2}}\mathrm{e}^{-\varepsilon_i/kT} \tag{24}$$

$$= \frac{1}{\tau_a + \tau_s}\frac{\omega_d}{2\omega_i}\frac{h^3}{(2\pi mkT)^{3/2}}\mathrm{e}^{-\varepsilon_i/kT} \tag{25}$$

where $\tau_s = \Gamma_s^{-1}$ and $\tau_a = \Gamma_a^{-1}$ are respectively the lifetimes for radiative stabilization and autoionization. Since the lifetime for stabilization is generally much longer, this can be written:

$$\alpha_i^{dr}(T) = \Gamma_s\frac{\omega_d}{2\omega_i}\frac{h^3}{(2\pi mkT)^{3/2}}\mathrm{e}^{-\varepsilon_i/kT} \tag{26}$$

(note that modern calculations do not need to make use of this approximation). Γ_s can be expressed in terms of the absorption oscillator strength f_{bd} for transition $b \rightarrow d$, b is an excited state (or the ground state) of the recombined ion $\mathrm{X}_b^{(q-1)+}$ that cannot further autoionize and to which the autoionizing state d can decay.

$$\alpha_i^{dr} = CT^{-3/2}\frac{\omega_b}{\omega_i}\nu_{bd}^2 f_{bd}\mathrm{e}^{-\varepsilon_i/kT} \tag{27}$$

where

$$C = \frac{(2\pi)^{1/2}e^2h^3}{ck^{3/2}m^{5/2}} \tag{28}$$

and ν_{bd} is the wave number of the emitted radiation.

The DR rate for an ion is obtained by summing over all the levels b and d. Burgess (1964a) pointed out the fact that the summation over statistical weights and Boltzmann factors can diverge formally, or can be very large if many states participate in the DR process. This is reduced by the fact that the approximation used to derive Eq. (26) breaks down for large n, i.e. that the autoionization no longer dominates over stabilization. Burgess (1964a) calculated the rate coefficient for recombination onto He^+ using values for Γ_s calculated by extrapolating the collisional excitation cross section to below threshold. A prescription for calculating DR rate coefficients was presented in the classic work of Burgess (1965), in which he demonstrated by numerical experiment that when the sum over b and d is performed on equation (27) the dependence on the nuclear charge and level energy separate, and the rate can be written as a sum over the oscillator strengths of the stabilizing radiative transitions and a polynomial in the energies of the same stabilizing transitions. These polynomials, known together as the Burgess General Formula (GF), allow the rate coefficient for DR to be calculated using an analytic function of nuclear charge, atomic number, and temperature. This remains the standard set of rate coefficients against which others are compared, and which are in widespread use in various calculations of ionization balance.

The GF is meant to be used for DR where the channels which dominate the total rate are into high n levels near the DR series limit. This allows all these high n levels to be treated approximately as a single resonance at the energy of the series limit. It is most accurate when the temperature is comparable to the dominant core excitation, i.e. $\varepsilon_i/kT \sim 1$. It is not meant to be used where the dominant recombination channels are those at low energies far away from the series limit. The GF models DR as a dipole core excitation followed by the inverse decay. It does not allow for autoionization into excited states, non-dipole core excitation, or alternative radiative stabilization pathways by either the core or Rydberg electron. Comparison with experiment (Savin, 1999) shows the GF, and modifications by Merts and by Burgess and Tworkowski (1976), to be reliable to approximately a factor of 2.

The importance of using accurate term energies rather than configuration-average energies in the calculation of DR rate coefficients was pointed out by Shore (1969). This is because of the Boltzmann factor in Eq. (27), and also because of the effect on the overlap of the resonance energies. Shore (1969) calculated DR rate coefficients for various ions of the H-like, Li-like, Na-like isoelectronic sequences, in addition to C^+ and Ca^+ ions using monoconfigurational screened hydrogenic wave functions including the effect of finite stabilization. These results demonstrate a qualitative difference between recombination onto ions where $\Delta n = 0$ transitions are allowed in the core excitation, such as Li- or Be-like ions, and those in which they are not, such as H-like ions. In the former case, capture states are those with $n > 100$, while in the latter case capture occurs primarily to states with $n < 50$. The Burgess (1965) formula provides results which are most accurate for ions dominated by the high-n capture states. Larger errors can result for ions where the low-n states dominate. For high Z the dielectronic capture and stabilization can occur predominantly through states with $n \leq 4$. The stabilization transition therefore can correspond to a spectroscopically resolvable emission line, although with an energy which is shifted from the corresponding line in the parent ion due to the partial screening provided by the recombining electron. These satellite lines have diagnostic value and are discussed in Section VI.A.2.

The calculations of Shore (1969) neglected exchange effects and channel coupling, both of which are expected to reduce the autoionization rates. The effects of stabilization and resonance overlap, in addition to exchange and channel coupling, were examined by Burgess and Tworkowski (1976) using the Coulomb-Born approximation for recombination onto H-like ions with $1 \leq Z \leq 40$. Comparison with the GF shows agreement to within 30% or better. Compilations of DR recombination rate coefficients calculated using the GF have been made by Aldrovandi and Pequignot (1973, 1976), and remain in widespread use.

Experiment

Experimental treatments of DR divide into those involving plasma measurement and those involving direct measurement of reaction yield using a beam or trap. In plasma measurements ion fractions are measured or inferred from spectra and then the recombination rate is derived under assumptions about the ionization rate. This procedure was carried out by Breton et al. (1978), who observed time variability of spectra from a tokamak in which the time variability comes from sawtooth heating due to an MHD instability. By measuring the spectra of two ions simultaneously (Mg-like and Na-like Mo^{30+} and Mo^{31+}), whose abundances peak near 2 keV in equilibrium, the ionization and DR rate coefficients could be disentangled. Brook et al. (1978) measured DR at $kT = 100$ eV for Fe^{8+}-Fe^{10+} by adding Fe to a theta-pinch plasma. The measured rate coefficients are approximately 50% of those calculated by Jacobs et al. (1977a), and are much less than those predicted by the Burgess (1965) GF. Isler, Crume and Arnurius (1982) measured relative abundances of iron ions in a tokamak where coronal equilibrium is achieved. DR rate coefficients were inferred by assuming collisional ionization rates. The results lead to inferred DR rate coefficients which are approximately $\sim$10 % of those predicted by the Burgess (1965) GF.

A related technique is the observation of DR satellites from plasma experiments. Such a measurement was carried out by Bitter et al. (1979) for He-like Fe in tokamak. These were found to agree with calculations of Jordan (1969) and Summers (1974). Decaux et al. (1991a) measured satellite spectra of Fe^{25+} and compared with various available calculations, showing agreement in the satellite intensity factors to within $\simeq 10\%$. Decaux et al. (1991b) compared experiment with HF calculations using the technique of Karim and Bhalla (1991) for $n = 3 - 8$ DR satellites of the Fe XXV Kα resonance line, and discussed the diagnostic use of the DR satellites for deriving the plasma temperature.

Measurements using traps and related techniques include those of Briand et al. (1984), who studied the energies of the K shell resonance in Ar^{12+} – Ar^{15+} using an electron beam ion source (EBIS). Rates for DR onto He-like argon were measured by Ali et al. (1990) also using an EBIS. Knapp et al. (1989) measured DR satellites from recombination into Ni^{27+} using an electron beam ion trap (EBIT), and inferred cross sections at the resonance energies. Beiersdorfer et al. (1992) measured DR satellites for He-like iron using an EBIT, along with extensive comparison with theoretical predictions for the strengths of these features. Good agreement was found between experiment and theory for the strongest lines, within the 20% experimental error, although for weak lines much greater discrepancies were found.

Beam experiments divide into those performed at high energy, using highly stripped ions, and those performed at energies similar to those expected in thermal equilibrium. An example of the former is the measurement of Tanis et al. (1981), who measured the Kα radiation produced following electron capture by highly stripped S^{13+} – S^{16+} with neutral argon at 13 MeV. This fluorescence process is the high energy analog of DR. Similar techniques were used by Clark et al. (1985) in a study of K shell excitation in Si^{11+} + He at 95 MeV, and by Schultz et al. (1987) who measured cross sections for the correlated emission of two K X-rays following the collision of S^{15+} ions with H_2 in the energy range between 70 and 160 MeV.

Merged beam experiments allow reactions to be measured at low energies, close to what is expected for thermal equilibrium. Key to merged beam measurements is reduction of background ions in the interaction region, which can be an important contaminant at low beam energies. Experimental measurements of DR were carried out for C^+ recombining to C using merged beams by Mitchell et al. (1983). This resulted in a lower limit which exceeds that calculated by Lagattuta and Hahn (1982a). Also experimental measurement of DR for Mg^+ using merged beams was carried out by Belic et al. (1983), with measured cross sections found to slightly exceed those calculated by Lagattuta and Hahn (1982a). Dittner et al. (1983) carried out measurement of DR in Li-like C and B using merged beams, using a high energy ion beam from a tandem VandeGraf accelerator. This has the advantage of low background due to the high beam energy, and showed good agreement with Lagattuta and Hahn (1982a) in the region of the $2s - 2p$ resonance for B. In C^{2+} a discrepancy with theory was found near threshold, in which the measurement is lower, possibly due to errors in the theoretical calculation of the $2p4d$ and $2p4f$ levels. Merged beam experimental measurement of DR in Boron-like N, O, F were carried out by Dittner et al. (1988) which resolved the ^2D, ^2P, ^2S states of the $2s2p^2$ electrons.

Theory

As mentioned above, the GF provides DR rate coefficients which are easily applied and accurate to within a factor ∼2 for temperatures $kT \sim \varepsilon_i$. Improvements to these rates divide into several categories: improved term energies and bound-state wavefunctions, associated with more accurate structure calculations; inclusion of other types of transitions such as autoionization into excited states, non-dipole core excitation and stabilization by decay to excited levels; and examination of the computational formalism, such as the isolated resonance approximation and the use of perturbation theory to calculate matrix elements. Improvements to the structure initially made use of single configuration non-relativistic Hartree-Fock wavefunctions in LS coupling, in order to study the systematic behavior of DR and related processes for many ions.

Study of processes which affect DR rate coefficients, including Auger and radiative transition probabilities, and inner shell excitation, were carried out by Hahn and coworkers. For example, inner shell excitation in electron-ion collisions in which the incident electron energy exceeds the first ionization threshold is the high energy analog of DR. The relation between this process and DR was explored by Hahn (1977), who pointed out the importance of inner shell excitation followed by autoionization. The importance of Auger ionization to the total ionization cross section for highly charged ions was also pointed out by Hahn (1978). Excitation probabilities, both to discrete and continuum states, were calculated for the inner- and outer-shell electrons, using an improvement to the Bethe approximation. The result showed a decrease in the relative transition strength to the continuum as the degree of ionization Z_I increases. The branching ratios for the Auger ionization and fluorescence decay were fitted as functions of Z_I for ionized targets. The Auger ionization and electron fluorescence cross sections were compared with the corresponding direct processes. Calculations of a related process, excitation followed by double autoionization of the ion Fe^{15+}, were carried out by Lagattuta and Hahn (1981a) using single configuration bound state and distorted wave continuum orbitals. McLaughlin and Hahn (1982) calculated cross sections for the resonant-excitation of the $1s$ electrons accompanied by the capture of an incident electron for the target ions Si^{11+} and S^{13+}. A systematic study of the dependence of the Auger and radiative transition probabilities of high Rydberg states on their principal and orbital quantum numbers was carried out by Gau and Hahn (1978), leading to a simple empirical l-dependence. The scaling behavior of the transition probabilities associated with DR were studied by Retter et al. (1978), showing that $\Gamma_s \propto Z^4$, $\Gamma_a \sim$ const. These were tested against numerical computations using single configuration Hartree-Fock wavefunctions, for the Be and Ne isosequences. This simple scaling was found to break down at high Z, and a polynomial expression in Z was given which is better approximation. Relativistic effects were shown to be important for Fe.

Calculations of DR using single configuration non-relativistic Hartree-Fock wavefunctions in LS coupling include those of Hahn (1980), who studies the scaling of α_{DR} with principal quantum number and with nuclear charge. A correction to Burgess (1965) general formula was suggested based on these results, which were carried out only for the Be and Ne isosequences. The importance of the contributions of high Rydberg states to DR of Ar^{7+}, Fe^{15+} and Mo^{31+} were studied by Lagattuta and Hahn (1981a), leading to derivation of approximate Auger rate coefficients and fluorescence yields for such states. Lagattuta and Hahn (1981b) calculated the DR rate for Na-like Mo^{31+} and pointed out the importance of cascades to all excited levels, not just the ground level, which reduces the total rate, and of including doubly excited states which increases the total rate. Lagattuta and Hahn (1982b) demonstrated the importance of $2p-3d$ core excitations and Auger decays from excited states using a calculation of DR for Cl^{7+} (Ne-like). These effects cause departures from n^{-3} scaling for the transition probabilities. Lagattuta and Hahn (1982a) calculated DR of Mg^{+} and pointed out the importance of cascades to autoionizing levels, which leads to a reduction of the net rate. Lagattuta and Hahn (1983a) calculated DR for C^{+}, for which the dominant excitation is $2s-2p$. The capture states are at high $n > 100$, and so are densely packed in energy close to threshold. Lagattuta and Hahn (1983b) calculated DR for Ar^{14+}, examining the influence of n^{-3} scaling and pointing out the effects of $1s$ excitation at high energy. McLaughlin and Hahn (1983a) calculated DR for C^{3+}, and McLaughlin and Hahn (1983b) calculated DR for B^{2+} with an improved treatment of high n states. McLaughlin and Hahn (1983c) calculated DR for O^{5+} and discussed scaling of Γ_a and Γ_s vs. Z for various ions in the isosequence. Lagattuta et al. (1986) discussed the effect on the DR cross section of electric-field-induced mixing of high Rydberg state levels, for both Mg^{+} and Ca^{+} target ions. Omar and Hahn (1987) calculated DR for Ca^{12+}, Ca^{11+}, Ca^{10+}. Moussa et al. (1988) calculated DR into Ne-like Mg^{2+}, P^{3+}, Cl^{7+}, in which DR involves $\Delta n \neq 0$ core excitation, and results were compared with the experiment of Dittner et al. (1983). Nasser and Hahn (1989) calculate DR for N^{2+}, O^{3+} in order to compare with the experiments of Dittner et al. (1988). Ramadan and Hahn (1989) calculated DR for the B-like ions of C, O, Ar and Fe. They pointed out the importance of accurate energies for $\Delta n = 0$. Owing to shortcomings of the single configuration Hartree-Fock treatment for this purpose, these authors use the HFR code. They estimate field effect enhancement based on state counting arguments, and derive an expression for the reduction: $r_F \sim n_f/(1+l_{max})$, and $n_f = 3.2 \times 10^8/F^{1/4}$, in which F is the field strength in V cm^{-1} and l_{max} is the maximum l which contributes to DR. Agreement is obtained with the experiment by Dittner et al. (1988) using $r_F = 2$ for C^{+}, but the experimental uncertainty is large. Metastables in the recombining ion can affect experimental results from beams, and these were calculated by Hahn (1989) and by Hahn and Bellantone (1989), who calculated DR cross sections for metastable O^{6+} and found them to be large, $\sim 10^{-15}$ cm^2 for resonances, leading to rate coefficients which are $\sim 10^{-9}$ cm^3 s^{-1}. With some field enhancement and assuming that the initial ion beam is a mixture of metastable $1s2s$ (^1S and ^3S) states, the overall feature of the experimental data of Andersen et al. (1992a) was reproduced, including the broad peaks at the incident-electron kinetic energies of 4.7 and 12.5 eV, and partially also at 2.5 and 6.8 eV. With a different mixture, the C^{4+} data were reproduced. Janjusevic and Hahn (1989) calculated DR rate coefficients and cross sections for the O^{3+} ion where the $2s$ and $2p$ electrons of the initial state are excited to higher, $n \geq 3$ states ($\Delta n \neq 0$ transitions). The $2p$ electron excitation dominates the $\Delta n \neq 0$ process, while the $2s$ excitation is suppressed by the cascade corrections that strongly affect the intermediate states $1s^2 2s2p3snl$ and $1s^2 2s2p3dnl$. The $2s$ contribution is approximately 15% of the $\Delta n \neq 0$ mode, while the total $\Delta n \neq 0$ contribution is roughly 10% of the $\Delta n = 0$ cross section. Bellantone and Hahn (1989) calculated DR cross sections and rate coefficients for the H-like and He-like C and O ions. The DR cross sections for the initial metastable states of the He-like ions were also estimated for a few low-lying resonance states near the DR threshold. Comparison between various electron coupling schemes was discussed and it was pointed out that configuration interaction (CI) will reduce the contrast between various coupling choices. Hahn (1993) obtained rate formulas for DR by fitting all of the existing DR data for ions with core charges (Z_c) less than 50 and the number of electrons in the target ions less than 13. A review of the physics of RR and DR was presented by Hahn (1997), in addition pointing out more exotic modes of recombination. These include off-shell dielectronic recombination (radiative DR = RDR), in which an electron capture is accompanied by simultaneous radiative emission and excitation of the target ion.

Similar techniques were used by Roszman (1979), who calculated the total rate of DR for Mo^{32+} (Ne-like) using radial orbitals obtained from central field solution and a Hartree-Fock calculation for ground states. The structure was LS term resolved, not configuration averaged. Agreement with the GF for the total rate is good in the temperature range 1.0-6.0 keV, but poor below 1.0 keV, which is attributed to the GF use of hydrogenic Coulomb wavefunctions for continuum and hydrogenic wavefunctions for bound states. Roszman (1987a) calculated DR for members of the fluorine isoelectronic sequence, Ar^{9+}, Fe^{17+}, and others using the single-configuration, LS-coupled, frozen-core approximation. These calculations employed a different treatment for the ground state orbitals, in which the Hartree-Fock exchange is replaced with Cowan HXR exchange potential, and continuum exchange is treated using a semi-classical exchange potential. A significant discrepancy is found with the only other available calculation, that of Jacobs et al. (1977a). This may be due to the overestimate of the decays to autoionizing levels by Jacobs et al. (1977a), as will be discussed below. The results also differ from the rate coefficients calculated using the GF. Similar results were found by Roszman (1987b) from calculations of DR for O-like Ar^{10+} and Fe^{18+} using similar techniques. Roszman (1987c) calculated DR for ions of the Li isoelectronic sequence: Ne^{7+}, Ar^{15+}, Fe^{23+}, and Kr^{33+}. When compared with McLaughlin and Hahn (1983a) a large discrepancy is found, which is attributed to an incorrect assumption by McLaughlin and Hahn (1983a) that all transitions from states $1s3pn'l'$ and $1s4pn'l'$ to $1s2pn''l''$ are treated as stabilizing, while in fact many are not since, for $n'' > n_0$, they are not below the first ionization limit. Roszman (1989a) used the same technique to calculate rate coefficients for O^{5+} and O^{2+}. Comparison with Badnell (1988) and the Burgess (1965) general formula shows differences of $\simeq$40%. The effect of density dependent correction formulas for DR as proposed by Jordan, Burgess, and Shore (all unpublished) are examined by Roszman (1989b), along with the effects of metastables. Another single-configuration Hartree-Fock calculation is that of Younger (1983), who calculated DR for He-like ions of C, Al, Ar, and Fe using DW and including CI for a limited set of states. The results compare well with those of Bely-Dubau et al. (1979a).

Jacobs et al. (1977a) pointed out that autoionization can occur to another level besides the ground level of the recombining ion, and that this may be more probable than the inverse of the initial capture. This would lead to a greater autoionization probability and a smaller net recombination cross section. Also, the autoionizing level can be collisionally ionized as well, if the density is high, leading to a net reduction in the recombination cross section. These processes were incorporated into DR rate coefficients for: $Fe^{8+} - Fe^{24+}$ (Jacobs et al., 1977a), and all ions of Si (Jacobs et al., 1977b), S (Jacobs et al., 1979), Ca, and Ni (Jacobs et al., 1980). These calculations were widely adopted and were later shown to be inaccurate owing to inclusion of autoionization into excited states which are energetically inaccessible (Badnell, 1986a). For example, for Fe^{22+} Jacobs et al. (1977a) included dipole autoionization of $1s^2 2s3p(^1P)nl \rightarrow 1s^2 2s3s(^1S)E_c l_c$, but Badnell (1986a) showed that this is only energetically allowed for $n > 19$. At $T=10^7$ K this translates into a factor 2.5 difference in the total rate. Badnell (1986a) also showed that non-dipole autoionizing transitions are important for this case.

The effects of fine structure were included in single configuration intermediate coupling calculations of DR rate coefficients for excited configurations of iron ions by Dasgupta (1995). Comparison with Savin et al. (1999a) shows adequate agreement, although their work leaves out important autoionizing channels by not explicitly calculating capture to states with $n \geq 15$. Scaled rate coefficients for O and F-like ions were calculated by Dasgupta and Whitney (1990) and Dasgupta (1995).

MCDF orbitals were used for DR calculations by Chen and coworkers. Chen (1986c) carried out such calculations for the He isoelectronic sequence. Relativistic effects drastically alter the satellite structure of Fe^{24+}, but only affect the total rate by 20%. Relativistic effects can alter the rate coefficients by as much as a factor of 3 by altering the Auger energies for higher Z elements (e. g. Mo^{40+}). In non-relativistic treatments and LS coupling the total rate is dominated by a few capture levels, while relativistic effects redistributes the rate to more levels. Calculations were carried out for Ne-like ions (Z=18, 26 and greater) by Chen (1986b) and for F-like ions (Z=26 and greater) by Chen (1988a). Coster-Kronig channels are those in which an ion with an inner shell vacancy decays by autoionization of an electron with the same principal quantum number as the initial vacancy. The influence of these channels on DR rate coefficients were examined in the calculations of Chen (1988b). The total DR coefficients for B^{3+}, N^{5+}, and F^{7+} ions are reduced by 60%, 13%, and 4%, respectively, due to the inclusion of Coster-Kronig channels. These effects are found to be negligible for $Z> 10$. Chen and Crasemann (1988) carried out DR calculations for Be-like ions with atomic numbers Z = 30, 34, 36, 42, 47, and 54. Effects of relativity and configuration interaction on the DR satellite spectra and rate coefficients were studied by comparing the theoretical results from nonrelativistic and relativistic single-configuration and multiconfiguration Hartree-Fock calculations with and without Breit interaction by Chen (1988c). Explicit calculations for H-like Ne, Cr, Mo, and Xe show that relativistic and CI effects are important in calculating satellite spectra. For the light ions, nonrelativistic calculations in intermediate coupling with configuration interaction may be sufficient. For medium heavy and heavy ions, however, *ab initio* relativistic calculations in intermediate coupling with CI including the Breit interaction are necessary. DW calculations using MCDF orbitals were carried out for Li-like ions by Chen (1991). It was shown that the total rate coefficients for the fine-structure states for ions with $Z\geq4$ can differ by as much as one order of magnitude at low temperatures due to the effects of relativity and intermediate coupling. Comparison with Roszman (1987a), finds Δn=0 rate coefficients 20% larger for Ne^{7+} at low temperature, which is likely due to Roszman (1987a) neglect of $1s2pnl$ for $l > 8$ and the use of non-relativistic $2s - 2p$ energies. For $\Delta n > 0$, computed rate coefficients are lower at low T and higher at high T, than those of Roszman (1987a). The discrepancy at low temperatures is likely due to discrepancy in Auger energies, and at high temperatures it is due to inclusion of K excitation channels in the work of Chen. DW calculations using MCDF orbitals have been carried out for B-like ions by (Chen, Reed, Guo and Savin, 1998). Comparison with experiment (Savin et al., 1999a) shows that the MCDF rate coefficients agree with experiment to within $\simeq$ 30%. The discrepancy may be due to the neglect of $l \geq 8$ Rydberg states, and possibly also due to overestimate of resonance energies.

Badnell showed the importance of the intermediate coupling and CI effects on DR rate coefficients in a series of papers reporting calculations using his AUTOSTRUCTURE code in Fe^{22+} and Fe^{21+} . This enables the relatively rapid calculation of large numbers of radiative and autoionization transition rates for arbitrary atomic configurations which are needed to calculate DR rate coefficients. Badnell (1986a) calculated configuration-mixing *LS* coupling or intermediate coupling autoionization rate coefficients for Fe^{24+}, and pointed out omissions in the state contribution in work on the same ion by Bely-Dubau et al. (1979a). Calculations using the same techniques for Fe^{21+} and Fe^{22+} were carried out by Badnell (1986b). This was also done for Be-like ions (Badnell, 1987), B-like ions (Badnell et al., 1991) $S^+ - S^{5+}$, (Badnell, 1991) and oxygen ions (Badnell, 1989, 1992). Intermediate coupling calculations were carried out by Badnell and Pindzola (1989a) for the boron isoelectronic sequence, by Badnell and Pindzola (1989b) for oxygen and by Badnell and Pindzola (1989c) for Na-like P and Cl. The effects of coupling are expected to be less important for highly charged ions, i.e., charge greater than 20, since the change from *LS* coupling does not open significant additional radiative channels. DR for the ground and excited states of He-like C and O were calculated by Badnell et al. (1990), and for Li-like Al by Badnell (1990). These were compared with R-matrix calculations by Terao and Burke (1990), and the importance of high angular momentum states and stabilization were pointed out. The importance of fine structure and CI were examined in detail for He-like ions by Pindzola et al. (1990), and compared with storage ring experimental results. Gorczyca and Badnell (1996b) demonstrated the importance of CI in Na-like ions, including Fe^{15+}.

Calculations of DR cross sections are most often done perturbatively, using bound state wavefunctions which are calculated separately from the continuum. Gorczyca et al. (1996) compared calculations using R-matrix with an optical potential against perturbative methods for calculating DR in the Ar^{15+} ion, showing agreement between the methods. This provides validation for the use of R-matrix methods for cases where the isolated resonance approximation is likely to be inaccurate. Rate coefficients which use continuum wavefunctions calculated in the R-matrix method and which combines both RR and DR into a unified rate coefficient have been calculated by Nahar and Pradhan (1994) and Nahar (1995, 1996a). Total recombination rate coefficients were calculated using R-matrix for DR into Si, Si^+, S^+, S^{2+}, C^+, C, N^+, O^{2+}, F^{3+}, Ne^{4+}, Na^{5+}, Mg^{6+}, Al^{7+}, Si^{8+}, and S^{10+}, (Nahar, 1995) and for iron ions (Nahar, 1996a).

Important to any close-coupling treatment of DR is the effect of radiation damping. This corresponds physically to the effect of radiative decays on the resonant capture state, and which formally determines the width of the resonance and therefore its effect on the rate coefficient. The importance of this effect, and the limitations of R-matrix calculations of DR, were discussed by Gorczyca et al. (2002), by comparing computational techniques applied to recombination into Fe^{16+}. They showed the importance of accurate treatment of resonance damping, adequate numerical resolution of resonances and inclusion of radiative decays to autoionizing states, and that these effects can be treated more efficiently and accurately using perturbative calculations.

Recent Developments

In a series of papers beginning with Savin et al. (1997), measurements were made of the resonance strengths and energies for several iron ions in the Li-Ne isoelectronic sequences using the heavy-ion Test Storage Ring in Heidelberg, Germany. This apparatus has the combined advantages of low background and negligible metastable content. Savin et al. (1999a) measured the energy dependent cross section for $Fe^{17+} \rightarrow Fe^{16+}$ and $Fe^{18+} \rightarrow Fe^{17+}$ Δn=0 DR and calculated DR rate coefficients. They found significant discrepancies between rate coefficients inferred from their measured cross sections and those of other published calculations. In a comparison with the calculations of Jacobs et al. (1977a) and Roszman (1987a), who only published Maxwellian-averaged rate coefficients, Savin et al. (1999a) demonstrated that such comparison can be used to identify discrepant calculations, but cannot clearly identify the approximation responsible for the error, and that agreement between measured and calculated rate coefficients is not a reliable test of the validity of a calculation. The accuracy of DR calculations can best be evaluated by comparison of resonance strengths and energies in the cross section. Savin et al. (1999a) show that single configuration *LS* coupling calculations overestimate $Fe^{18+} \rightarrow Fe^{17+}$ by a factor 1.6. This may be due to the use of *LS* coupling which leaves out important autoionizing channels, or it could be due to inaccurate resonance energies.

Savin et al. (2002a) measured resonance strengths and energies for DR of $Fe^{18+} \rightarrow Fe^{17+}$ via $n = 2 \rightarrow n' = 2$ and $n = 2 \rightarrow n' = 3$ core excitations. They have also calculated these resonance strengths and energies using two independent techniques: the perturbative multiconfiguration Breit-Pauli (MCBP) and multiconfiguration Dirac-Fock (MCDF) methods, finding reasonable agreement between experimental results and theoretical calculations. The left panel (a) of figure 9 shows the results of measurements made using tokamaks by Isler, Crume and Arnurius (1982) and Wang et al. (1988b), theoretical calculations by Jacobs et al. (1977a), Roszman (1987a), and Dasgupta and Whitney (1994) and those adopted in the compilation of Mazzotta et al. (1998) and the RR rate coefficients calculated by Arnaud and Raymond (1992). This shows the dispersion in rate coefficients obtained by various workers is a factor ~10 at low temperatures, and a factor ~3 at coronal temperatures, far greater than the estimated experimental uncertainties. The right panel (b) of Figure 9 shows the storage ring measurements of Savin et al. (2002a), along with calculations using MCBP (AUTOSTRUCTURE) and MCDF. Savin et al. (2002b) measured the resonance strengths and energies for DR of $Fe^{19+} \rightarrow Fe^{18+}$ Δn=0 core excitations. They have also calculated the DR resonance strengths and energies using four different theoretical techniques: AUTOSTRUCTURE, HULLAC, MCDF, and R-matrix methods. On average the theoretical resonance strengths agree to within $\leq$ 10%. However, the 1 σ scatter in the comparison is 30%, so that calculations of individual emission lines due to DR will have a scatter of approximately this magnitude, although the ensemble will be more accurate.

Savin et al. (2003) measured DR resonance strengths and energies for $Fe^{20+} \rightarrow Fe^{19+}$ for $Fe^{21+} \rightarrow Fe^{20+}$ via $\Delta n = 0$ core excitations. They have also calculated these resonance strengths and energies using three techniques: multiconfiguration Breit-Pauli (MCBP) method using AUTOSTRUCTURE, and MCDF and FAC. Although there is general agreement between experiment and theoretical calculations, discrepancies occur for collision energies $\leq$3 eV. Nonetheless, the storage ring experiments and the careful comparison with various computational platforms provide crucial benchmarks. These make it clear which computational techniques and approximations are most reliable, and the level of accuracy which can be expected. These techniques can then be applied on a large scale to provide DR cross sections and rate coefficients for astrophysical applications.

Other storage ring measurements include those of DeWitt et al. (1995) for He^{+}, Zong et al. (1997) for Ar^{15+}, Mannervik et al. (1998) for C^{3+}, Glans et al. (1999) for F^{6+}, Glans et al. (2001) for N^{4+}, Bohm et al. (2002, 2003) for O^{5+}, Bohm et al. (2001) for Ne^{7+}, Fogle et al. (2003) for Ni^{17+}, and Nikolić et al. (2004) for Na^{8+}; these are summarized by Glans et al. (2004). Many of these include comparison with calculations which utilize relativistic many-body perturbation theory, and take into account QED effects in the position and strengths of resonances. Kenntner et al. (1995) measured DR for Li-like Cl and Si and Fogle et al. (2005) has measured DR for Be-like C, N and O using similar apparatus. Measurements of DR have been done using a single-pass merged-beam by Andersen et al. (1992a,b) for He-like and Li-like ions of nitrogen, fluorine, and silicon. These authors point out the importance of resonances associated with the $1s2s(^3S)$ metastable state in the He-like case. They also point out the importance of intermediate coupling in determining the resonance structure and hence the DR rate coefficient in situations when the electron velocities sample resonances close to the ionization threshold for the metastable state. The use of merged beams for DR and for electron collisional excitation and for charge transfer has been reviewed by Phaneuf et al. (1999), and the use of storage rings for measurements of recombination is reviewed by Schippers (1999).

Building on the experimental results of Savin and coworkers, large scale calculations of state-selected cross sections and rate coefficients for DR in intermediate coupling using the AUTOSTRUCTURE (Badnell et al., 2003) code have been carried out by Badnell, Gorczyca, and coworkers. These include calculations for the various isoelectronic sequences H-Na (Altun et al., 2004, 2005, 2006; Badnell, 2006; Colgan et al., 2003, 2004, 2005; Mitnik and Badnell, 2004; Zatsarinny et al., 2003, 2004a,b, 2005a,b, 2006). In a complementary effort Gu (2003b) has used FAC to calculate total DR rate coefficients for the H-like through Ne-like isoelectronic sequences for the 7 elements Mg, Si, S, Ar, Ca, Fe and Ni. Together these remove the shortcomings of early calculations, namely that of LS coupling and the choice of energetically allowed channels for applications at coronal temperatures. For applications at temperatures characteristic of photoionized plasmas, large uncertainties remain owing to the use of *ab initio* energy level structure intrinsic in this work. This has been shown by the storage ring measurements of Schippers et al. (2004), who demonstrate the existence of strong resonances in the recombination cross section for Mg^{8+} at electron energies 20-70 meV. They point out that errors in the location of these resonances of only 100 meV can result in changes of a factor up to a factor $\sim$3 in the total recombination rate coefficient at low temperatures. However, with these calculations and their experimental validation, the rate coefficients for DR at coronal temperatures for many ions of astrophysical interest have reached a level accuracy previously unattained.

One remaining area of uncertainty is the role of external fields on DR. According to Badnell et al. (2003), this renders pointless efforts to compute field-free rate coefficients to an accuracy of better than 20%. It has long been known that the high Rydberg states that frequently dominate the DR process can be Stark-mixed by weak electric fields (Burgess and Summers, 1969), such as the plasma microfield (Jacobs, et al., 1976), and so increase the partial rate coefficients by factors of 2 or more over a wide range of n. Recently, the picture has been further complicated by the discovery that magnetic fields, when crossed with an electric field, strongly affect the electric field enhancement, by reducing it in most cases (Bartsch et al., 1999; Robicheaux and Pindzola, 1997). This suppression of the electric field enhancement improves the applicability of field-free DR rates, but does not remove the uncertainty due to field effects in modeling of real plasmas. The importance of field effects, and the field strengths themselves, can be derived through collisional radiative modeling of the dynamic part of the plasma microfield (Badnell et al., 2003). Previously it appeared that a reasonable approach would be to use the values of the plasma microfield for the electric field strength for use in the generation of field dependent data as input to plasma modeling, but the added sensitivity to the magnetic field makes this impractical.

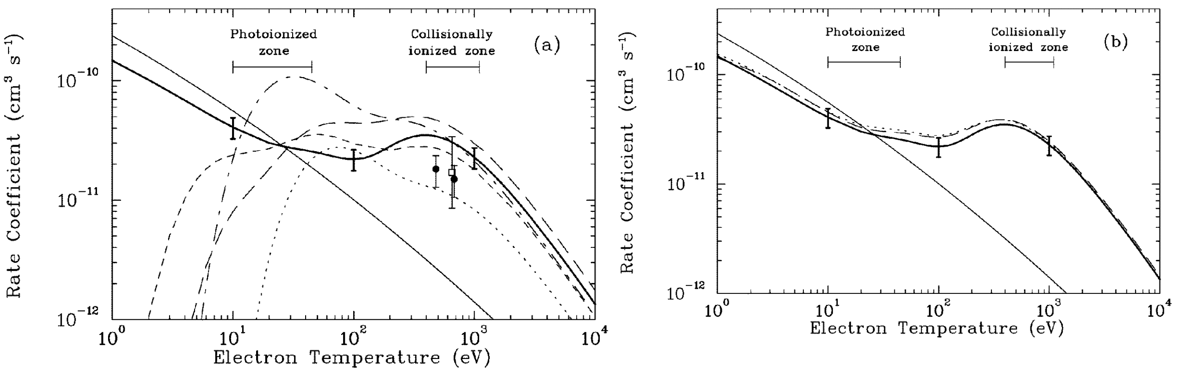

FIG. 9 Left panel (a): Fe^{18+} – Fe^{17+} rate coefficient for recombination. The thick solid curve represents the experimentally derived rate coefficient from Savin et al. (2002b). The thick error bars show the estimated experimental uncertainty of 20%. Symbols show tokamak results of Isler, Crume and Arnurius (1982) (filled circles) and Wang et al. (1988b) (open squares). Curves are DR rate coefficients calculated by Jacobs et al. (1977a) as fitted by Shull and van Steenberg (1982a,b) (dotted curve), Roszman (1987a) (short-dashed curve), and of Dasgupta and Whitney (1994) (long-dashed curve), and recommended DR rate coefficient of Mazzotta et al. (1998) (dot-long-dashed curve), and recommended RR rate coefficient of Arnaud and Raymond (1992) (thin solid curve). None of the experimental or theoretical DR rate coefficients include RR. The range of temperatures at which these processes are likely to occur in equilibrium are denoted for photoionized and collisionally ionized plasmas. Right Panel (b): As in (a) the thick solid curve represents the rate coefficient derived from the storage ring experiment of Savin et al. (2002a), and the thin solid curve shows the recommended RR rate. The dotted curve shows the MCBP calculations and the dashed curve shows the MCDF calculations of the DR rate coefficents calculated by Savin et al. (2002a). Both calculations are for capture into states including capture states for all values of nl (i.e. $n_{max} = \infty$) and both include DR via $1 \rightarrow 2$, $2 \rightarrow 2$, and $2 \rightarrow 3$ core excitations. None of the experimental or theoretical DR rate coefficients in (a) or (b) include RR. From Savin et al. (2002a).

3. Collisional Excitation

Background

Collisional excitation or deexcitation, by electrons or protons, is closely associated with discrete diagnostics, since it is the dominant mechanism affecting the level populations associated with many diagnostic features. However, it also is key to the calculation of synthetic spectra and for cooling. For spectrum synthesis, comprehensiveness is important in order to accurately calculate cooling rate coefficients and pseudo-continuum emission due to large arrays of blended weak lines.

In tabulating collisional excitation data it is customary to work with the collision strength (Hebb and Menzel, 1940), rather than the cross section. The collision strength between a given pair of levels Ω_{ij} is defined such that $\Omega_{ij} = \Omega_{ji}$, and the excitation cross section is given by

$$\sigma_{ij} = \frac{\pi a_0^2}{\omega_i k_i^2}\Omega_{ij} \tag{29}$$

where ω_i is the statistical weight of level i. The Maxwellian averaged collision strength is denoted Υ_{ij} and preserves this symmetry.

Although, calculations are of greater practical importance to collisional excitation than experiments owing to the large number of transitions which may be of interest, measurement of plasma spectra can be used to infer collision rates. This makes use of assumptions about the excitation mechanism and with independent measurements of the gas density and temperature. Examples include the measurements of Datla et al. (1976), who deduced ionization rate coefficients for He-like B and C from the time histories of the lines emitted by these ions ions in a theta-pinch plasma and compared theoretical estimates using the semi-classical formula of Burgess with experimental results, corrected for the effects of metastables. Johnston and Kunze (1971) determined electron collision-excitation rate coefficients experimentally for n=2, 3, and 4 levels of Be-like N^{3+}, O^{4+}, Ne^{6+}, and Si^{8+} using plasma produced in a theta pinch device. Tondello and McWhirter (1971) measured excitation rate coefficients for eighteen transitions in Ne^{7+}. A review of methods and some results was presented by Kunze (1972).

A general review of experimental techniques and results is given by Dunn et al. (1995). The use of merged beams for electron collisional excitation and for charge transfer has been reviewed by Phaneuf et al. (1999). Recent measurements of $2s - 2p$ excitation in Li-like ions C^{3+} and O^{5+} have been carried out using merged beams by Greenwood et al. (1999) and Lozano et al. (2001), and for S^{3+} by Smith et al. (2000a). Measurements of selected transitions have provided crucial checks on calculations (Beiersdorfer et al., 2002) for spectra such as Fe^{16+}, and the EBIT apparatus has been used to benchmark cross sections and density dependent line ratios for N^{5+}, Ar^{13+} and Fe^{21+} (Chen et al., 2004).

An early review of computational techniques for collisional excitation is that of Bely (1966). These include the Born approximation, in addition to other computational methods, which require the consideration of many partial waves and so are slow when carried out on older computers. For this reason the Bethe approximation was widely used in early work. This is based on the fact that at very high energy distant encounters are most important and the projectile remains outside the atom most of the time. Then the cross section can be expressed as a proportionality with the oscillator strength of the transition. The proportionality is expressed as a Gaunt factor, and values of effective $\bar{g}$ were derived by Van Regemorter (1962). This allowed the use of radiative transition probabilities directly in modeling of collisional plasmas. This formula was used, for example, in calculation of structure and collision strengths for Fe^{7+} by Czyzak and Krueger (1966) and compared with and results from Hartree-Fock with exchange self-consistent wavefunctions. This approximation is no longer in widespread use, since more accurate methods can now be conveniently applied to large numbers of transitions.

Coulomb Born Oppenheimer (CBO) calculations of collisional excitation in H-like ions were performed by Burgess et al. (1970) and Golden and Sampson (1971). Screened hydrogenic calculations of collisional excitation for atoms with less than 4 electrons were performed by Sampson and Parks (1974). Golden et al. (1981) calculated scaled collision strengths for hydrogenic ions using the CBO method, and Clark et al. (1982) calculated scaled collision strengths for excitation of highly charged ions.

An early mention of the importance of CI for collisional excitation rate coefficients was by Layzer (1951). Jones (1970) extended the Eissner and Nussbaumer CI code to include relativity, and illustrated that drastic changes in A values can occur depending on the treatment of CI. Ermolaev and Jones (1972) explored the importance of CI in He-like ions and mixing between ^1P and ^3P, especially for $Z > 2$ using both Breit-Pauli and Z-expansion techniques. Nussbaumer (1972a) discussed the importance of CI for the ion C^{2+}. Flower (1972) estimated collision strengths and showed that Li-like lines are useful temperature diagnostics in solar corona if 2-2 and 2-3 lines can both be measured. Bely-Dubau (1973) and Flower and Pineau des Forets (1973) performed CI calculations for Fe^{12+}. The pitfalls of CI calculations which have deficient sets of configurations and can lead to errors were examined by Nussbaumer (1973), with the ion Fe^{12+} (Flower and Pineau des Forets, 1973) used as an example. Loulergue and Nussbaumer (1973) demonstrated the effects of blending on the 17.06 Å line in a CI calculation of the structure and excitation rate coefficients for Fe^{16+}. Jones (1974) calculated collision strengths for He-like ions of Si, Ca, Fe comparing the results of LS coupling and intermediate coupling using a DW method. The effects of relativity were examined by Walker (1974), who calculated electron impact excitation of the $n = 1$ and $n = 2$ states of hydrogenic ions in the Coulomb-Born approximation using Dirac wavefunctions.

A comparison of distorted wave and close coupling calculations of collision strengths for transitions in C^{2+} excited by electron collisions (Flower and Launay, 1972) indicates that the distorted wave method is sufficiently accurate for many astrophysical and laboratory applications. DW calculations for many ions have been carried out by Bhatia, Mason and coworkers, cited in Section VI. Calculations using similar techniques have been made for S^{10+} (Landi and Bhatia, 2003a), Ca^{6+} (Landi and Bhatia, 2003b), Fe^{17+} (Cornille et al., 1992), Fe^{20+} (Phillips et al., 1996), Ne^{2+} (Landi and Bhatia, 2005c), Ca^{13+} (Landi and Bhatia, 2005b), Ca^{12+} (Landi and Bhatia, 2005a), and Ar^{11+} (Eissner et al., 2005). Fawcett and Mason (1991) calculated collision strengths and oscillator strengths for Fe^{8+}. Collisional excitation rate coefficients for H-like and He-like ions calculated using a relativistic DW method have been calculated by Sampson et al. (1983) and Zhang and Sampson (1987). This has also been applied to the F (Sampson et al., 1991), Na (Sampson et al., 1990), B (Sampson et al., 1986; Zhang and Sampson, 1994a,b), Li (Zhang et al., 1990), Be (Zhang and Sampson, 1992), and C (Zhang and Sampson, 1996) isoelectronic sequences. Collections of references to calculations of collisional excitation have been provided by Kato (1976), Raymond and Smith (1977), Mewe and Gronenschild (1981), and Mewe et al. (1985, 1986). Reviews of calculations of available electron excitation cross sections for many ions of interest were presented as part of a 1994 conference on collisions by Fossi and Landini (1994), Cornille et al. (1994a), Mason (1994), Pradhan (1994), Dufton and Kingston (1994), Bhatia et al. (1994), Lang and Summers (1994), Kato (1994), Sampson et al. (1994), Berrington (1994), McWhirter (1994), Dubau (1994), and Callaway (1994).

Recent Developments

Close coupling calculations are available for an increasing fraction of transitions needed to model coronal plasmas. R-matrix calculations of collisional excitation have been carried out for hydrogenic ions of C (Aggarwal and Kingston, 1991a), Ne (Aggarwal and Kingston, 1991b), Si (Aggarwal and Kingston, 1992a), Ca (Aggarwal and Kingston, 1992b), Fe (Aggarwal and Kingston, 1993). R-matrix intermediate coupling calculations have been made for He-like and Li-like Ar and Fe by Whiteford et al. (2001, 2002). Calculations for Be-like ions have been reviewed by Berrington (1994). The breakdown of the isolated resonance approximation and the importance of accurate treatment of radiation damping in calculations of collisional excitation, in contrast with the situation for DR, was pointed out by Badnell and Pindzola (1993). The point is that two or more Rydberg series of resonances will interfere only if they overlap because coupling through the background is weak, or absent. In contrast, for electron-impact excitation there is strong coupling through the background. There is no dipole selection rule and consequently number of resonances increase greatly, so that close-coupling technique or a perturbative approach to overlapping resonances are needed. Such a situation is seldom met in photoionization and DR cross section because the number of accessible resonances is limited by dipole selection rules.

A comparison of relativistic DW and R-matrix calculations for Fe^{21+} was carried out by Gu (2004). In order to test for the importance of channel coupling and breadown of the isolated resonance approximation, the two calculations were compared using the same energy level structure, and good agreement between the two methods was found for most transitions, for both resonance structure and for the background cross section. This is in contrast to Badnell and Pindzola (1993), who demonstrated factor ~2 errors in the dominant resonant contributions to the excitation of Mg-like ions. Thus uncertainties introduced by the DW + isolated resonance approximation can be significant. R-matrix calculation of excitation of many X-ray transitions have been carried out by the Iron project (Hummer et al., 1993). This work is continuing and the results are contained in the TIPTOPbase database (Cunto and Mendoza, 1992). A sample of publications include those for Fe^{20+} (Butler and Zeippen, 2000), Fe^{19+} (Butler and Zeippen, 2001a), Fe^{18+} (Butler and Zeippen, 2001b), Fe^{11+} (Binello et al., 1998a,b), the oxygen isosequence (Butler and Zeippen, 1994), Ca^{7+} (Landi et al., 2004), Fe^{15+} (Eissner et al., 1999), the Cl isosequence (Pelan and Berrington, 1995), Fe^{13+} fine structure (Storey et al., 1996), the B isosequence (Zhang et al., 1994) and for Fe^{2+} (Zhang, 1996). R-matrix calculations have been made for the fine structure levels of Fe^{12+} and for Fe^{10+} (Gupta and Tayal, 1998, 1999). Most of these do not include levels in the $n = 4$ manifold, but do account for relativistic effects using the Breit-Pauli Hamiltonian and intermediate coupling. Exceptions include the R-matrix calculations for He-like O by Delahaye and Pradhan (2002) and He-like Ne by Bautista et al. (2003). The mission of the Iron Project has been extended into the X-ray region by the UK RmaX Network (http://amdpp.phys.strath.ac.uk/UK_RmaX).

Close-coupling calculations which include $n = 4$ and intermediate coupling have been carried out for Fe^{20+} by Badnell and Griffin (2001) and for Fe^{21+} by Badnell et al. (2001), and show general consistency with the Iron Project results. The difference between collision strengths calculated using the close-coupling approximation from those calculated using DW is illustrated in Figure 10, taken from Eissner et al. (1999). This shows the effective collision strength for the $3s^2\ ^1S_0 \rightarrow 3s3p\ ^3P_1^o$ transition in Fe^{14+} as a function of temperature for close-coupling (circles) and DW calculations (squares). The difference at low temperatures is due to the cumulative effect of resonances, which are not accounted for by DW method. At the temperature corresponding to the peak abundance of this ion in coronal equilibrium, log(T)≃6.4, the two methods give very nearly the same result. The role of CI in collisional calculations is illustrated in Figure 11. This shows comparison of the effective collision strength for the $2s^22p^2(^3P_0^e) \rightarrow 2s^22p^2(^1D_2^e)$ transition in Fe^{20+} as a function of temperature calculated using BPRM (Butler and Zeippen, 2000) with those of Aggarwal (1991) which used MCDF. The latter, although it includes a more complete treatment of relativistic interactions, omits the n=3 configurations and so under predicts the resonance structure at high temperature, where these resonances can be excited.

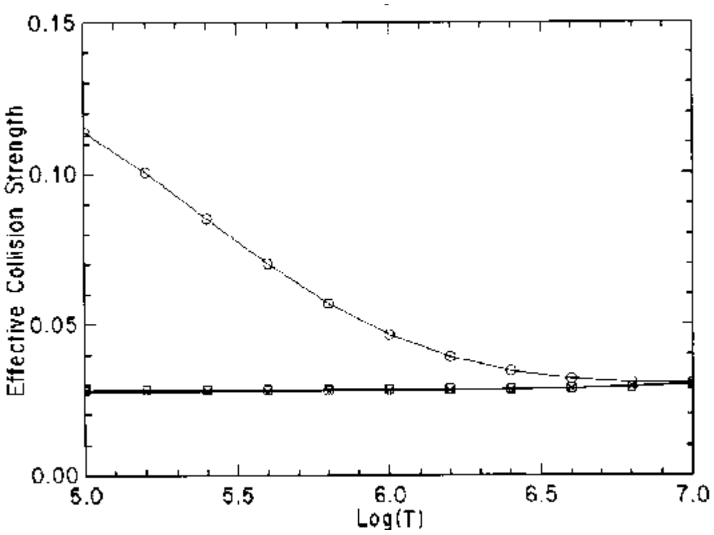

FIG. 10 The effective collision strength for the $3s^2\,^1S0 \rightarrow 3s3p^3P_1^o$ transition in Fe^{14+} as a function of temperature for close-coupling (circles) and DW calculations (squares). from Eissner et al. (1999)

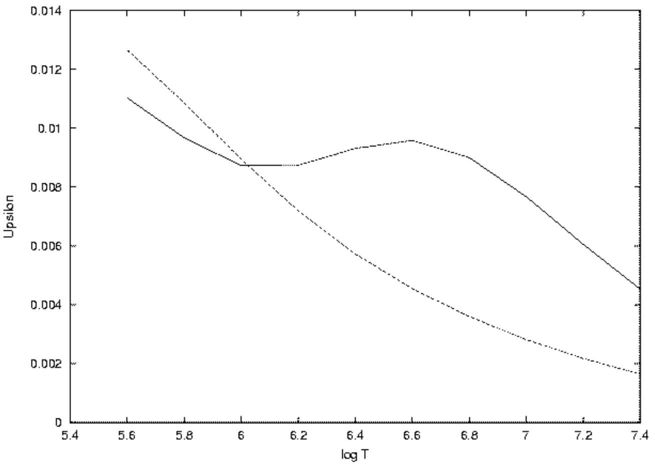

FIG. 11 Comparison of the collision strength for the $2s^22p^2(^3P_0^e) \rightarrow 2s^22p^2(^1D_2^e)$ transition in Fe^{20+} calculated using BPRM (solid curve; (Butler and Zeippen, 2000)) with calculated using MCDF by Aggarwal (1991) (dashed) as a function of temperature (from Butler and Zeippen (2000))

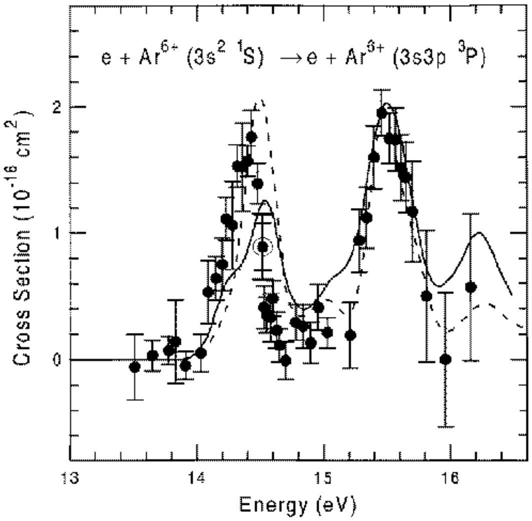

FIG. 12 Comparison of the collision strength for the $3s^2\ {}^1P_0 \rightarrow 3s3p\ {}^3D$ transition in Ar^{6+} calculated using an R matrix calculation (solid curve) (Griffin et al., 1993), an isolated-resonance DW calculate (dashed curve), and experimental merged beam measurements (Smith et al., 2003). from Smith et al. (2003)

Measured line ratios and absolute rate coefficient are important for validating calculations. Absolute cross sections have been measured for electron impact excitation of a few ions, for example C^{3+} $2s(^2S_{1/2}) \rightarrow 2p(^2P_{1/2,3/2})$ for energies near threshold by Savin et al. (1995) (see also Janzen et al. (1999) for further work and references to other measurements), for Fe^{16+} by Brown et al. (2001b), and Beiersdorfer et al. (2002, 2004), and for Fe^{20+} – Fe^{23+} by Chen et al. (2005). These serve as important tests for close-coupling calculations such as those of Chen and Pradhan (2002). An example is shown in figure 12, which shows a comparison of the collision strength for the $3s^2(^1P_0) \rightarrow 3s3p(^3D)$ transition in Ar^{6+} calculated using an R matrix calculation (Griffin et al., 1993); an isolated-resonance DW calculations and experimental merged beam measurements (Smith et al., 2003). These illustrate the importance of resonances, which are more prominent in the spin-forbidden transition shown here, and the difficulty in accurately calculating resonance strength. An added uncertainty in experimental measurements comes from the fact that experiments such as those shown in Figure 12 must detect the scattered electrons in order to discriminate between various excitation channels, and the angular scattering distribution must be understood in order to correct for the electrons which miss the detectors. Similar comparisons have been performed by Djurić et al. (2002).

Bibliographies of the available data for collisional excitation were published by Itikawa et al. (1984) and Itikawa (1991, 1996, 2002), all designed primarily for fusion applications, and by Pradhan and Gallagher (1992). Reviews organized by isosequence include the aforementioned conference proceedings from 1994 (e.g. Berrington (1994) etc.). Much recent work relevant to X-ray astronomy is contained in the CHIANTI database. These include papers by Dere et al. (1997), Landi et al. (1999), Dere et al. (2001), Young et al. (2003), Landi et al. (2004) Landi and Phillips (2005), and Landi et al. (2005), and papers describing the Arcetri spectral code (Landi and Landini, 1998, 2002).

4. Radiative Transition Probabilities

Background

Traditional modeling of coronal plasmas assumed that radiative decay to the ground level is more rapid than excitation or decay to excited levels. As a consequence, all dipole-allowed line emission and cooling could be calculated without explicit reference to the rate coefficients for radiative decay. Recent plasma models, such as APEC (Smith et al., 2001), calculate all level populations explicitly, and therefore require transition probabilities for transitions in all decay paths of excited levels.

Radiative transition probabilities are conveniently parameterized in terms of the oscillator strength, which has a value of unity by definition for a classical point charge. Non-relativistic quantum mechanical oscillator strengths for hydrogen have been tabulated by Menzel and Pekeris (1935). It is also customary to define the oscillator strength for hydrogen in terms of the semi-classical Kramers expression:

$$f_K(n,n') = \frac{32}{3\pi\sqrt{3}} \left(\frac{1}{n'^2} - \frac{1}{n^2}\right)^{-3} \left(\frac{1}{n^3 n'^5}\right) g_I(n',n) \tag{30}$$

along with a Gaunt factor $g_I(n',n)$. These are tabulated in, e. g., Baker and Menzel (1938).

Classic tabulations of these include the H-like oscillator strengths of Wiese et al. (1966), along with the compilations of NIST (Fuhr et al., 1999). For hydrogen-like ions without relativity exact calculation is possible (Bethe and Salpeter, 1972). Treatment of non-dipole allowed processes such as 2 photon decay (Shapiro and Breit, 1959) and magnetic dipole rate coefficients (Parpia and Johnson, 1972) requires treatment of the effects of QED and nuclear size.

Examples of DW calculations include: transition probabilities for lines from Al-like ions (Nussbaumer, 1977), transition probabilities within the $2s^2 - 2s2p - 2p^2$ manifold in the Be isosequence (Muehlethaler and Nussbaumer, 1976), radiative data for the Mg isosequence (Christensen et al., 1986), transition probabilities for ground configuration of S^{3+} (Johnson et al., 1986), transition probabilities for transitions within the ground configuration of S^{2+} and other Si-like ions (Huang, 1985), and oscillator strengths for He-like allowed lines and collision strengths among fine structure levels (Zhang and Sampson, 1987). It is worth noting that, although ground state fine structure transitions often fall outside of what is typically considered the X-ray band, the structure and transition probabilities are relevant to the X-ray spectrum from these ions seen in absorption, and they may also be useful for study of higher energy transitions which belong to the same isoelectronic sequence. Martin et al. (1993) calculated transition probabilities in the lithium sequence. DW calculations of oscillator strengths have been carried out for $2s-2p$ transitions Be, B, C, N, and O (Fawcett et al., 1978), and for $\Delta n=0$, 1 transitions in the O, S, P (Fawcett, 1986a,b,c) and C (Fawcett, 1987) isosequences.

Cowan et al. (1984) presented theoretical calculation of wavelengths and oscillator strengths for Fe^{9+}. They pointed out the importance of spin-orbit and configuration-mixing effects in the calculation of wavelengths and oscillator strengths for heavy-element moderately charged ions. This technique involves calculation of the energy level structure and line spectrum for a variety of ions by collecting available experimental data from laboratory and solar measurements, adjusting in order to obtain smooth variation along isoelectronic sequence, and then using these levels to calculate the structure of model ions using a semi-empirical code (Cowan, 1981). This was done for Fe^{11+} and Fe^{12+} $3p-3d$ and $3s-3p$ transitions (Bromage et al., 1978a), Be-like and B-like iron (Bromage et al., 1978b), the $2p^2-2p3d$ transition array of Fe^{20+} and isoelectronic spectra (Bromage and Fawcett, 1977a), the $2s^22p^n-2s^22p^{n-1}4d$ Fe^{17+} and Fe^{18+} lines (Bromage et al., 1977a), much of which was updated by Cornille et al. (1992), the $2p^3-2p^23d$ transition array in Fe^{19+} and isoelectronic ions (Bromage and Fawcett, 1977b), and the $3s^23p^n-3s^23p^{n-1}3d$ transitions in Fe^{9+} and Fe^{10+} (Bromage et al., 1977b). A compilation of collisional excitation and radiative decay rate coefficients for lines of $2s^22p^k$, $2s2p^{k+1}$, and $2p^{k+2}$ configurations, and for the O, N, C, B, and Be isoelectronic sequences of Ti, Cr, Fe, Ni was produced by Feldman et al. (1982). A compilation of transition probabilities for Cr, Fe, Ni ions in the B, C, N, O, and F isosequences was produced by Feldman et al. (1980).

Recent Developments

Close-coupling transition probabilities for many dipole-allowed transitions of interest have been calculated by the Opacity Project (Seaton, 1987) and are contained in the the TOPbase database (Cunto and Mendoza, 1992). These use LS coupling and are tabulated with theoretical wavelengths, and therefore are not directly applicable to synthesis of spectra and do not include forbidden transitions. Their application to observations has been aided by the work of Fuhr et al. (1999) who have matched these with experimental wavelengths where possible and redistributed the oscillator strength among fine structure levels. Other CI calculations of transition probabilities include oscillator strengths of F-like ions for $18< Z <33$ using CIV3 (Blackford and Hibbert, 1994). Iron Project calculations include intermediate coupling and relativistic effects in the Breit-Pauli approximation. These include extensive work on forbidden transitions within the ground configuration of complex ions, whose wavelengths generally place them outside the scope of this review (Galavis et al., 1997). An annotated bibliography of transition probabilities for allowed and forbidden transitions with some overlap to the X-ray and EUV band is presented by Biemont and Zeippen (1996). Quinet (2000) calculated the wavelengths and oscillator strengths using HFR for the $3p4s$, $3p4d$, $3p5s$ and $3p5d$ transitions in Fe^{8+}–Fe^{13+} appearing in the soft X-ray region. Close coupling calculations of transition probabilities for fine structure transitions in S^{3+} have been calculated by Tayal (1999). Storey and Zeippen (2000) presented transition probabilities for transitions within the ground configuration of the carbon and oxygen iso-electronic sequences. Opacity Project line strengths have been incorporated into the line list for use in absorption line studies by Verner, Verner and Ferland (1996). These used a compilation of experimental energy levels similar to that used by NIST and Opacity Project wavelengths derived using LS coupling rules for lines originating from ground-term multiplets in the spectral region 1–200 Å . Experimental measurements of radiative lifetimes for excited levels of many ions have been reviewed by Träbert (2002).

B. Photoionized Plasmas

In gases exposed to strong ionizing radiation, or in the absence of strong mechanical or non-radiative heating, the ionization balance can be determined by the effects of photoionization and recombination. In this case the gas temperature is determined by a balance between heating and cooling due to photon interactions. Heating processes include slowing down of fast photoelectrons, and Compton scattering, while cooling is due to emission processes analogous to those in a coronal plasma. Early discussion of this was by Tarter et al. (1969) and Tarter and Salpeter (1969). Traditional application for photoionization models was HII regions and planetary nebulae (Flower, 1968, 1983), but it is now apparent that photoionization is dominant in many X-ray sources as well, such as active galaxies (e. g., Figures 1 and 4).

The condition for photoionization to dominate over collisions depends on the rate of mechanical heating, if any, and on the ratio of the ionizing flux to the gas density, n, which is called the photoionization parameter. Various definitions are in use, those most widely quoted are $U=N/(\mathrm{n}c)$ where N is the number flux of ionizing photons (i.e., photons with energies greater than 1 Ry), and $\xi=4\pi F/\mathrm{n}$, where F is the energy flux of ionizing photons, typically in the 1-1000 Ry energy range.

The choice of convention for ionization parameter definition is arbitrary. Any accurate calculation of photoionization rate coefficients or heating must take into account the shape of the ionizing spectrum in detail; the ionization parameter serves as a constant of proportionality for use in describing model results. Certain choices of ionization parameter are more directly related to the problem to be solved, which explains in part the origins of the differing conventions. Photoionization rate integrals can be written

$$\text{rate} = \int_{\varepsilon_{th}}^{\infty} F_\varepsilon \sigma(\varepsilon) \frac{d\varepsilon}{\varepsilon} \tag{31}$$

where ε_{th} is the ionization threshold energy for the bound level in question, F_ε is the ionizing flux in units erg cm^{-2} s^{-1} erg^{-1}, and the photoionization cross section is $\sigma(\varepsilon)$. This quantity scales with energy above threshold as $\sigma(\varepsilon) \propto \varepsilon^{-\gamma}$ where $\gamma \sim 3$. So the photoionization rate and heating integrals are always dominated by the behavior at threshold if $d\log(F_\varepsilon)/d\log(\varepsilon) \leq \gamma$. In classical photoionized nebulae, such as HII regions or planetary nebulae, the behavior of the model depends most sensitively on the ionizing photon flux at 1 Ry. The total number of ionizing photons N is also weighted toward the flux at 1 Ry unless F_ε increases faster than $\propto \varepsilon^1$. However, photons at 1 Ry have less influence on the ionization of ions typically observed in the X-ray band than do photons at energies greater than ∼0.25 keV. Study of X-ray photoionized plasmas differs from classical photoionized nebulae in that it is often possible to directly observe the photons responsible for the ionization of gas responsible for line emission or absorption, which is motivation for an ionization parameter which is more closely coupled to the continuum in the X-ray band than is N. This has led to the suggestion by Netzer (1996) of the use of the parameter $U_X = N_X/(\mathrm{n}c)$ where N_X is the number flux of ionizing photons above 0.1 keV. The choice of ξ is motivated by the fact that it is more heavily weighted toward the X-ray band by using ionizing energy flux rather than number flux. Also, heating by Compton scattering is proportional to the photon energy flux. ξ has units implied (typically erg s cm^{-1}), while U is dimensionless. The study of photoionized gases in which the pressure is prescribed rather than the density has led to the further definition of an ionization parameter $\Xi = F/(cP)$, where P is the gas pressure (Krolik et al., 1981). This quantity is dimensionless. It is important to note that no matter what definition of ionization parameter is adopted, it serves only as a convenient scaling quantity. Real calculations take into account the full frequency dependence of the radiation spectrum, and so do not depend ultimately on the convention which is used.

Since the ionizing radiation spectrum may not, in general, be a pure thermal spectrum, photoionization is not conveniently parameterized by a rate coefficient depending on temperature. Rather, it is customary to consider the full energy dependent cross section, and perform the calculation of the ionization rate by integrating this over the photon flux distribution. Photoionization cross sections are also important for calculations of the inverse process, RR, via the Milne relation (Osterbrock and Ferland, 2006). In the case of RR, cross sections to excited levels are important. In many cases of astrophysical interest the equilibrium populations of excited levels are negligible, so that for the purpose of calculating the ionization rates, it is only necessary to consider photoionization from the ground level or term. For this reason many traditional calculations were applied only to the ground term. Recent calculations have addressed rate coefficients for excited levels, which are increasingly being self-consistently included in level population calculations for most ions. An added feature of photoionization is that, owing to the non-thermal nature of the radiation field, ionization from inner electronic shells can be important for ions with 3 or more electrons. In contrast, EII generally results in a smaller contribution from inner shell ionization. A thermal electron energy distribution has too few electrons at the high energies needed for inner shell ionization (at least $5-10$ times the valence threshold), although excitation-autoionization is important for many isoelectronic sequences.

1. Photoionization

Background

Analytic expressions for the photoionization cross section of hydrogen can be obtained in the same way as for bound-bound transition oscillator strengths if the upper level is allowed to have an imaginary principle quantum number, ik. The oscillator strength can then be written

$$f_{nk} = \frac{32}{3\pi\sqrt{3}} \left(\frac{1}{n^2} + \frac{1}{k^2}\right)^{-3} \left(\frac{1}{k^3 n^5}\right) g_{II}(n,k) \tag{32}$$

where $g_{II}(n,k)$ is the bound-free Gaunt factor (Karzas and Latter, 1961; Menzel and Pekeris, 1935). The cross section involves the density of states, and if this is calculated in the limit of large n then a reasonably accurate approximation is

$$\sigma(E) = (2.815 \times 10^{29}) \frac{g_{II}(n,k)}{n^5 \nu^3} \tag{33}$$

This is a hydrogenic approximation and is independent of angular momentum. The Gaunt factor can take angular momentum into account; the assymptotic dependence of the cross section on energy is $\propto \varepsilon^{-l-7/2}$ (Fano & Cooper, 1968). The exact analytic non-relativistic cross section for l=0,1 is given by Bethe and Salpeter (1972).

A widely used simple parameterization of photoionization cross sections is that of Seaton (1958). This has been fitted to monoconfigurational Hartree-Fock results for the moderately ionized ions important to planetary nebulae by Henry and Williams (1968), Henry (1970), Chapman and Henry (1971) and Chapman and Henry (1972). Photoionization cross sections for He-like ions were calculated by Brown (1971). Photoionization cross sections using Hartree-Slater wavefunctions were calculated by Barfield (1979), who derived a simple scaling behavior along isonuclear sequences which could be used to relate ionic cross sections to those for neutrals. Reilman and Manson (1978, 1979) performed the first large scale calculations of photoionization cross sections using Hartree-Slater wavefunctions, resulting in tabulations of cross sections for all ions of the elements with Z up to 30, including inner shells. Cross sections for excited levels of many ions based on a hydrogenic approximation were calculated by Clark et al. (1986).

The behavior of photoionization cross sections near the thresholds in multi-electron ions is affected by resonance structure due to quasi-bound states. Accurate models for these require calculations using the close-coupling approximation. Near inner shell edges these take the form of photo-excited core (PEC) resonances below the threshold, and the net effect is to fill in the cross section below threshold and smooth the inner shell edge.

Recent Developments

A large scale compilation of close coupling calculations is included in the Opacity Project (Seaton, 1987), with results contained in the TOPbase, which is in turn part of TIPTOPbase (Cunto and Mendoza, 1992) http://cdsweb.u-strasbg.fr/topbase/home.html. Also included as part of TIPTOPbase is the Iron Project database and the OP server, which can calculate Rosseland mean opacities (Mihalas, 1978) for various elemental mixtures using the Opacity Project cross sections. These are LS coupling calculations including channel couplings, carried out for ground states and excited states for all ions of elements with Z up to 30. A widely used compilation was presented by Verner and Yakovlev (1995), who calculated central field cross sections including inner shells based on the Dirac-Slater potential, for most astrophysically important ions. These were scaled to fit the behavior of the R-matrix calculations near threshold, while also having the correct behavior in the high energy asymptotic limit. These are convenient to use, and provide an approximation to the resonance structure near threshold, and therefore can be used to calculate integral quantities such as photoionization rates. However they do not contain the detailed resonance structure near threshold, and so should not be applied to calculations of monochromatic opacity or synthetic spectra. Opacity Project opacities have been recently revised to include inner-shell contributions, using the AUTOSTRUCTURE package, and these are available through the Opacity Project on line database TIPTOPbase (Badnell et al., 2005). Figure 13 shows a comparison of BPRM calculations for O^{4+} with experiment (Champeaux et al., 2003) in the vicinity of the threshold for ground state ionization, showing the extensive resonance structure and general consistency between the measured and calculated cross section.

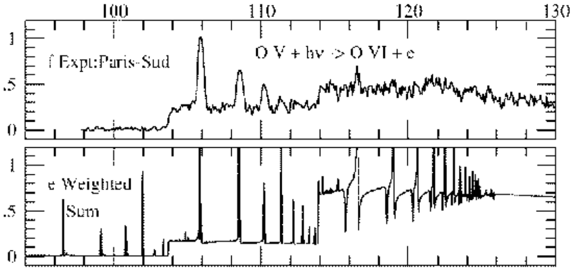

FIG. 13 Comparison of BPRM calculation of the photoionization of O^{4+} with experiment (Champeaux et al., 2003) in the energy range 90-130 eV. Below 103 eV the cross section is due to ionization from the $2s2p$ excited configuration, and the $2s^2$ above, from Nahar (2004).

Even when the total ionization rate is so low that the gas is neutral, or if photoionization is not the dominant ionization mechanism, the spectrum of the radiation field transmitted in the X-ray band is affected by the photoionization cross section. Thus a knowledge of the cross section is needed to interpret observations of X-ray absorption. In this case, spectroscopic accuracy can be important, since features in the cross section can be used to diagnose the conditions in the absorbing gas (Paerels et al., 2001). Examples of such features include the line features due to K shell photoexcitation in oxygen and its ions, which is abundant in the interstellar medium. The importance of this process has been emphasized by Pradhan (2000) and Pradhan et al. (2003). An early detection of interstellar oxygen K absorption was by Schattenburg and Canizares (1986).

The calculation of photoionization from inner shells is affected by the resonance structure associated with excitation of states with one np excited electron and a K shell vacancy. They decay predominantly by spectator Auger transitions, in which the np electron does not participate, and have widths nearly independent of principle quantum number n. This leads to a series of resonances with constant width close to the threshold for photoionization, thereby smearing and lowering the location of the edge. This effect, called Auger damping, has also been observed in the laboratory (Farhat et al., 1997). It was emphasized and pointed out earlier in calculations of inner shell ionization by Gorczyca and McLaughlin (2000) for oxygen (c. f., Gorczyca and Robicheaux (1999)), and Ne (Gorczyca, 2000). Computation of these effects using an R-matrix technique relies on the use of an optical potential to mimic the decays to spectator channels not explicitly included in the close coupling expansion. BPRM photoionization cross sections including Auger damping have been carried out for inner shells of all ions of iron (Bautista et al., 2003, 2004; Kallman et al., 2004; Mendoza et al., 2004; Palmeri et al., 2002, 2003a,b), and for oxygen (Garcia et al., 2005). An example of these effects is shown in figure 14, which shows the photoionization cross sections of Fe^{16+} and Fe^{22+} near the threshold for the K shell, taken from Bautista et al. (2004). The left panels show the resonance structure with the effects of damping by resonances with $n > 2$ included, while the right panels show the resonance structure with damping

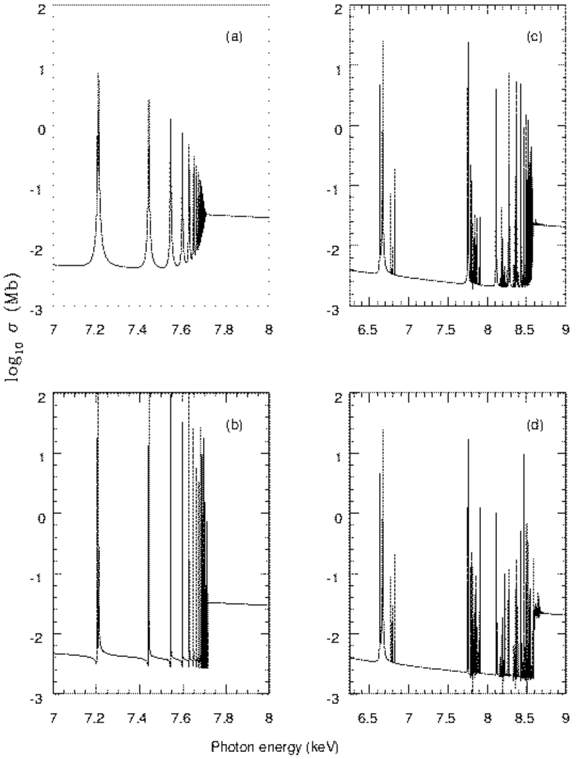

FIG. 14 High-energy total photoabsorption cross sections of the ground level of: (a) Fe^{16+} including radiative and Auger damping effects; (b) Fe^{16+} excluding damping effects for resonances with $n > 2$; (c) Fe^{22+} including damping; (d) Fe^{22+} excluding damping for resonances with $n > 2$. This demonstrates that when damping is included the resonance widths are constant for high n leading to a smearing of the K edge. From Bautista et al. (2004).

by resonances with $n > 2$ excluded.

The vacancies created by inner shell photoionization are filled by fluorescence or Auger decays. The rates for these processes have been calculated by Jacobs and Rozsnyai (1986) using configuration-average energy levels and by Kaastra and Mewe (1993) based on isoelectronic scaling from the calculations of McGuire (1969, 1970, 1971a,b, 1972). The validity of these approximations has been discussed by Gorczyca et al. (2003) and Gorczyca et al. (2006). Level resolved intermediate coupling calculations of K Auger and fluorescence rates have been calculated for iron by Bautista et al. (2003, 2004), Mendoza et al. (2004), and Palmeri et al. (2002, 2003a,b).

2. Radiative Recombination (RR)

Radiative recombination (RR) is more important as a line emission mechanism in photoionized plasmas than in coronal plasmas and therefore receives more discussion in this context. Rate coefficients can be calculated using detailed balance arguments via the Milne relation (Osterbrock and Ferland, 2006). The rate coefficient can be expressed in the form defined by Seaton (1959) for hydrogenic ions:

$$\begin{aligned}\alpha_n(Z,T) = \; & \tfrac{1}{c^2}\left(\tfrac{2}{\pi}\right)^{1/2}(mkT)^{-3/2}2n^2e^{I_n/kT} \\ & \int_{I_n}^{\infty}(h\nu)^2e^{-h\nu/kT}\sigma_n(Z,h\nu)d(h\nu) \qquad (34)\end{aligned}$$

where I_n is the ionization potential and the photoionization cross section can be written

$$\sigma_n(Z,h\nu) = \frac{2^6\alpha\pi a_0^2}{3\sqrt{3}}\frac{n}{Z^2}(1+n^2\epsilon)^{-3}g_{II}(n,\epsilon) \qquad (35)$$

where α is the fine structure constant, a_0 is the Bohr radius, and energy conservation requires that $h\nu = hRcZ^2(1/n^2+\epsilon)$. The Kramers-Gaunt factor can be expanded as a polynomial in $u = n^2\epsilon$, and the rate coefficient can be expressed as:

$$\alpha_n(Z,T) = DZ\frac{\lambda^{1/2}}{n}x_nS_n(\lambda) \qquad (36)$$

where $D = \frac{2^6}{3}\left(\frac{\pi}{3}\right)^{1/2}\alpha^4ca_0^2 = 5.197\times10^{14}\mathrm{cm}^3\ \mathrm{s}^{-1}$ and $\lambda = hRcZ^2/(kT) = 157890Z^2/T$, $x_n = \lambda/n^2$,

$$S_n(\lambda) = \int_0^{\infty}\frac{g_{II}(n,\epsilon)e^{-x_nu}}{1+u}du \qquad (37)$$

and $u = n^2\epsilon$. Seaton (1959) uses the asymptotic expansion for $g_{II}(n,\epsilon)$ to evaluate $S_n(\lambda)$. Numerical tables for $S_n(\lambda)$ and for the total recombination rate coefficients for $\alpha_{\Sigma}(Z,T) = \Sigma_{n=1}^{\infty}\alpha_n(Z,T)$ and for the spectrum of recombining electrons have been published by Seaton (1959). When $RZ^2/n^2 \gg kT$ then $\alpha_n(1,T) \propto n^{-1}T^{-1/2}$ and when $RZ^2/n^2 \ll kT$ then, for $Z = 1$,

$$\begin{aligned}\alpha_n(1,T) \propto \quad & n^{-3}T^{-3/2}(\ln\left(\tfrac{n^2T}{157890}\right) - 0.5772 \\ & +8.56\times10^{-3}T^{1/3} - 2.3\times10^{-5}T^{2/3}) \qquad (38)\end{aligned}$$

The first term in the brackets becomes less important at high temperatures, corresponding to the fact that excited levels contribute more at low temperatures than at high temperatures.

Such calculations are typically tabulated as total recombination rates, in which all the possible radiative transitions from the lowest continuum state (i.e., the ground state of the next highest ion stage) to the bound states of a given ion are summed. This requires a sum over all the rate coefficients into excited levels of an ion, and implicitly assumes that all recombinations to excited levels decay to the ground level. Such sums traditionally use ground state photoionization cross sections appropriate to the ion, together with hydrogenic photoionization cross sections for the excited levels. Tarter (1971) calculated RR rate coefficients for many ions of astrophysical interest, as did Gould (1978). A widely used compilation is by Aldrovandi and Pequignot (1973, 1976) who calculated RR and DR rate coefficients for many ions of astrophysical interest, calculated using the Burgess (1965) general formula for DR and the Milne relation. Pequignot et al. (1991) calculated total and effective RR coefficients for all ions with Z≤10 for important optical and UV transitions of these ions. Woods et al. (1981) calculated RR rate coefficients for iron, using the cross sections of Reilman and Manson (1979). Pradhan (1983) calculated the RR for the ground states of Li-like ions. Verner and Ferland (1996) calculated rate coefficients for RR based on Opacity Project photoionization cross sections. Gu (2003c) has provided total RR rate coefficients for the H-like through Ne-like isoelectronic sequences for the 7 elements Mg, Si, S, Ar, Ca, Fe and Ni, and Gu (2003d) has provided X-ray line emission rate coefficients for Fe^{17+} – Fe^{23+} due to both RR cascades and DR. The need for tabulations of total rate coefficients or of effective rate coefficients is reduced by advances in computer speed, which allow plasma modeling codes to calculate or make use of state-specific recombination rates.

3. Dielectronic Recombination (DR)

Dielectronic recombination (DR) in photoionized plasmas is generally less important than in coronal plasmas, but it is not negligible. As shown in figure 9, the contributions of radiative and DR are comparable for Fe^{18+} DR at temperatures characteristic of photoionized plasmas. For Fe^{19+} – Fe^{22+} DR dominates RR by a factor of 2 or more (Savin et al., 2002a,b, 2003). Theoretical rate coefficients are less certain at low temperatures, owing to the fact that the electron velocity distribution samples low energy states. Theory cannot calculate the resonance energies for the relevant DR resonances at low energy with sufficient precision. Netzer (2004) and Kraemer et al. (2004) provide examples of the sensitivity of astrophysical results to DR rates in photoionized plasmas, and also point out the consequences of errors in the rate coefficients which are in widespread use for astrophysical modeling.

The importance of low temperature DR was pointed out by Storey (1981), who showed that the $C^{2+}\ 2p^2\ {}^3D \rightarrow 2s2p\ {}^1P_0\lambda2296$ line observed from planetary nebulae is likely excited by DR. This was extended to ions of C, N, and O by Nussbaumer and Storey (1983), who calculated rates for these ions using LS coupling. The associated satellite spectra were calculated by Nussbaumer and Storey (1984). These were extended to Mg, Al, Si by Nussbaumer and Storey (1986) and to Ne by Nussbaumer and Storey (1987). Calculations of low temperature DR are most affected by the uncertainties in the low energy resonance structure, and this in turn is affected by the assumption of LS coupling in many calculations. LS coupling can be applied when the fine structure splitting is small compared to the term separation which is caused by the Coulomb interaction.

Recent experimental measurements using storage rings (Savin, 2000; Savin et al., 2002b) and calculations using AUTOSTRUCTURE (Altun et al., 2004, 2005, 2006; Badnell, 2006; Colgan et al., 2003, 2004, 2005; Mitnik and Badnell, 2004; Zatsarinny et al., 2003, 2004a,b, 2005a,b, 2006) of DR include intermediate coupling structure calculations, and so are likely to be more accurate for low temperature DR than previous calculations. Nonetheless, as pointed out by Schippers et al. (2004) and by Gu (2003b), DR at low temperatures continues to be a major source of uncertainty in calculations of ionization balance under photoionization conditions.

4. Charge Transfer

Background

Charge transfer is of potential importance in photoionized plasmas owing to the fact that the charge transfer rate coefficient for an ion with neutral H or He can exceed that for electron recombination by a factor $\geq 10^4$ (Kingdon and Ferland, 1996). Photoionized plasmas can have a hydrogen neutral fraction as great as ~ 0.1 coexisting with several times ionized metals, depending on the shape of the ionizing spectrum. Another application for charge transfer rate coefficients was pointed out by Savin et al. (2004a), who calculated the rate coefficients for $H^+ + H_2 \rightarrow H + H_2^+$ using recently published theoretical cross sections, and showed that uncertainties in these rate coefficients can affect the cooling and formation of primordial structures such as stars and galaxies.

The importance of charge transfer in the interstellar medium was pointed out by Field and Steigman (1971) and Steigman et al. (1971) who also calculated rate coefficients for $C^{2+} + He \rightarrow C^+ + He^+$ (Steigman, 1975) and discussed the influence of charge transfer on the O^+ and N^+ ionization balance. The potential importance of charge transfer and, for the first time, charge transfer involving ions more than singly ionized on the structure of planetary nebula was pointed out by Pequignot, Stasinska and Aldrovandi (1978) and Pequignot (1980a). This led to efforts to calculate cross sections and rates, including calculations of the charge transfer of N^+ with H, and of C^+ and S^+ with H and He using a distorted wave calculation by Butler and Dalgarno (1979, 1980a). Butler and Dalgarno (1980b) calculated the charge transfer of a variety of multiply charged ions with H and He using a Landau-Zener calculation. Watson and Christensen (1979) calculated charge transfer of C^{3+} +H and N^{3+}+H using close-coupling approximation. A review and compilation by Kingdon and Ferland (1996) provides a collection of rate coefficients in a form useful for modeling.

Recent Developments

The most accurate calculations at the low energies of interest to astrophysics (≤ 1 eV/amu) are techniques similar to molecular calculations, using the molecular-orbital close-coupling (MOCC) technique (Heil et al., 1985). Recent MOCC calculations include O^{3+} + H (Wang et al., 2003), Si^{4+} + He (Stancil et al., 1997), N^{4+} + H (Zygelman et al., 1997), S^{4+} + H (Stancil et al., 2001), and S^{4+} + He Wang et al. (2003). These show large ($\geq 10^2$) differences with Landau-Zener calculations in some cases. Recent measurements include Si^{3+}, Si^{4+}, Si^{5+} + He (Tawara et al., 2001), Ne^{3+} + H (Rejoub et al., 2004), Ne^{2+} + H (Mroczkowski et al., 2003), C^{4+} + H (Bliek et al., 1997), N^{2+} + H (Pieksma et al., 1997), C^+ + H (Stancil et al., 1998a,b).

A review of the charge transfer process is given by Janev and Winter (1985). Recent reviews of charge transfer data for photoionized plasmas are given in Stancil (2001) for theory and in Havener (2001) for experiment. Although quantum mechanical MOCC calculations provide the most reliable results when no experimental data are available (Stancil, 2001), still large discrepancies between theory and experiment at collision energies of less than a few hundreds eV/amu point to the difficulty of theory at this energy range and the need for benchmark measurements (Havener, 2001).

C. Charge Transfer in Cometary and Planetary Atmospheres

The discovery of X-ray emission from comets by the ROSAT X-ray astronomy satellite (Lisse et al., 1996) led to the appreciation of the importance of charge transfer of solar wind nuclei with neutrals in comets and gaseous planets. This process has a distinct spectral signature associated with the cascade of the captured electron from the excited state where capture initially occurs. The most probable states are determined by the energetics of the collision and the level structure of the reactants.

Haberli et al. (1997) extended this idea to look at individual spectral lines produced from C, O, and Ne ions. The excited state of the ion following capture was assumed to have a principal quantum number n which is the nearest integer to the quantity $q^{0.75}$, where q is the charge on the ion, followed by a cascading decay of $\Delta n = 1$. This assumption leads to X-ray spectra which fits to the observed X-ray spectra in a subset of the cases. A recent review of the physics of cometary X-ray emission was presented by Cravens (2002). EBIT simulations of cometary charge exchange were performed by Beiersdorfer et al. (2003). Additional models for the cascade, level populations and X-ray line emission associated with cometary charge transfer have been calculated by Kharchenko and Dalgarno (2000).

Measurements for various species have been carried out using beam techniques. Total cross sections for C, N and O are tabulated by Phaneuf et al. (1987), Havener et al. (1989), and Huq et al. (1989). For interpreting X-ray spectra, and for testing theoretical calculations, state-selective measurements are needed. This need, along with the relatively low collision energy, make the X-ray astronomy data needs distinct from those for fusion plasmas. Techniques for measuring state-selected charge transfer include energy loss spectroscopy and photon emission spectroscopy. Energy loss spectropscopy provides greater counting rates, while photon emission spectroscopy which allows higher energy resolution. Measurements have been made using energy loss spectroscopy of O^{2+} in H, H_2 and He (McLaughlin et al., 1990), C^{4+} ions in collisions with H_2 and O_2 (McLaughlin et al., 1992), Fe^{3+} and Fe^{4+} ions with H and He atoms (McLaughlin et al., 1993), S^{2+} with H and H_2 (Wilson et al., 1990b), and S^{3+} with H, H_2 and He (Wilson et al., 1990a). Using similar techniques, Kimura et al. (1987) have studied highly stripped Ne, O, N and C in collisions with H and H_2, and Kamber et al. (1996) have studied N^{3+} colliding with H_2, He, Ne, and Ar. Beam measurements have been made using photon emission spectroscopy to obtain state selective cross sections of single electron charge transfer of C^{4+} on H and H_2 (Hoekstra et al., 1990), O^{3+} on H and H_2 (Beijers et al., 1996), C^{4+}, N^{5+}, O^{6+} with H, H_2 and He (Dijkkamp et al., 1985a), C^{6+}, N^{6+}, O^{6+}, and Ne^{6+} onto H_2, He, Ar (Dijkkamp et al., 1985b). Similar techniques have been used to study C^{5+} and N^{6+} with He and H_2 (Suraud et al., 1991), and C^{5+} and N^{6+} with He and H_2 (Ciric et al., 1985). Double charge exchange can be an important loss process for highly charged ions incident on neutrals, but in many cases it leads to the production of autoionizing states, and therefore does not contribute to X-ray emission. Cross sections with molecular targets other than H_2 have been measured for ions of C, N, O, and Ne colliding with He, H_2, CO_2, and H_2O by Greenwood et al. (2001). Some of these experimental data have been collected at the ORNL/UGA charge transfer database website, http://cfadc.phy.ornl.gov/astro/ps/data/home.html, including both total and state-specific cross sections and rates, along with fits to many of these.

Computational techniques for charge exchange collisions include the classical trajectory Monte-Carlo technique (Cornelius et al., 2000), in which the motion of the projectile, target and electron are calculated by integrating Hamilton's equations including only the Coulomb interactions. This technique is of limited use at energies below 1 keV/amu, where the structure of the projectile ion is important. Another method is the semi-classical impact parameter close coupling method, in which the wavefunction of the electrons is calculated from a set of orbitals appropriate to the projectile ion. This technique is most suitable to systems with a small number of electrons (Kumar and Saha, 1998; Saha, 1995), and so has not been applied to the study of many ions. The Landau -Zener model has also been widely applied, and involves the use of avoided level crossings in order to determine the cross sections for various processes. It turns out that especially for energies below 200 eV/amu there are considerable differences between experiment and theory both in relative and state-selective cross sections.

VIII. DISCUSSION

Basic needs and physical processes important to atomic data for X-ray astronomy have been known since the advent of solar X-ray astronomy. This has led to steady production of rate coefficients and cross sections for use in modeling and interpreting observed astrophysical X-ray spectra, and with considerable overlap with the needs for fusion plasmas. Prior to the launch of $Chandra$ and $XMM-Newton$ a great deal of work had been done toward the goal of developing an atomic database for coronal plasmas. Much of this was devoted to the study of discrete diagnostics, since the spatial and temporal structure of the X-ray emission limits the accuracy of global modeling for the Sun.

The launch of instruments capable of observing spectra from extrasolar objects with comparable resolution and good counting statistics has added motivation for data production and it has changed the emphasis somewhat from that of studies of solar X-rays. Extrasolar objects often cannot be spatially resolved and the sensitivity to temporal variability is limited. Arguments based on other knowledge of their properties motivates attempts to construct global models based on a single set of physical conditions, such as the assumption of a single temperature or a cooling flow for the coronal emission from a cluster of galaxies. For some objects a simple distribution of conditions is assumed, such as a differential emission measure analysis performed for a cool star. In addition, the spectra of distant objects often do not have sufficient statistical accuracy to allow the application of detailed discrete diagnostics. This creates a greater need for global modeling, in which the ionization balance and spectrum can be calculated based on simple assumptions about the conditions, such as temperature and density. In addition extrasolar data have broadened the range of physical processes of interest to include charge exchange, photoionized plasmas, inner shell processes, and opacities associated with interstellar gas.

Significant advances in the calculation and measurement of atomic cross sections and rate coefficients needed for X-ray astronomy have occurred in parallel with the launch of the new observatories. Notable among these are the energetic application of experimental apparatus such as the EBIT and storage rings, and the improvements in computer technology and campaigns to calculate large quantities of data such as the Iron Project and Opacity Project. At the same time, long term efforts to compile reliable data from more traditional laboratory sources have continued to yield results, and the advent of free on line databases, such as the NIST database, has aided in their use. Other important databases are those developed primarily for the fusion energy program at ORNL (http://www-cfadc.phy.ornl.gov/) and ALADDIN and AMBDIS at the IAEA (http://www-amdis.iaea.org/). As a result, there now exist accurate experimental datasets for line wavelengths and cross sections or rate coefficients for some key processes, along with computations using the most accurate known algorithms for many quantities. Laboratory measurements have been made for DR of many ions, and comparison with calculations allows benchmarking of computational techniques. Comprehensive calculations of state-specific DR, which have been benchmarked against the measurements, are available for many ions of interest. Measurements of EII exist for most ions of astrophysical interest, although verification is needed for many of these. Calculations, including close-coupling calculations with adequate treatment of intermediate coupling, relativistic effects, CI and radiation damping, have been made for radiative transition probabilities and electron impact collision strengths of many ions of interest. Measurements of absolute electron impact excitation cross sections have proven to be crucial in benchmarking these calculations. Beam measurements have yielded state-selective cross sections for charge exchange for many ions of interest to solar system X-ray studies.

In addition to the databases discussed above, a great deal of useful data has been collected and made publicly available as part of the databases associated with analysis packages such as CHIANTI (Landi and Bhatia, 2005a), APEC (Smith et al., 2001), and MEKAL/SPEX (Kaastra, Mewe and Nieuwenhuijzen, 1996). It is important to point out that the ultimate source of all databases and compilations is extensive computational and experimental work, and that the credit for this work is often neglected when the compilation or database is used. Astrophysicists and modelers should, whenever possible, attempt to cite original sources even when using the compilation or database as a guide or repository for atomic data.

As a result of accuracy demanded by the new instruments for X-ray astronomy some of the atomic calculations which were in widespread use for modeling astrophysical plasmas are no longer adequate for application to many observations. The approximations necessitated by early computers or analytic work provide valuable insight and constraints on the more recent work, and therefore have been crucial in the development of modern tools. However, there are few remaining processes or ions for which rate coefficients calculated using simple approximations are all that is available. These include the use of the Born approximation, or CBO, in collisional ionization cross sections, the Bethe approximation for collisional excitation, *ab initio* wavelengths for strong lines in the X-ray band, the Burgess general formula for DR, hydrogenic or central field cross sections for photoionization or radiative recombination, and Landau-Zener rate coefficients for charge exchange. An added consequence of the capabilities of new computers is that it is no longer necessary to use total recombination rates when calculating ionization balance. Rather, collisional-radiative models (eg. (Summers et al., 2006)) can be quickly calculated which take into account state-specific recombination and ionization rates, and so are applicable to a wide range of gas densities and radiation environments.

Areas where there are still critical needs include the accumulation of energy level structures and transition wavelengths which are of sufficient accuracy. These are needed for applications including line identification, where the observations have an accuracy of 10^{-3} in many cases, and for calculations of DR at low temperature. Experiments have the most promise for useful work in this area, but new theoretical techniques are needed for this challenge as well. There are few experimental measurements of inner shell photoabsorption for ions of interest to astronomy. Similarly, many lines in observed spectra such as that of NGC 3783 remain unidentified, and these may be associated with inner shell transitions not typically observed from coronal plasmas. X-ray processes involving molecules, including detailed spectra associated with charge transfer, and inner shell opacities, have not been studied for many species. Experimental work is needed to continue the campaign to measure all the DR and CI rate coefficients needed to benchmark the calculation of coronal ionization balance in both electron ionization and photoionization driven plasmas, and in cometary and planetary atmospheres.

The most probable choices for future X-ray instrumentation will likely be only a partial continuation of the trends of the recent past. Both technological challenges and astronomical priorities suggest that X-ray astronomy satellites following *Chandra* and $XMM-Newton$ will have significantly greater sensitivity, so that the number of objects which can be observed spectroscopically, the statistical quality of the spectra and the ability to study time variability will all be greatly enhanced. However, it is less likely that either the spectral resolution or the spectral bandpass will be improved in such instruments. Thus, spectral resolution comparable to that available from the best optical or UV instruments will not be attained. In view of this it seems likely that the interpretation of data from such future missions will continue to rely on tools similar to those currently in use, tools which attempt to calculate ionization, excitation and synthesize the spectrum over a wide range of wavelengths. New targets for these observations will likely include galaxies, clusters of galaxies, and intergalactic gas in order to study the formation of structure, nucleosynthesis, and cosmological parameters. More sensitive instruments will also study spectra of fainter nearby objects such as stars and supernova remnants, and allow improved statistics and more detailed study of time variability of the brightest objects. This is in contrast to what might be expected if the trend toward both greater spectral resolution and greater sensitivity were to occur, which might lead to more extensive application of discrete diagnostics and a reduced reliance on global modeling. If so, the atomic data needed for the foreseeable future will not be greatly altered, in the sense that the precision required will be comparable to the best currently available, and physical processes of interest will span those covered in this review. Spectra with improved statistical accuracy, or time resolution, are likely to reveal physical effects which have not been incorporated into the available atomic database. These may include departures from ionization equilibrium, non-stationary processes, optical depth effects, the effects of magnetic fields, and interactions with energetic particles and non-Maxwellian electron energy distributions. This implies the need for cross sections at energies both significantly above and below the traditional range of energies prescribed by coronal equilibrium. In addition, it is likely that X-ray astronomers will further explore molecular, or solid matter in astrophysics using charge transfer and also absorption features near edges or inner shell lines.

Acknowledgments

We thank Manuel Bautista, Nigel Badnell, Greg Madejski, Alfred Müller, Daniel Savin for careful reading many valuable comments and suggestions. We also thank Prof. Claude Canizares and the Center for Space Research for access to the MIT libraries. This work was supported in part by a grant from NASA though the Astrophysics Theory program.

References

Abrahamsson, K., et al., 1993, Nucl. Instrum. Methods B, 79, 26

Aggarwal, K. M., 1991, Astrophys. J. Suppl. Ser., 77 677

Aggarwal, K. M., and Kingston, A. E., 1991a, J. Phys. B, 24, 4583

Aggarwal, K. M., and Kingston, A. E., 1991b, J. Phys. B, 44, 517

Aggarwal, K. M., and Kingston, A. E., 1992a, Phys. Scr, 46, 193

Aggarwal, K. M., and Kingston, A. E., 1992b, J. Phys. B, 25, 751

Aggarwal, K. M., and Kingston, A. E., 1993, Astrophys. J. Suppl. Ser., 85, 187

Aichele, K., et al., 1998, J. Phys. B., 31, 2369

Aichele, K., Steidl, M., Hartenfeller, U., Hathiramani, D., Scheuermann, F., Westermann, M., Salzborn, E., and Pindzola, M. S., 2001a, J. Phys. B, 34, 4113

Aichele, K., Shi, W., Scheuermann, F., Teng, H., Salzborn, E., Müller, A., 2001b, Phys. Rev. A , 63, 014701

Aitken, K. L., and Harrison, M. F. A., 1971, J. Phys. B., 4, 1176

Aitken, K. L., Harrison,. F. A., and Rundel, R. D., 1971, J. Phys. B., 4, 1189

Ait-Tahar, S., Grant, I. P. and Norrington, P. H., 1996, Phys. Rev. A , 54, 3984.

Aldrovandi, S. M. V. and Pequignot, D., 1973, Astron. Astrophys., 25, 137

Aldrovandi, S. M. V. and Pequignot, D., 1976, Astron. Astrophys., 47, 321

TABLE II Glossary

Acronym	Meaning	Section
AMA	Angular Momentum Average	VII.A.2
APEC	Atomic Physics Emission Code	VII.A
BP	Breit-Pauli	III
BPRM	Breit-Pauli R-Matrix Code Package	III
CB	Coulomb Born Approximation	III
CBE	Coulomb Born with Exchange	III
CBO	Coulomb Born Oppenheimer	III
CCD	Charge Coupled Device	II
CI	Configuration Interaction	III
DI	Direct Ionization	VII.A.1
DR	Dielectronic Recombination	VII.A.2
DW	Distorted Wave Aprroximation	III
EA	Excitation-Autoionization	VII.A.2
EBIS	Electron Beam Ion Source	IV
EBIT	Electron Beam Ion Trap	IV
ECIP	Exchange Classical Impact Parameter	VII.A.1
EII	Electron Impact Ionization	VII.A.1
FAC	Flexible Atomic Code	III
GF	Burgess General Formula	VII.A.2
HETG	High Energy Transmission Grating	II
HFR	Hartree-Fock Relativistic Code	III
HRS	High Rydberg States	VII.A.2
HULLAC	Hebrew University LLNL Code	III
HXR	Hartree-Fock Exchange PotentialIII	
LLNL	Lawrence Livermore Nat'l Lab	III
LTE	Local Thermodynamic Equilibrium	III
MBPT	Many Body Perturbation Theory	III
MC	Multi Configuration	III
MCBP	Multi Configuration Breit Pauli	III
MCDF	Multi Configuration Dirac Fock	III
MCHF	Multi Configuration Hartree Fock	III
ORNL	Oak Ridge National Laboratory	III
QED	Quantum Electrodynamic	III
READI	Resonant Excitation Auto-Double-ionization	VII.A.1
REDA	Resonant Excitation Double Autoionization	VII.A.1
RGS	Reflection Grating Spectrograph	II
RTE	Resonant Transfer of Excitation	VII.A.2
SCF	Self Consistent Field	III

Ali, R., Bhalla, C. P., Cocke, C. L., and Stockli, M., 1990, Phys. Rev. Lett., 64, 633

Allen, J. W. and Dupree, A. K., 1969, Astrophys. J., 155, 27

Altun, Z., Yumak, A., Badnell, N. R., Colgan, J., and Pindzola, M. S., 2004, Astron. Astrophys., 420, 775

Altun, Z., Yumak, A., Badnell, N. R., Colgan, J., and Pindzola, M. S., 2005, Astron. Astrophys., 433, 395

Altun, Z., Yumak, A., Badnell, N. R., Loch, S. D., & Pindzola, M. S. 2006, Astron. Astrophys., 447, 1165

Andersen, L. H., Pan, G.-Y., Schmidt, H. T., Pindzola, M. S., and Badnell, N. R., 1992a, Phys. Rev. A , 45, 6332

Andersen, L. H., Pan,G.-Y., Schmidt, H. T., Badnell, N. R., and Pindzola, M. S., 1992b, Phys. Rev. A , 45, 7868

Ansari, B., and Alam, C., 1975, Sol. Phys., 41, 97.

Antonucci, R. R. J., and Miller, J. S., 1985, Astrophys. J., 297, 621

Arnaud, M.and Raymond, J., 1992, Astrophys. J., 398, 394

Arnaud, M.and Rothenflug, R., 1985, Astron. Astrophys. Suppl. Ser., 60, 425

Avgoustoglou, E., Johnson, W. R., Plante, D. R.,Sapirstein, J., Sheinerman, S., and Blundell, S. A., 1992, Phys. Rev. A , 46, 5478

Badnell, N. R., 1986a, J. Phys. B, 19, 1541

Badnell, N. R., 1986b, J. Phys. B, 19, 3827

Badnell, N. R., 1987, J. Phys. B, 20, 2081

Badnell, N. R., 1988, J. Phys. B, 21, 749

Badnell, N. R., 1989, Phys. Scr., T28, 33

Badnell, N. R., 1990, J. Phys. B, 23, L565

Badnell, N. R., 1991, Astrophys. J., 379, 356

Badnell, N. R., 1992, Phys. Rev. A , 46, 660

Badnell, N. R., and Moores, D. L., 1994, At. Data Nucl. Data Tables, 57, 329

Badnell, N. R., 1997, J. Phys. B, 30, 1

Badnell, N. R., and Griffin, D. C., 2001, J. Phys. B, 34, 681

Badnell, N. R., and Pindzola, M. S., 1989a, Phys. Rev. A , 39, 1685

Badnell, N. R., and Pindzola, M. S., 1989b, Phys. Rev. A , 39, 1690

Badnell, N. R., and Pindzola, M. S., 1989c, Phys. Rev. A , 39, 6165

Badnell, N., and Pindzola, M., 1993, Phys. Rev. A , 47, 2937

Badnell, N. R., Pindzola, M. S., and Griffin, D. C., 1990, Phys. Rev. A , 41, 2422

Badnell, N. R., Pindzola, M. S., Andersen, L. H., Bolko, J., and Schmidt, H. T., 1991, J. Phys. B, 24, 4441

Badnell, N. R., Pindzola, M. S., Dickson, W. J., Summers, H. P., Griffin, D. C., and Lang, J., 1993, Astrophys. J. Lett., 407, L91

Badnell, N. R., Pindzola, M. S., Bray, I., and Griffin, D. C., 1998, J. Phys. B, 31, 911

Badnell, N. R., Griffin, D. C. And Mitnik, D., 2001, J. Phys. B, 34, 5071

Badnell, N. R., et al., 2003, Astron. Astrophys., 406, 1151

Badnell, N.R., Bautista, M. A., Butler, K., Delahaye, F., Mendoza, C., Palmeri, P., Zeippen, C.J., and Seaton, M.J., 2005, Mon. Not. R. Astron. Soc., 360, 458

Badnell, N. R. 2006, Astron. Astrophys., 447, 389

Baker, J., and Menzel, D., 1938, Astrophys. J., 88, 52

Ballance, C. P., Griffin, D. C., Ludlow, J. A., and Pindzola, M. S., 2004, J. Phys. B, 37, 4779

Bannister, M. E., 1996, Phys. Rev. A , 54, 1435

Barfield, W. D., 1979, Astrophys. J., 229, 856

Bar-Shalom, A., Klapisch, M., and Oreg, J., 2001, J. Quant. Spec. Radiat. Transf., 71, 169.

Bartiromo, R., Bombarda, F., and Giannella, R., 1985, Phys. Rev. A , 32, 531

Bartschat, K., and Bray, I., 1996, J. Phys. B, 30, L577

Bartschat, K., and Bray, I., 1997, J. Phys. B, 30, L109

Bartsch, T., et al., 1999, Phys. Rev. Lett., 82, 3779

Bates, D. R. and Dalgarno, A., 1962, in 'Atomic and Molecular Processes,' Ed. D. R. Bates p. 245 (Academic Press: New York and London),

Bautista, M. A., Kallman, T. R., and Pradhan, A. K., 2000, Conference Proceedings, NASA/CP-2000-209968; Rept-2000-04370-0; NAS 1.55:209968, http://heasarc.gsfc.nasa.gov/docs/heasarc/atomic/,

Bautista, M. A., 1997, Astrophys. J., 122, 167

Bautista, M. A., 2000, J. Phys. B, 33, 71

Bautista, M.A., and Kallman, T.R., 2000, Astrophys. J., 544, 581

Bautista, M. A., and Kallman, T. R., 2001, Astrophys. J. Suppl. Ser., 134, 139

Bautista, M. A., Mendoza, C., Kallman, T. R., and Palmeri, P., 2003, Astron. Astrophys., 403, 339

Bautista, M. A., Mendoza, C., Kallman, T. R., and Palmeri, P., 2004, Astron. Astrophys., 418, 1171

Becker, C., Knopp, H., Jacobi, J., Teng, H., Schippers, S., Müller, A., 2004, J. Phys. B, 37, 1503

Behar, E., and Netzer, H., 2002, Astrophys. J., 570, 165

Behar, E., Sako, M., and Kahn, S. M., 2001a, Astrophys. J., 563, 497

Behar, E., Cottam, J., and Kahn, S. M., 2001b, Astrophys. J., 548, 966

Behring, W. E., Cohen, L., and Feldman, U., 1972, Astrophys. J., 175, 493

Beiersdorfer, P., 2003, Ann. Rev. Astron. Astrophys., 41, 343

Beiersdorfer, P., et al., 1990, Rev. Sci Inst., 61, 2338

Beiersdorfer, P., et al., 1992, Phys. Rev. A , 46 3812

Beiersdorfer, P., Phillips, T., Jacobs, V. L., Hill, K. W., Bitter, M., von Goeler, S., and Kahn, S. M., 1993, Astrophys. J., 409, 846

Beiersdorfer, P., et al., 2002, Astrophys. J. Lett., 576, L169

Beiersdorfer, P.,et al., 2003, Science, 300, 1558

Beiersdorfer, P., et al., 2004, Astrophys. J., 610, 616

Beijers, J. P. M., Hoekstra, R., and Morgenstern, R., 1996, J. Phys. B, 29, 1397

Belic, D. S., Dunn, G. H., Morgan, T. J., Mueller, D. W., and Timmer, C., 1983, Phys. Rev. Lett., 50, 339

Bellantone, R., and Hahn, Y., 1989, Phys. Rev. A , 40, 6913

Bell, K.L., Gilbody, H.B., Hughes, J.G., Kingston, A.E., and Smith, F.J., 1983, J. Phys. Chem. Ref. Data, 12, 891

Bely, O., 1966, Annales d'Astrophysique, 29, 683

Bely, O., 1968, J. Phys. B, 1, 23

Bely, O., and van Regemorter, H., 1970, Ann. Rev. Ast. Ap., 8, 329

Bely-Dubau, F., 1973, Astron. Astrophys., 25, 431

Bely-Dubau, F., Gabriel, A. H., and Volonte, S., 1979, Mon. Not. R. Astron. Soc., 186, 405

Bely-Dubau, F., Gabriel, A. H., and Volonte, S., 1979, Mon. Not. R. Astron. Soc., 189, 801

Bely-Dubau, F., et al., 1982a, Mon. Not. R. Astron. Soc., 201, 1155

Bely-Dubau, F., Faucher, P., Dubau, J., and Gabriel, A. H., 1982b, Mon. Not. R. Astron. Soc., 198,

Bely-Dubau, F., et al., 1983, Phys. Lett. A, 93, 189

Berrington, K. A., 1994, At. Data Nucl. Data Tables, 57, 71

Bethe, H. A. and Salpeter, E. E., 1972, Quantum Mechanics of One- and Two-Electron Atoms (Berlin: Springer). ,

Bevington, P. R., 1969, 'Data Reduction and Error Analysis for Physicists', New York: McGraw-Hill, 1969,

Bhalla, C. P., Gabriel, A. H., and Presnyakov, L. P., 1975, Mon. Not. R. Astron. Soc., 172, 359

Bhalla, C. P., and Karim, K. R., 1986b, Rev. Sci Inst., 57, 2055

Bhalla, C. P., and Karim, K. R., 1988, Rev. Sci Inst., 59, 1527

Bhatia, A. K., and Doschek, G. A., 1992, At. Data Nucl. Data Tables, 52, 1

Bhatia, A. K., and Doschek, G. A., 1993a, At. Data Nucl. Data Tables, 53, 195

Bhatia, A. K., and Doscheck, G. A., 1995a, At. Data Nucl. Data Tables, 60, 145

Bhatia, A. K., and Doschek, G. A., 1995b, At. Data Nucl. Data Tables, 60, 97

Bhatia, A. K., and Doschek, G. A., 1996, At. Data Nucl. Data Tables, 64, 183

Bhatia, A. K., and Doschek, G. A., 1998, At. Data Nucl. Data Tables, 68, 49

Bhatia, A. K., and Doschek, G. A., 1999, At. Data Nucl. Data Tables, 71, 69

Bhatia, A. K., and Doschek, G. A., 2003, At. Data Nucl. Data Tables, 85, 1

Bhatia, A. K., and Kastner, S. O., 1980, Sol. Phys., 65, 181

Bhatia, A. K., and Kastner, S. O., 1985, Sol. Phys., 96, 11

Bhatia, A. K., and Kastner, S. O., 1999, Astrophys. J., 516, 482

Bhatia, A. K., and Landi, E., 2003a, Astrophys. J., 585, 587

Bhatia, A. K., and Landi, E., 2003b, Astrophys. J. Suppl. Ser., 147, 409

Bhatia, A. K., and Landi, E., 2003c, At. Data Nucl. Data Tables, 85, 169

Bhatia, A. K., and Landi, E., 2003d, At. Data Nucl. Data Tables, 85, 317

Bhatia, A. K., and Mason, H. E., 1980a, Astron. Astrophys., 83, 380

Bhatia, A. K., and Mason, H. E., 1981, Astron. Astrophys., 103, 324

Bhatia, A. K., and Mason, H. E., 1983, Astron. Astrophys. Suppl. Ser., 52, 115

Bhatia, A. K., and Mason, H. E., 1986a, Astron. Astrophys., 155, 413

Bhatia, A. K., and Mason, H. E., 1986b, Astron. Astrophys., 155, 417

Bhatia, A. K., and Mason, H. E., 1997, At. Data Nucl. Data Tables, 66, 119

Bhatia, A. K., Seely, J. F., and Feldman, U., 1987, At. Data Nucl. Data Tables, 36, 453

Bhatia, A. K., Fawcett, B. C., Phillips, K. J. H., Lemen, J. R., and Mason, H. E., 1989b, Mon. Not. R. Astron. Soc., 240, 421

Bhatia, A. K., Kastner, S. O., Keenan, F. P., Conlon, E. S., and Widing, K. G., 1994, Astrophys. J., 427, 497

Bhatia, A. K., Doschek, G. A., and Eissner, W., 2002, At. Data Nucl. Data Tables, 82, 211

Bhatia, A. K., Landi, E., and Mason, H. E., 2003, At. Data Nucl. Data Tables, 83, 71

Biemont, E., and Zeippen, C. J., 1996, Phys. Scr., T65, 192

Biemont, E., P. Quinet, A.Ya., Faenov, I., Skobolev, J., Nilsen, V.M., Romanova,M., Scholz, L., Karpinski and A. Szydlowski, 2000, Phys. Scr., 61, 555.

Binello, A. M., Mason, H. E., and Storey, P. J., 1998a, Astron. Astrophys. Suppl. Ser., 131, 153

Binello, A. M., Mason, H. E., and Storey, P. J., 1998b, Astron. Astrophys. Suppl. Ser., 127, 545

Bitter, M., Hill, K. W., Sauthoff, N. R., Efthimion, P. C., Meservey, E., Roney, W., von Goeler, S., Horton, R., Goldman, M., and Stodiek, W., 1979, Phys. Rev. Lett., 43, 129

Bitter, M., et al., 1984, Phys. Rev. A , 29, 661

Blackford, H. M. S., and Hibbert, A., 1994, At. Data Nucl. Data Tables, 58, 101

Blanchet, L.,Cornille, M., Dubau, J., Faucher, P., and Lion, J., 1985, Astron. Astrophys., 152, 417

Bliek, F. W., Hoekstra, R., Bannister, M. E., and Havener, C. C., 1997, Phys. Rev. A , 56, 426

Blumenthal, G. R., Drake, G. W. F., and Tucker, W. H., 1972, Astrophys. J., 172, 205

Bohm, S., et al., 2001, Phys. Scr., T92, 395

Bohm, S., et al., 2002, Phys. Rev. A , 65, 052728

Bohm, S., Müller, A., Schippers, S., Shi, W., Ekl ow, N., Schuch, R., Danared, H., and Badnell, N. R., 2003, Astron. Astrophys., 405, 1157

Boiko, V. A., Faenov, A. Y., Pikuz, S. A., and Safranova, U. L., 1977, Mon. Not. R. Astron. Soc., 181, 107

Boiko, V. A., Faenov,A. I., and Pikuz, S. A., 1978, J. Quant. Spec. Radiat. Transf., 19, 11

Breton, C., DeMichelis, C., Finkenthal, M., and Mattioli, M., 1978, Phys. Rev. Lett., 41, 110

Briand, J. P., Charles,P., Arianer, J., Laurent, H., Goldstein, C., Dubau, J., Loulergue, M., and Bely-Dubau, F., 1984, Phys. Rev. Lett., 52, 617

Brickhouse, N.S., Raymond, J.C., and Smith, B.W., 1995, Astrophys. J. Supp. Ser., 97, 551

Brinkman, B. C., et al., 2000, Proc. SPIE, 4012, 81

Brinkman, A. C., Kaastra, J. S., van der Meer, R. L. J., Kinkhabwala, A., Behar, E., Kahn, S. M., Paerels, F. B. S., and Sako, M., 2002, Astron. Astrophys., 396, 761

Bromage, G. E., and Fawcett, B. C., 1977a, Mon. Not. R. Astron. Soc., 178, 605

Bromage, G. E., and Fawcett, B. C., 1977b, Mon. Not. R. Astron. Soc., 178, 591

Bromage, G. E., Fawcett, B. C., and Cowan, R. D., 1977a, Mon. Not. R. Astron. Soc., 178, 599

Bromage, G. E., Cowan, R. D., and Fawcett, B. C., 1977b, Phys. Scr., 15, 177

Bromage, G. E., Fawcett, B. C., and Cowan, R. D., 1978a, Mon. Not. R. Astron. Soc., 183, 19

Bromage, G. E., Fawcett, B. C., Ridgeley, A., and Cowan, R. D., 1978b, Optical Society of America Journal A, 68, 48

Brook, E., Smith,A. C. H., and Harrison, M. F. A., 1978, J. Phys. B, 11, 3115

Brown, R. T., 1971, Astrophys. J., 170, 387

Brown, G. V., Beiersdorfer, P., Liedahl, D. A., Widmann, K., and Kahn, S. M., 1998, Astrophys. J., 502, 1015

Brown, G. J. N., Scott, M. P., and Berrington, K. A., 1999, J. Phys. B, 32 737

Brown, G. V., et al., 2001a, Phys. Scr., T92, 130

Brown, G. V., Beiersdorfer, P., and Widmann, K., 2001b, Phys. Rev. A , 63, 032719

Bruch, R. et al., 1979, Phys. Rev. A , 19, 587

Bruch, R., et al., 1987, Phys. Rev. A , 35, 4114

Bruch, R., Schneider, D., Chen, M. H., Chung, K. T., and Davis, B. F., 1992, Phys. Rev. A , 45, 4476

Brueckner, K. A., 1955, Phys. Rev., 97, 1353

Bryans, P., Badnell, N. R., Gorczyca, T. W., Laming, J. M., Mitthumsiri, W., and Savin, D. W., 2006, ArXiv Astrophysics e-prints, arXiv:astro-ph/0604363,

Burgess, A., 1964a, Mem. R. Astron. Soc., 69, 1

Burgess, A., 1965, Astrophys. J., 141, 1588

Burgess, A., and Chidichimo, M. C., 1983, Mon. Not. R. Astron. Soc., 203, 1269

Burgess, A., and Sheorey, V. B., 1974, J. Phys. B, 7, 2403

Burgess, A., and Summers, H. P., 1969, Astrophys. J., 157, 1007

Burgess, A., and Summers, H. P., 1976, Mon. Not. R. Astron. Soc., 174, 345

Burgess, A.and Tworkowski, A.S., 1976, Astrophys. J. Lett., 205, L105

Burgess, A., Hummer, D. G., and Tully, J. A., 1970, Royal Society of London Philosophical Transactions Series A, 266, 225

Burgess, A., Summers, H. P., McWhirter, R. W. P., and Cochrane, D. M., 1977, Mon. Not. R. Astron. Soc., 179, 275

Burke, P. G., and Berrington, K. A., 1993, Atomic and Molecular Processes: an R-matrix Approach (Bristol and Philadelphia: IOP Publishing) ,

Burkhalter, P. G.,Cohen, L., Cowan, R. D., and Feldman, U., 1979, Optical Society of America Journal A, 69, 1133

Butler, S. E. and Dalgarno, A., 1979, Astrophys. J., 234, 765

Butler, S. E. and Dalgarno, A., 1980a, Astron. Astrophys., 85, 144

Butler, S. E. and Dalgarno, A., 1980b, Astrophys. J., 241, 838

Butler, K. and Moores, D. L., 1985, J. Phys. B, 18, 1247

Butler, K., and Zeippen, C. J., 1994, Astron. Astrophys. Suppl. Ser., 108, 1

Butler, K., and Zeippen, C. J., 2000, Astron. Astrophys. Suppl. Ser., 143, 483

Butler, K., and Zeippen, C. J., 2001a, Astron. Astrophys., 372, 1078

Butler, K., and Zeippen, C. J., 2001b, Astron. Astrophys., 372, 1083

Callaway, J., 1994, At. Data Nucl. Data Tables, 57, 9

Canizares, C. R., et al., 2000, Astrophys. J. Lett., 539, L41

Canizares, C. R., et al., 2005, Publ. Astron. Soc. Pac., 117, 1144

Champeaux, J.-P., Bizau, J.-M., Cubaynes, D., Blancard, C., Nahar, S., Hitz, D., Bruneau, J., and Wuilleumier, F. J., 2003, Astrophys. J. Suppl. Ser., 148, 583

Chantrenne, S. J., Gregory, D. C., Buie, M. J., and Pindzola, M. S., 1990, Phys. Rev. A , 41, 140.,

Chapman, R. D., and Henry, R. J. W., 1971, Astrophys. J., 168, 169

Chapman, R. D., and Henry, R. J. W., 1972, Astrophys. J., 173, 243

Chen, G. X., Pradhan, A. K., and Eissner, W., 2003, J. Phys. B, 36, 453

Chen, M. H., Reed, K. J., Guo, D. S., and Savin, D. W., 1998, Phys. Rev. A , 58, 4539

Chen, M. S., 1986a, At. Data Nucl. Data Tables, 34, 301

Chen, M. H., 1986b, Phys. Rev. A , 34, 1073

Chen, M. H., 1986, Phys. Rev. A , 33, 994

Chen, M. H., 1988a, Phys. Rev. A , 38, 2332

Chen, M. H., 1988b, Phys. Rev. A , 38, 6430

Chen, M. H., 1988c, Phys. Rev. A , 38, 3280

Chen, M.H., 1991, Phys. Rev. A , 44, 4215

Chen, M. H., and Crasemann, B., 1988, Phys. Rev. A , 38, 5595

Chen, G. X., and Pradhan, A. K., 2002, Phys. Rev. Lett., 89, 013202

Chen, M.H., et al., 1990, Phys. Rev. Lett., 64, 1350

Chen, H., Beiersdorfer, P., Heeter, L. A., Liedahl, D. A., Naranjo-Rivera, K. L., Träbert, E., Gu, M. F., and Lepson, J. K., 2004, Astrophys. J., 611, 598

Chen, H., et al., 2005, Astrophys. J., 618, 1086

Christensen, R. B., Norcross, D. W., and Pradhan, A. K., 1986, Phys. Rev. A , 34, 4704

Ciric, D., Brazuk, A., Dijkkamp, D., de Heers, F. J., and Winter, H., 1985, J. Phys. B, 18, 3629

Clark, R. E. H., Sampson, D. H., and Goett, S. J., 1982, Astrophys. J. Supp. Ser., 49, 545

Clark, M., Brandt, D., Swenson, J. K. and Shafroth, S. M., 1985, Phys. Rev. Lett., 54, 544

Clark, R.E.H., Cowan, R.D., and Bobrowicz, F.W., 1986, At. Data Nucl. Data Tables, 34, 415

Cohen, M., Fournier, K., and Goldstein, W., 1998, Phys. Rev. A , 57, 2651

Colgan, J., Pindzola, M. S., Whiteford, A. D., and Badnell, N. R., 2003, Astron. Astrophys., 412, 597

Colgan, J., Pindzola, M. S., and Badnell, N. R., 2004, Astron. Astrophys., 417, 1183

Colgan, J., Pindzola, M. S., and Badnell, N. R., 2005, Astron. Astrophys., 429, 369

Connerade, J. P., Peacock, N. J., and Speer, R. J., 1970, Sol. Phys., 14, 159

Corliss, C., and Sugar, J., 1982, J. Phys. Chem. Ref. Data, 11, 135

Cornelius, K. R., Wojtkowski, K., and Olson, R. E., 2000, J. Phys. B, 33, 2017

Cornille, M., Dubau, J., Loulergue, M., Bely-Dubau, F., and Faucher, P., 1992, Astron. Astrophys., 259, 669

Cornille, M., Dubau,J., and Jacquemot, S., 1994a, At. Data Nucl. Data Tables, 58, 1

Cornille, M., et al., 1994b, Astron. Astrophys. Suppl. Ser., 105, 77

Cowan, R.D., 1981, *The Theory of Atomic Structure and Spectra* (University of California Press, Berkeley).,

Cowan, R. D. and Mann, J. B., 1979, Astrophys. J., 232, 940

Cowan, R. D., Bromage, G. E., and Fawcett, B. C., 1984, Mon. Not. R. Astron. Soc., 210, 439

Cox, D.P., and Daltabuit, E., 1971, Astrophys. J., 167, 113

Cox, D.P., and Tucker, W.H., 1969, Astrophys. J., 157, 1157

Crandall, D. H., Phaneuf, R. A., and Gregory, D. C., 1979a, “Electron Impact Ionization of Multicharged Ions”, ORNL/TM-7020, Oak Ridge National Laboratory.,

Crandall, D. H., Phaneuf, R. A., Hasselquist, B. E., and Gregory, D. C., 1979b, J. Phys. B, 12, L249

Crandall, D. H., Phaneuf, R. A., Falk, R. A., Belic, D. S.,and Dunn, G. H., 1982, Phys. Rev. A , 25, 143

Crandall, D. H., Phaneuf, R. A., Gregory, D. C., Howald, A. M., Mueller, D. W., Morgan, T. J., Dunn, G. H., Griffin, D. C. , and Henry, R. J. W., 1986, Phys. Rev. A , 34, 1757

Cravens, T. E., 2002, Science, 296, 1042

Culhane, J. L., and Acton, L. W., 1974, Ann. Rev. Astron. Astrophys., 12, 359

Cunto, W., and Mendoza, C., 1992, Revista Mexicana de Astronomia y Astrofisica, 23, 107

Curdt, W., Landi, E., Wilhelm, K., and Feldman, U., 2000, Phys. Rev. A , 62, 22502

Czyzak, S. J., and Krueger, T. K., 1966, Astrophys. J., 144, 381

Dance, D. F., Harrison, M. F. A., and Rundel, R. D., 1967, Royal Society of London Proceedings Series A, 299, 525

Danjo, A., et al., 1984, J. Phys. Soc. Jpn., 43, 4091

Dasgupta, A., 1995, Astrophys. J. Suppl. Ser., 101, 401

Dasgupta, A.and Whitney, K.G., 1990, Phys. Rev. A , 42, 2640

Dasgupta, A.and Whitney, K.G., 1994, At. Data Nucl. Data Tables, 58, 77

Datla, R. U., Nugent, L. J., and Griem, H. R., 1976, Phys. Rev. A , 14, 979

Decaux, V., et al., 1991a, Phys. Rev. A , 43, 228

Decaux, V., Bitter, M., Hsuan, H., Hill, K. W., von Goeler, S., Park, H., and Bhalla, C. P., 1991b, Phys. Rev. A , 44, 6987

Decaux, V., Beiersdorfer, P., Osterheld, A., Chen, M., and Kahn, S. M., 1995, Astrophys. J., 443, 464

Decaux, V.,Beiersdorfer, P., Kahn, S. M., and Jacobs, V. L., 1997, Astrophys. J., 482, 1076

Decaux, V., Jacobs, V. L., Beiersdorfer, P.,Lie dahl, D. A., and Kahn, S. M., 2003, Phys. Rev. A , 6, 012509

Defrance, P., et al., 1990, J. Phys. B, 23, 2333

Delahaye, F., and Pradhan, A. K., 2002, J. Phys. B, 35, 3377

Dere, K.P., Landi, E., Mason, H. E., Monsignori Fossi, B.C., and Young, P.R., 1997, Astron. Astrophys. Suppl. Ser., 125, 149

Dere, K.P., Landi, E., Young, P. R., and DelZanna, G., 2001, Astrophys. J. Suppl. Ser., 134, 331

Derevianko, A., and Johnson, W.R., 1997, Phys. Rev. A , 56, 1288

Deutschman, W. A., and House, L. L., 1966, Astrophys. J., 144, 435

Deutschman, W. A., and House, L. L., 1967, Astrophys. J., 149, 451

DeWitt, D. R., Lindroth, E., Schuch, R., Gao, H., Quinteros, T., and Zong, W., 1995, J. Phys. B, 28, L147

Dijkkamp, D., Ciric, D., Vlieg, E., de Boer, A., and de Heer, F. J., 1985a, J. Phys. B, 18, 4763

Dijkkamp, D., Gordeev, Yu. S., Brazuk, A., Drentje, A. G., and de Heer, F. J., 1985b, J. Phys. B, 18, 737

Diserens, M. J.,Harrison, M. F. A., and Smith, A. C. H., 1984, J. Phys. B, 17, L621

Diserens, M. J.,Harrison, M. F. A., and Smith, A. C. H., 1988, J. Phys. B, 21, 2129

Dittner, P. F., et al., 1983, Phys. Rev. Lett., 51, 31

Dittner, P. F., Datz, S., Hippler, R., Krause, H. F., and Miller, P. D., 1988, Phys. Rev. A , 38, 2762

Djurić, N., et al., 2002, Phys. Rev. A , 65, 052711

Djuric, N., Bell, E., Guo, W., X. Q., Phaneuf, R. A., Bannister, M. E., Pindzola, M. S., and Griffin, D. C., 1993, Phys. Rev. A , 47, 4786

Dolder, K. T., Harrison, M. F. A., and Thonemann, P. C., 1961, Royal Society of London Proceedings Series A, 264, 367

Dolder, K. T., Harrison, M. F. A., and Thonemann, P. C., 1963, Royal Society of London Proceedings Series A, 274, 546

Doschek, G. A., 1972, Sp. Sci. Rev., 13, 765

Doschek, G. A., and Cowan, R. D., 1984, Astrophys. J. Suppl. Ser., 56, 67

Doschek, G. A. and Feldman, U., 1987, Astrophys. J., 313, 883

Drake, G.W., 1988, Can. J. Phys., 66, 586

Dubau, J., 1994, At. Data Nucl. Data Tables, 57, 21

Dubau, J., and Volonte, S., 1980, Rep. Prog. Phys., 43, 199

Dubau, J., Loulergue, M., and Steenman-Clark, L., 1980, Mon. Not. R. Astron. Soc., 190, 125

Dubau, J., Loulergue, M.,Gabriel, A. H., Steenman-Clark, L., and Volonte, S., 1981, Mon. Not. R. Astron. Soc., 195, 705

Dubau, J., Porquet, D.,and Zabaydullin, O. Z., 2003, J. Quant. Spec. Radiat. Transf., 81, 117

Dufton, P. L., and Kingston, A. E., 1994, At. Data Nucl. Data Tables, 57, 273

Dunn, G. H., Djuric, N.,Chung, Y.-S., Bannister, M., and Smith, A. C. H., 1995, Nucl. Instrum. Methods B, 98, 107

Duponchelle, M., Khouilid, M., Oualim, E. M., Zhang, H., and Defrance, P., 1997, J. Phys. B, 30, 729

Dyall, K. G., Grant, I. P., Johnson, C. T., Parpia, F. A. and Plummer, E. P., 1989, Comput. Phys. Commun., 55, 425.

Dzifcakova, E., 1992, Sol. Phys., 140, 247

Dzifcakova, E., 1998, Sol. Phys., 178, 317

Dzifcakova, E., and Kulinova, A., 2002, ESASP-477: Solspa2001, Proceedings of the Second Solar Cycle and Space Weather Euroconference, 9

Edlen, B., 1983, Phys. Scr, 28, 51

Edlen, B., 1984, Phys. Scr, 30, 135

Edlen, B., 1985, Phys. Scr, 31, 345

Edmonds, A. R., 1960, Angular Momentum in ‘Quantum Mechanics’ (Princeton University Press, Princeton, NJ).,

Eissner, W., Jones, M. and Nussbaumer, H., 1974, Comput. Phys. Commun., 8, 270.

Eissner, W., Galavís, M. E., Mendoza, C., and Zeippen, C. J., 1999, Astron. Astrophys. Suppl. Ser., 136, 385

Eissner, W., Landi, E., and Bhatia, A. K., 2005, At. Data Nucl. Data Tables, 89, 139

Engstrom, L., and Litzen, U., 1995, J. Phys. B, 28, 2565

Ericsson, G.W., 1977, J. Phys. Chem. Ref. Data, 6, 3

Ermolaev, A. M., and Jones, M., 1972, J. Phys. B, 5, L225

Faenov, A.Ya., Pikuz, S. A., and Shlyaptseva, A. S., 1994, Phys. Scr., 49, 41.

Falk, R. A., Dunn, G. H., Gregory, D. C., and Crandall, D. H., 1983a, Phys. Rev. A , 27, 762

Falk, R. A., Stefani, G., Camilloni, R., Dunn, G. H., Phaneuf, R. A., Gregory, D. C., and Crandall, D. H., 1983b, Phys. Rev. A , 28, 91

Fano, U. and Racah, G., 1959, Irreductible Tensorial Sets (Academic Press, New York).,

Fano, U., & Cooper, J. W., 1968, Reviews of Modern Physics, 40, 441

Farhat, A., et al., 1997, Phys. Rev. A , 56, 50

Fawcett, B. C., 1970, J. Phys. B, 3, 1152

Fawcett, B. C., 1971, J. Phys. B, 4, 1577

Fawcett, B. C., 1986a, At. Data Nucl. Data Tables, 35, 203

Fawcett, B. C., 1986b, At. Data Nucl. Data Tables, 35, 185

Fawcett, B. C., 1986c, At. Data Nucl. Data Tables, 34, 215

Fawcett, B. C., 1987, At. Data Nucl. Data Tables, 37, 367

Fawcett, B. C., and Cowan, R. D., 1975, Mon. Not. R. Astron. Soc., 171, 1

Fawcett, B. C., and Hayes, R. W., 1972, J. Phys. B, 5, 366

Fawcett, B. C., and Hayes, R. W., 1973, Phys. Scr., 8, 244

Fawcett, B. C., and Mason, H. E., 1989, At. Data Nucl. Data Tables, 43, 245

Fawcett, B. C., and Mason, H. E., 1991, At. Data Nucl. Data Tables, 47, 17

Fawcett, B. C., Kononov, E. Y., Hayes, R. W., and Cowan, R. D., 1972, J. Phys. B, 5, 1255

Fawcett, B. C., Cowan, R. D., and Hayes, R. W., 1974, Astrophys. J., 187, 377

Fawcett, B. C., Ridgeley, A., and Bromage, G. E., 1978, Phys. Scr, 18, 315

Fawcett, B. C., Bromage, G. E., and Hayes, R. W., 1979, Mon. Not. R. Astron. Soc., 186, 113

Feldman, U., and Cohen, L., 1968, Astrophys. J. Lett., 151, L55

Feldman, U., Doschek, G. A., Nagel, D. J., Behring, W. E., and Cohen, L., 1973, Astrophys. J. Lett., 183, L43

Feldman, U., Doschek, G. A., Cheng, C.-C., and Bhatia, A. K., 1980, Journal of Applied Physics, 51, 190

Feldman, U., Doschek, G. A., and Bhatia, A. K., 1982, Journal of Applied Physics, 53, 8554

Ferland , G. and Savin, D. W., 2001, Pub. Astron. Soc. Pacific, 113, 1024

Fernley, J.A., Taylor, K.T., and Seaton, M.J., 1987, J. Phys. B, 20, 6457

Field, G. B. and Steigman, G., 1971, Astrophys. J., 166, 59

Fischer, C. F., 1996, in 'Atomic, Molecular and Optical Physics Handbook,' Drake G., ed. (AIP Press, New York), pp. 242–257.

Fischer, C. F., Brage, T. and Jonsson, P., 1997, 'Computational Atomic Structure - An MCHF Approach' (Bristol: IOP)

Fite, W. L., and Brackmann, R. T., 1959, Phys. Rev., 113, 815

Fite, W. L., Kauppila, W. E., and Ott, W. R., 1968, Phys. Rev. Lett., 20, 409

Flower, D. R., 1968, IAU Symp. 34: 'Planetary Nebulae', 34, 205

Flower, D. R., 1972, Astron. Astrophys., 17, 201

Flower, D. R. 1983, IAU Symp. 103: Planetary Nebulae, 103

Flower, D. R., and Jordan, C., 1971, Astron. Astrophys., 14, 473

Flower, D. R., and Launay, J. M., 1972, J. Phys. B, 5, L207

Flower, D. R., and Pineau des Forets, G., 1973, Astron. Astrophys., 24, 181

Fogle, M., Eklöw, N., Lindroth, E., Mohamed, T., Schuch, R., and Tokman, M., 2003, J. Phys. B, 36, 2563

Fogle, M., Badnell, N. R., Glans, P., Loch, S. D., Madzunkov, S., Abdel-Naby, S. A., Pindzola,M. S., and Schuch, R., 2005, Astron. Astrophys., 442, 757

Fossi, B. C. M., and Landini, M., 1994, At. Data Nucl. Data Tables, 57, 125

Freeman, F. F., and Jones, B. B., 1970, Sol. Phys., 15, 288

Fuhr, J. R., et al., 1999, NIST Atomic Spectra Database, version 2.0

Gabriel, A. H., 1972, Mon. Not. R. Astron. Soc., 160, 99

Gabriel, A. H., and Jordan, C., 1969, Mon. Not. R. Astron. Soc., 145, 241

Gabriel, A., and Paget, T., 1972, J. Phys. B., 5, 673

Gabriel, A. H., and Phillips, K. J. H., 1979, Mon. Not. R. Astron. Soc., 189, 319

Galavs, M., Mendoza, C., and Zeippen, C. J., 1997, Astron. Astrophys. Suppl. Ser., 123, 159

Garca, J., Mendoza, C., Bautista, M. A., Gorczyca, T. W., Kallman, T. R., and Palmeri, P., 2005, Astrophys. J. Suppl. Ser., 158, 68

Gau, J. N., and Hahn, Y., 1978, Phys. Lett. A, 68, 197

Gau, N., Hahn, Y., and Retter, J. A., 1980, J. Quant. Spec. Radiat. Transf., 23, 147

Gianetti, D., Landi, E., and Landini, M., 2000, Astron. Astrophys., 360, 1148

Glans, P., et al., 1999, Nucl. Instrum. Methods B, 154, 97

Glans, P., Lindroth, E., Badnell, N. R., Eklow, N., Zong, W., Justiniano, E., and Schuch, R., 2001, Phys. Rev. A , 64, 043609

Glans, P., et al., 2004, Phys. Scr., T110, 212

Goldberg, L., Dupree, A. K., and Allen, J. W. 1965, Annales d'Astrophysique, 28, 589

Golden, L. B., and Sampson, D. H., 1971, Astrophys. J., 170, 181

Golden, L. B. and Sampson, D. H., 1977, J. Phys. B, 10, 2229

Golden, L. B., and Sampson, D. H., 1980, J. Phys. B., 13, 2645

Golden, L. B., Sampson, D. H., and Omidvar, K., 1978, J. Phys. B, 11, 3235

Golden, L. B., Clark, R. E. H., Goett, S. J., and Sampson, D. H., 1981, Astrophys. J. Suppl. Ser., 45, 603

Goldsmith, S., Feldman, U., Oren, L., and Cohen, L., 1972, Astrophys. J., 174, 209

Goldsmith, S., Katz, L. O., Crooker, A. M., and Cohen, L., 1973, Astrophys. J., 184, 1021

Goldstein, W. H., Osterheld, A., Oreg, J., and Bar-Shalom, A., 1989, Astrophys. J. Lett., 344, L37

Goldstone, J., 1957, Proc. Roy. Soc., A239, 267

Gorczyca, T. W., 2000, Phys. Rev. A , 61, 024702

Gorczyca, T. W. and Badnell, N. R., 1996, J. Phys. B, 29, L283

Gorczyca, T. W., and Badnell, N. R., 1996b, Phys. Rev. A , 54, 4113

Gorczyca, T. W. and Badnell, N. R., 2000, J. Phys. B, 33, 2511

Gorczyca, T. W., and McLaughlin, B. M., 2000, J. Phys. B, 33, L859

Gorczyca, T. W., and Robicheaux, F., 1999, Phys. Rev. A , 60, 1216

Gorczyca, T. W., Robicheaux, F., Pindzola, M. S., and Badnell, N. R., 1996, Phys. Rev. A , 54, 2107

Gorczyca, T. W., Badnell, N. R., and Savin, D. W., 2002, Phys. Rev. A , 65, 062707

Gorczyca, T. W., Kodituwakku, C. N., Korista, K. T., Zatsarinny, O., Badnell, N. R., Behar, E., Chen, M. H., and Savin, D. W., 2003, Astrophys. J., 592 636

Gorczyca, T. W.,Dumitriu, I., Hasoğlu, M. F., Korista, K. T., Badnell, N. R., Savin,D. W., and Manson, S. T., 2006, Astrophys. J. Lett., 638, L121

Gould, R. J., 1978, Astrophys. J., 219, 250

Grant, I., 1996, in 'Atomic, Molecular and Physics', Drake, G., ed.,

Grant, I. P., McKenzie, B. J., Norrington, P. H., Mayers, D. F., and Pyper, N. C., 1980, Computer Physics Communications, 21, 207

Greenwood, J. B.,Smith, S. J., Chutjian, A., and Pollack, E., 1999, Phys. Rev. A , 59, 1348

Greenwood, J. B., Williams, I. D., Smith, S. J., and Chutjian, A., 2001, Phys. Rev. A , 63, 062707

Gregory, D. C., Dittner, P. F., and Crandall, D. H., 1983, Phys. Rev. A , 27, 724

Gregory, D. C., Crandall, D. H., Phaneuf, R. A., Howald, A. M., Dunn, G. H., Falk, R. A., Mueller, D. W., and Morgan, T. J., 1985, Electron Impact Ionization of Multicharged Ions at ORNL: 1980 - 1984, ORNL/TM-9501, ,

Gregory, D. C. and Howald, A. M., 1986, Phys. Rev. A , 34, 97

Gregory, D. C., Meyer, F. W. , Müller, A. ,and Defrance, P., 1986, Phys. Rev. A , 34, 3657

Gregory, D. C., Wang, L. J., Meyer, F. W. , and Rinn, K., 1987, Phys. Rev. A , 35, 3256

Grevesse, N., Noels, A., and Sauval, A., 1996, in 'ASP Conf. Ser. 99, Cosmic Abundances,' ed. S. Holt and G. Sonneborn (San Francisco: ASP), 117,

Griffin, D. C., Bottcher, C., and Pindzola, M. S., 1982a, Phys. Rev. A , 25, 1374

Griffin, D. C., Pindzola, M. S., and Bottcher, C., 1987, Phys. Rev. A , 36, 3642

Griffin, D. C., and Pindzola, M. S., 1988, J. Phys. B, 21, 3253

Griffin, D. C., Pindzola, M. S., and Badnell, N. R., 1993, Phys. Rev. A , 47, 2871

Gronenschild, E. H. B. M., and Mewe, R., 1978, Astron. Astrophys. Suppl. Ser., 32, 283

Gronenschild, E. H. B. M., and Mewe, R., 1982, Astron. Astrophys. Suppl. Ser., 48, 305

Gu, M. F., 2003a, Astrophys. J., 582, 1241

Gu, M. F., 2003b, Astrophys. J., 590, 1131

Gu, M. F., 2003c, Astrophys. J., 589, 1085

Gu, M. F., 2003d, Astrophys. J., 593, 1249

Gu, M. F., 2004, Phys. Rev. A , 70, 062704

Gu, M. F., 2005, Astrophys. J. Suppl. Ser., 156, 105

Gu, M. F., Kahn, S. M., Savin, D. W., Behar, E., Beiersdorfer, P., Brown, G. V., Liedahl, D. A., and Reed, K. J., 2001, Astrophys. J., 563, 462

Gu, M. F., et al., 2004, Astrophys. J. Lett., 607, L143

Gu, M. F., Schmidt, M., Beiersdorfer, P., Chen, H., Thorn, D. B., Träbert, E., Behar, E., and Kahn, S. M., 2005, Astrophys. J., 627, 1066

Gupta, G. P.Deb, N. C. and Msezane, A. Z., 2000, At. Data Nucl. Data Tables, 74, 257

Gupta, G. P., and Tayal, S. S., 1998, Astrophys. J., 506, 464

Gupta, G. P., and Tayal, S. S., 1999, Astrophys. J., 510, 1078

Gwinner, G., Savin, D. W., Schwalm, D., Wolf, A., Schippers, S., Müller, A., Badnell, N. R., and Chen, M. H., 2001, Phys. Scr., T92, 319

Haberli, R. M., Gombosi, T. I., DeZeeuw, D. L., Combi, M. R., and Powell, K. G., 1997, Science, 276, 939

Hagelstein, P. L., and Jung, R. K., 1987, At. Data Nucl. Data Tables, 37, 121

Hahn, Y., 1977, Phys. Rev. Lett. , 39, 82

Hahn, Y., 1978, Phys. Rev. A , 18, 1028

Hahn, Y., 1980, Phys. Rev. A , 22, 2896

Hahn, Y., 1986, Phys. Lett. A, 119, 293

Hahn, Y., 1989, Phys. Scr., T28, 25

Hahn, Y., 1993, J. Quant. Spec. Radiat. Transf., 49, 81

Hahn, Y., 1997, Rep. Prog. Phys., 60, 691

Hahn, Y., and Bellantone, R., 1989, Phys. Rev. A , 40, 6117

Hamdan, M., Burkinshaw, K., and Hasted, J. B., 1978, P. Phys. B., 11, 331,

Hamilton, A. J. S., Chevalier, R. A., and Sarazin, C. L., 1983, Astrophys. J. Supp. Ser., 51, 115

Harra-Murnion, L. K., et al., 1996, Astron. Astrophys., 308, 670

Hartree, D. R., 1957, The Calculation of Atomic Structures (John Wiley and Sons Inc.: New York) ,

Havener, C. C., 2001, ASP Conf. Ser. 247: 'Spectroscopic Challenges of Photoionized Plasmas', 247, 17

Havener, C. C., Huq, M. S., Krause, H. F., Schulz, P. A., and Phaneuf, R. A., 1989, Phys. Rev. A , 39, 1725

Hayton, S. J. T., and Peart, B., 1994, J. Phys. B, 27 5331

Hebb, M. H., and Menzel, D. H., 1940, Astrophys. J., 92, 408.,

Heil, T. G., Bottrell, G. J., and Bottcher, C., 1985, Nucl. Instrum. Methods B, 9, 448

Henry, H. J. W., 1970, Astrophys. J., 161, 1153.

Henry, H. J. W., 1979, J. Phys. B, 12, L309

Henry, R. J. W. and Msezane, A. Z., 1982, Phys. Rev. A , 26, 2545

Henry, H. J. W. and Williams, R., 1968, Pub. Astron. Soc. Pacific, 80, 669

Hibbert, A., 1975, Comput. Phys. Commun., 9, 141

Hoekstra, R., Beijers, J. P. M., Schlatmann, A. R., Morgenstern, R., and de Heer, F. J., 1990, Phys. Rev. A , 41, 4800

Hooper, J. W., Lineberger, W. C., and Bacon, F. M., 1966, Phys. Rev., 141, 165

House, L. L., 1969, Astrophys. J. Suppl. Ser., 18,21

Howald, A. M., Gregory, D. C., Meyer, F. W., Phaneuf, R. A., Müller, A., Djuric, N., and Dunn, G. H., 1986, Phys. Rev. A , 33, 3779

Huang, K.-N., 1985, At. Data Nucl. Data Tables, 32, 503

Hudson E T, Bartschat, K., Scott, M. P., Burke, P. G., and Burke V. M., 1996, J. Phys. B, 29, 5513

Hummer, D. G., Berrington, K. A., Eissner, W., Pradhan, A. K., Saraph, H. E., and Tully,J. A., 1993, Astron. Astrophys., 279, 298

Huq, M. S., Havener, C. C.,and Phaneuf, R. A., 1989, Phys. Rev. A , 40, 1811

Inokuti, M., and Kim, Y., 1968, Phys. Rev., 173, 154

R. C. Isler, E. C. Crume, and D. E. Arnurius, 1982, Phys. Rev. A , 26, 2105

Itikawa, Y., 1991, At. Data Nucl. Data Tables, 49, 209

Itikawa, Y., 1996, At. Data Nucl. Data Tables, 63, 315

Itikawa, Y., 2002, At. Data Nucl. Data Tables, 80, 117

Itikawa, Y., Takayanagi, K., and Iwai, T., 1984, At. Data Nucl. Data Tables, 31, 215

Itoh, H., 1979, Pub. Astron. Soc. Japan, 31, 541

Jacobs, V. L., Davis,J., and Kepple, P. C., 1976, Phys. Rev. Lett., 37, 1390

Jacobs, V. L., and Rozsnyai, B. F., 1986, Phys. Rev. A , 34, 216

Jacobs, V.L., Davis, J., Kepple, P.C., and Blaha, M., 1977a, Astrophys. J., 211, 605

Jacobs, V.L., Davis, J., Kepple, P.C., and Blaha, M., 1977b, Astrophys. J., 215, 690

Jacobs, V.L., Davis, J., Rogerson, J.E., and Blaha, M., 1979, Astrophys. J., 230, 627

Jacobs, V. L., Davis, J., Rozsnyai, B. F., and Cooper, J. W., 1980, Phys. Rev. A , 21, 1917

Jain, N. K. and Narain, U., 1978, Astron. Astrophys. Suppl. Ser., 31, 1

Janev. R. K. and Winter, H., 1985, Phys. Rep., 117 265

Janjusevic, M., and Hahn, Y., 1989, Phys. Rev. A , 40, 5641

Janzen, P. H., Gardner, L. D., Reisenfeld, D. B., Savin, D. W., Kohl, J. L., and Bartschat, K., 1999, Phys. Rev. A , 59, 4821

Johnson, C. T., Kingston, A. E., and Dufton, P. L., 1986, Mon. Not. R. Astron. Soc., 220, 155

Johnston, W. D., and Kunze, H.-J., 1971, Phys. Rev. A , 4, 962

Jones, M., 1970, J. Phys. B, 3, 1571

Jones, M., 1974, Mon. Not. R. Astron. Soc., 169, 211

Jordan, C., 1969, Mon. Not. R. Astron. Soc., 142, 501

Jordan, C., 1970, Mon. Not. R. Astron. Soc., 148, 17

Juett, A. M., Schulz, N. S., and Chakrabarty, D., 2004, Astrophys. J., 612, 308

Jupen, C., Isler, R. C., and Träbert, E., 1993, Mon. Not. R. Astron. Soc., 264, 627

Kaastra, J.S., Mewe, R., and Nieuwenhuijzen, H., 1996, in 'UV and X-Ray Spectroscopy of Astrophysical and Laboratory Plasmas,' ed. K. Yamashita,

Kaastra, J.S., 1992, 'An X-Ray Spectral Code for Optically Thin Plasmas' (Internal SRON-Leiden Rep., updated version 2.0) ,

Kaastra, J. S., and Mewe, R., 1993, Astron. Astrophys. Suppl. Ser., 97, 443

Kaastra, J. S., et al., 2004, Astron. Astrophys., 428, 57

Kahn, S. M., Behar, E., Kinkhabwala, A., and Savin, D. W., 2004, Frontiers of X-ray astronomy. Edited by A. C. Fabian, K. A. Pounds, R. D. Blandford. (Cambridge (UK): Cambridge University Press), ISBN 0-521-53487-9, 2004. ,

Kallman, T. R., Palmeri, P., Bautista, M. A., Mendoza, C., and Krolik, J. H., 2004, Astrophys. J. Suppl. Ser., 55, 675

Kamber, E. Y., Akg ung or, K., Leather, C., and Brenton, A. G., 1996, Phys. Rev. A , 54, 1452

Karim, K. R., and Bhalla, C. P., 1986, Phys. Lett. A, 116, 172

Karim, K. R., and Bhalla, C. P., 1988a, Phys. Rev. A , 37, 840

Karim, K. R., and Bhalla, C. P., 1988, Phys. Rev. A , 37, 2599

Karim, K. R. and Bhalla, C. P., 1988, Phys. Rev. A , 37, 1507

Karim, K. R., and Bhalla, C. P., 1989a, Nucl. Instrum. Methods B, 40, 366

Karim, K. R., and Bhalla, C. P., 1989b, Phys. Rev. A , 39, 3548

Karim, K. R., and Bhalla, C. P., 1990, Phys. Rev. A , 42, 3555

Karim, K. R., and Bhalla, C. P., 1991, Phys. Rev. A , 43, 615

Karim, K. R., and Bhalla, C. P., 1995, J. Phys. B, 28, 5229

Karim, K. R., Bhalla, C. P., Ruesink, M., Biel, S., and Wilson, M., 1991, J. Phys. B, 24, L375

Karim, K. R., Ruesink, M., and Bhalla, C. P., 1992, Phys. Rev. A , 46, 3904

Karstensen, F., and Schneider, M., 1978, J. Phys. B., 11, 167

Karzas, W., and Latter, R., 1961, Astrophys. J. Suppl. Ser., 6, 167

Kastner, S. O., 1983, Astrophys. J., 275, 922

Kato, T., Masai, K., and Arnaud, M., 1991, National Institute for Fusion Science, Nagoya, Japan, Research Report, NIFS-DATA-14

Kato, T., 1976, Astrophys. J. Suppl. Ser., 30, 397

Kato, T., 1994, At. Data Nucl. Data Tables, 57, 181

Kato, T., and Nakazaki, S., 1989, At. Data Nucl. Data Tables, 42, 313

Kato, T., Safronova, U., Shlypteseva, A., Cornille, M., Dubau, J., and Nilsen, J., 1997, At. Data Nucl. Data Tables, 67, 225

Kaufman, V., and Martin, W. C., 1991a, J. Phys. Chem. Ref. Data, 20, 775

Kaufman, V., and Martin, W. C., 1991b, J. Phys. Chem. Ref. Data, 20, 83

Kaufman, V., and Martin, W. C., 1993, J. Phys. Chem. Ref. Data, 22, 279

Keenan, F. P., Kingston, A. E., and McKenzie, D. L., 1986, Astrophys. J., 303, 486

Kelly, R. L., 1987, J. Phys. Chem. Ref. Data Suppl., 16, 1

Kenntner, J., et al., 1995, Nucl. Instrum. Methods B, 98, 142

Kharchenko, V., and Dalgarno, A., 2000, JGR, 105, 18351

Kieffer, L. J., and Dunn, G. H., 1966, Rev. Mod. Phys., 38, 1

Kimura, M., Kobayashi, N., Ohtani, S., and Tawara, H., 1987, J. Phys. B, 20, 3873

Kingdon, J. B., and Ferland, G. J., 1996, Astrophys. J. Suppl. Ser., 106, 205

Kinkhabwala, A., et al., 2002, Astrophys. J., 575, 732

Kisielius, R., Hibbert, A., Ferland, G. J., Foord, M. E., Rose, S. J., van Hoof, P. A. M.,and Keenan, F. P., 2003, Mon. Not. R. Astron. Soc., 344, 696

Knapp, D., et al., 1989, Phys. Rev. Lett. , 62, 2104

Knopp, H., Teng, H., Ricz, S., Schippers, S., Müller, A., 2001, Phys. Scr., T92, 379

Kotochigova, S., Kirby, K., Mohr, P., and Tupitsyn, S., 2005, in "X-ray Diagnostics for Astrophysical Plasmas", AIP, R. Smith ed.,

Kraemer et al., 2004, Astrophys. J., 604, 556

Krolik, J. H., McKee, C. F., and Tarter, C. B., 1981, Astrophys. J., 249, 422

Krongold, Y., Nicastro, F., Brickhouse, N. S., Elvis, M., Liedahl, D. A., and Mathur, S., 2003, Astrophys. J., 597, 832

Kumar, S., and Saha, K., 1998, J. Phys. B, 31, L937

Kunze, H.-J., 1972, Sp. Sci. Rev., 13, 565

Kunze, H.-J., Gabriel, A. H., and Griem, H. R., 1968, Phys. Rev., 165, 267

Lagattuta, K. J., and Hahn, Y., 1981a, Phys. Lett. A, 84, 468

Lagattuta, K. J., and Hahn, Y., 1981b, Phys. Rev. A , 24, 785

Lagattuta, K.and Hahn, Y., 1982a, J. Phys. B, 15, 2101

Lagattuta, K., and Hahn, Y., 1982b, Phys. Rev. A , 26, 1125

Lagattuta, K., and Hahn, Y., 1983a, Phys. Rev. Lett., 50, 668

Lagattuta, K., and Hahn, Y., 1983b, Phys. Rev. A , 27, 1675

Lagattuta, K. J., and Hahn, Y., 1984, Phys. Rev. A , 30, 316

Lagattuta, K., Nasser, I., and Hahn, Y., 1986, Phys. Rev. A , 33, 2782

Landi, E., and Bhatia, A. K., 2003a, Astrophys. J. Suppl. Ser., 149, 251

Landi, E., and Bhatia, A. K., 2003b, Astrophys. J., 589, 1075

Landi, E., and Bhatia, A. K., 2005a, Astron. Astrophys., 444, 305

Landi, E., and Bhatia, A. K., 2005b, At. Data Nucl. Data

Tables, 90, 177

Landi, E., and Bhatia, A. K., 2005, At. Data Nucl. Data Tables, 89, 195

Landi, E., and Landini, M., 1998, Astron. Astrophys. Suppl. Ser., 133, 411

Landi, E., and Landini, M., 2002, Astron. Astrophys., 384, 1124

Landi, E., and Phillips, K., 2005, Astrophys. J. Suppl. Ser., 160, 286

Landi, E., Landini, M., Dere, K.P., Young, P.R., and Mason, H.E., 1999, Astron. Astrophys. Suppl. Ser., 135, 339

Landi, E., Storey, P. J., and Zeippen, C. J., 2004, Astrophys. J., 607, 640

Landi, E., Dere, K. P., Young, P. R., del Zanna, G., Mason, H. E., and Landini, M., 2005, AIP Conf. Proc. 774: 'X-ray Diagnostics of Astrophysical Plasmas: Theory, Experiment, and Observation', 774, 409

Landini, M., and Monsignori Fossi, B.C., 1972, Astron. Astrophys. Suppl. Ser., 7, 291

Lang, J., and Summers, H. P., 1994, At. Data Nucl. Data Tables, 57, 215

Layzer, D., 1951, Astron. J., 56, 43

Lee, J. C., Ogle, P. M., Canizares, C. R., Marshall, H. L., Schulz, N. S., Morales, R., Fabian, A. C., and Iwasawa, K., 2001, Astrophys. J. Lett., 554, L13

Lemen, J. R., Phillips, K. J. H., Cowan, R. D., Hata, J., and Grant, I. P., 1984, Astron. Astrophys., 135, 313

Lennon, M.A., Bell, K.L., Gilbody, H.B., Hughes, J.G., Kingston, A.E., Murray, M.J., and Smith, F.J., 1988, J. Phys. Chem. Ref. Data, 17, 1285

Lepson, J. K., Beiersdorfer, P., Behar, E., and Kahn, S. M., 2003, Astrophys. J., 590, 604

Lepson, J. K., Beiersdorfer, P., Behar, E., and Kahn, S. M., 2005a, Nucl. Instrum. Methods B, 235, 131

Lepson, J. K., Beiersdorfer, P., Behar, E., and Kahn, S. M., 2005b, Astrophys. J., 625, 1045

Liedahl, D.A., 2000, in 'Atomic Data Needs for X-Ray Astronomy,' ed. M.A.Bautista, T.R.Kallman, and A.K.Pradhan (NASACP-2000-209-968; Greenbelt:NASA/GSFC), 151

Liedahl, D., 2003, Atomic Data for X-Ray Astronomy, 25th meeting of the IAU, Joint Discussion 17, 22 July 2003, Sydney, Australia, 17

Liedahl, D.A., Osterheld, A.L., and Goldstein, W.H., 1995, Astrophys. J., 438, L115

Lin, C.D., Johnson, W.R., and Dalgarno, A., 1977, Phys. Rev. A , 15, 154

Lin, S.-H., Hsue, C.-S., and Chung, K.T., 2001a, Phys. Rev. A , 64, 12709

Lin, S.-H., Hsue, C.-S., and Chung, K.T., 2001b, Phys. Rev. A , 65, 32706

Linkemann, J., M uller, A., Kenntner, J., Habs, D., Schwalm, D., Wolf, A., Badnell, N. R., and Pindzola, M. S., 1995, Phys. Rev. Lett., 74, 4173

Lisse, C. M., et al., 1996, Science, 274, 205

Loch, S. D., Colgan, J., Pindzola, M. S., Westermann, M., Scheuermann, F., Aichele, K., Hathiramani, D., and Salzborn, E., 2003, Phys. Rev. A , 67, 042714

Loch, S. D., et al., 2005, Phys. Rev. A , 71, 012716

Loch, S. D., Pindzola, M. S., Ballance, C. P., and Griffin, D. C., 2006, J. Phys. B, 39, 85

Lotz W., 1967, Astrophys. J. Suppl. Ser., 14, 207

Lotz, W., 1968, Z. Phys., 216, 241

Loulergue, M., 1971, Astron. Astrophys., 15, 216

Loulergue, M., and Nussbaumer, H., 1973, Astron. Astrophys., 24, 209

Loulergue, M., and Nussbaumer, H., 1975, Astron. Astrophys., 45, 125

Lozano, J. A., Niimura,M., Smith, S. J., Chutjian, A., and Tayal, S. S., 2001, Phys. Rev. A , 63, 042713

Müller, A., 2001, in 'Physics of Ion Impact Phenomena', edited by D. Mathur, Springer Series in Chemical Physics, Vol.54 (Springer Verlag, Berlin, Heidelberg, 1991) p. 13 - 90

Müller, A., Tinschert, K., Achenbach, C., Becker, R., and Salzborn, E., 1985, J. Phys. B, 18, 3011

Müller, A., Huber, K., Tinschert, K., Becker, R., and Salzborn, E., 1985c, J. Phys. B, 18, 2993

Müller, A., Teng, H., Hofmann, G., Phaneuf, R. A., and Salzborn, E., 2000, Phys. Rev. A , 62, 062720

Man, K., F., Smith, A. C. H., and Harrison, M. F. A., 1987, J. Phys. B., 20, 2571

Man, K., F., Smith, A. C. H., and Harrison, M. F. A., 1993, J. Phys. B., 26, 1365

Mann, J. B., 1983, At. Data Nucl. Data Tables, 29, 407

Mannervik, S., Dewitt, D., Engström, L., Lidberg, J., Lindroth, E., Schuch, R., and Zong, W., 1998, Phys. Rev. Lett., 81, 313

Marchalant, P. J., and Bartschat, K., 1997, J. Phys. B, 30 4373

Marchalant, P. J., Bartschat, K., and Bray, I., 1997, J. Phys. B, 30 L435

Mariska, J. T., 1993, "The Solar Transition Region", by John T. Mariska, pp. 290. ISBN 0521382610. Cambridge, UK: Cambridge University Press, January 1993.

Martin, W. C., and Zalubas, R., 1979, J. Phys. Chem. Ref. Data, 8, 817

Martin, W. C., and Zalubas, R., 1983, J. Phys. Chem. Ref. Data, 12, 323

Martin, S.O., Peart, B., and Dolder, K.T., 1968, J. Phys. B, 1, 537

Martin, W. C., Zalubas, R., and Musgrove, A., 1990, J. Phys. Chem. Ref. Data, 19, 821

Martin, I., Karwowski, J., Diercksen, G. H. F., and Barrientos, C., 1993, Astron. Astrophys. Suppl. Ser., 100, 595

Masai, K., 1997, Astron. Astrophys., 324, 410

Masai, K., and Ishida, M., 2004, Astrophys. J., 607, 76

Mason, H. E., 1994, At. Data Nucl. Data Tables, 57, 305

Mason, H. E., and Storey, P. J., 1980, Mon. Not. R. Astron. Soc., 191, 631

Mason, H. E., and Bhatia, A. K., 1983, Astron. Astrophys. Suppl. Ser., 52, 181

Mason, H. E., Doschek, G. A., Feldman, U., and Bhatia, A. K., 1979, Astron. Astrophys., 73, 74

Massey, H. S. W., and Bates, D. R., 1942, Rep. Prog. Phys., 9, 62.

Matsumoto, A., et al., 1990, J. Phys. Soc. Jpn., 59, 902.

Mauche, C., 2005, in ' AIP Conf. Proc. 774: X-ray Diagnostics of Astrophysical Plasmas: Theory, Experiment, and Observation, 774, p. 133

Mazzotta, P., Mazzitelli, G., Colafrancesco, S., and Vittorio, N., 1998, Astron. Astrophys. Suppl. Ser., 133, 403

McDowell, M. R. C., and Williamson, J. H., 1963, Phys. Lett., 4, 159

McGowan, J. W., and Clarke, E. M., 1968, Phys. Rev., 167, 43

McGuire, E. J., 1969, Phys. Rev. , 185, 1

McGuire, E. J., 1970, Phys. Rev. A , 2, 273

McGuire, E. J., 1971a, Phys. Rev. A , 3, 1801

McGuire, E. J., 1971b, Phys. Rev. A , 3, 587
McGuire, E. J., 1972, Phys. Rev. A , 5, 1052
McGuire, E. J., 1977, Phys. Rev. A , 16, 62
McGuire, E. J., 1982, Phys. Rev. A , 26, 125
McKenzie, D. L., 1987, Astrophys. J., 322, 512
McKenzie, D. L., Landecker, P. B., Broussard, R. M., Rugge, H. R., Young, R. M., Feldman, U., and Doschek, G. A., 1980, Astrophys. J., 241, 409
McLaughlin, D. J., and Hahn, Y., 1982, Phys. Lett. A, 88, 394
McLaughlin, D. J., and Hahn, Y., 1983a, Phys. Rev. A , 27, 1389
McLaughlin, D. J., and Hahn, Y., 1983b, Phys. Rev. A , 28, 493
McLaughlin, D. J., and Hahn, Y., 1983c, J. Phys. B, 16, L739
McLaughlin, T. K., Wilson, S. M., McCullough, R. W., and Gilbody, H. B., 1990, J. Phys. B, 23, 737
McLaughlin, T. K., McCullough, R. W., and Gilbody, H. B., 1992, J. Phys. B, 25, 1257
McLaughlin, T. K., Hodgkinson, J. M., Tawara, H., McCullough, R. W., and Gilbody, H. B., 1993, J. Phys. B, 26, 3587
McWhirter, R. W. P., 1994, At. Data Nucl. Data Tables, 57, 39
Meekins, J. F., Kreplin, R. W., Chubb, T. A., and Friedman, H., 1968, Science, 162, 891
Mendoza, C., Kallman, T. R., Bautista, M. A., and Palmeri, P., 2004, Astron. Astrophys., 414, 377
Menzel, D., and Pekeris, C., 1935, Mon. Not. R. Astron. Soc., 96, 77
Mewe, R., 1972a, Astron. Astrophys., 20, 215
Mewe, R., 1972b, Sol. Phys., 22, 459
Mewe, R., 1975, Sol. Phys., 44, 383
Mewe, R.and Gronenschild, E.H.B.M., 1981, Astron. Astrophys. Suppl. Ser., 45, 11
Mewe, R., and Schrijver, J., 1975, Astrophys. Sp. Sci., 38, 345
Mewe, R., and Schrijver, J., 1978a, Astron. Astrophys. Suppl. Ser., 33, 311
Mewe, R., and Schrijver, J., 1978b, Astron. Astrophys., 65, 99
Mewe, R., Gronenschild, E.H.B.M., and van den Oord, G.H.J., 1985, Astron. Astrophys. Suppl. Ser., 62, 197
Mewe, R., Lemen, J.R., and van den Oord, G.H.J., 1986, Astron. Astrophys. Suppl. Ser., 65, 511
Mewe, R., Kaastra, J. S., Schrijver, C. J., van den Oord, G. H. J., and Alkemade, F. J. M., 1995a, Astron. Astrophys., 296, 477
Mewe, R., Kaastra, J.S., and Liedahl, D.A., 1995b, Legacy, 6, 16–19
Mihalas, D., 1978, Stellar Atmospheres (Freeman: San Francisco),
Mitchell, J. B. A., Ng, C. T., Forand, J. L., Levac, D. P., Mitchell, R. E., Sen, A., Miko, D. B., and McGowan, J. W., 1983, Phys. Rev. Lett., 50, 335
Mitnik, D. M., and Badnell, N. R., 2004, Astron. Astrophys., 425, 1153
Mitnik, D. M., Shaw, J. A., Pindzola, M. S., Griffin, D. C., and Badnell, N. R., 1998, Computer Physics Communications, 114, 368
Mitnik, D.M., Pindzola, M.S., Griffin, D.C., Badnell,N.R., 1999, J. Phys. B, 32, L479
Montague, R. G., Diserens, M. J., and Harrison, M. F. A., 1984, J. Phys. B, 17, 2085
Moores, D. L., and Pindzola, M. S., 1990, Phys. Rev. A , 42, 5384
Moores, D. L., Golden, L. B., and Sampson, D. H., 1980, J. Phys. B., 13, 385
Moussa, A. H., Ramadan, H. H., and Hahn, Y., 1988, Phys. Rev. A , 38, 5076
Mroczkowski, T., Savin, D. W., Rejoub, R., Krstić, P. S.,and Havener, C. C., 2003, Phys. Rev. A , 68, 032721
Muehlethaler, H. P., and Nussbaumer, H., 1976, Astron. Astrophys., 48, 109
Mueller, D. W., Morgan, T. J., Dunn, G. H., Gregory, D. C., and Crandall, D. H., 1985a, Phys. Rev. A , 31, 2905
Nagy, P., et al., 1980, J. Phys. B., 13, 1249
Nahar, S.N., 1995, Astrophys. J. Suppl. Ser., 101, 423
Nahar, S.N., 1996a, Astrophys. J. Suppl. Ser., 106, 213
Nahar, S. N., 2004, Phys. Rev. A , 69, 042714
Nahar, S. N., and Pradhan, A. K., 1994, Phys. Rev. A , 49, 1816
Nasser, I., and Hahn, Y., 1989, Phys. Rev. A , 39, 401
Netzer, H., 1996, Astrophys. J., 473, 781
Netzer, H., 2004, Astrophys. J., 604, 551
Nilsen, J., 1986, J. Phys. B., 19, 2401
Nilsen, J., 1987, At. Data Nucl. Data Tables, 37, 191
Nilsen, J., 1988, At. Data Nucl. Data Tables, 38, 339
Nikolić, D., et al. 2004, Phys. Rev. A , 70, 062723
Nussbaumer, H., 1972a, Astron. Astrophys., 16, 77
Nussbaumer, H., 1973, Astron. Astrophys., 27, 303
Nussbaumer, H., 1977, Astron. Astrophys., 58, 291
Nussbaumer, H.and Storey, P.J., 1983, Astron. Astrophys., 126, 75
Nussbaumer, H.and Storey, P.J., 1984, Astron. Astrophys., 56, 293
Nussbaumer, H., and Storey, P. J., 1986, Astron. Astrophys. Suppl. Ser., 64, 545
Nussbaumer, H., and Storey, P. J., 1987, Astron. Astrophys. Suppl. Ser., 69, 123
Oelgoetz, J., and Pradhan, A. K., 2001, Mon. Not. R. Astron. Soc., 327, L42
Oelgoetz, J., and Pradhan, A. K., 2004, Mon. Not. R. Astron. Soc., 354, 1093
Omar, G., and Hahn, Y., 1987, Phys. Rev. A , 35, 918
Osterbrock, D. E., and Ferland, G. J., 2006, Astrophysics of gaseous nebulae and active galactic nuclei, 2nd. ed. by D.E. Osterbrock and G.J. Ferland. Sausalito, CA: University Science Books, 2006,
Owocki, S. P., and Scudder, J. D., 1983, Astrophys. J., 270, 758
Paerels, F. B. S., and Kahn, S. M., 2003, Ann. Rev. Astron. Astrophys., 41, 291
Paerels, F., et al., 2001, Astrophys. J., 546, 338
Palmeri, P., Mendoza, C., Kallman, T. R., and Bautista, M. A., 2002, Astrophys. J. Lett., 577, L119
Palmeri, P., Mendoza, C., Kallman, T. R., and Bautista, M. A., 2003a, Astron. Astrophys., 403, 1175
Palmeri, P., Mendoza, C., Kallman, T. R., Bautista, M. A., and Meléndez, M., 2003b, Astron. Astrophys., 410, 359
Parkinson, J. H., 1973, Astron. Astrophys., 24, 215
Parkinson, J. H., 1975, Sol. Phys., 42, 183
Parpia, F. A., and Johnson, W. R., 1972, Phys. Rev. A , 26, 1142
Parpia, F. A., Froese Fischer, C., and Grant, I. P., 1996, Computer Physics Communications, 94, 249
Peart, B., et al., 1991, J. Phys. B, 24, 4453
Pelan, J., and Berrington, K. A., 1995, Astron. Astrophys. Suppl. Ser., 110, 209

Pequignot, D., Stasinska, G., and Aldrovand i, S. M. V., 1978, Astron. Astrophys., 63, 313

Pequignot, D., 1980a, Astron. Astrophys., 81, 356

Pequignot, D., Petitjean, P., and Boisson, C., 1991, Astron. Astrophys., 251, 680

Peterson, J. R., Kahn, S. M., Paerels, F. B. S., Kaastra, J. S., Tamura, T., Bleeker, J. A. M., Ferrigno, C., and Jernigan, J. G., 2003, Astrophys. J., 590, 207

Phaneuf et al., 1987, Report ORNL-6090/V5 U.S. Dept. of Energy, Washington DC,

Phaneuf, R. A.,Havener, C. C., Dunn, G. H., Müller, A., 1999, Rep. Prog. Phys., 62, 1143

Phillips, K. J. H., et al., 1982, Astrophys. J., 256, 774

Phillips, K. J. H., Lemen, J. R., Cowan, R. D., Doschek, G. A., and Leibacher, J. W., 1983, Astrophys. J., 265, 1120

Phillips, K. J. H., Bhatia, A. K., Mason, H. E., and Zarro, D. M., 1996, Astrophys. J., 466, 549

Phillips, K. J. H., Greer, C. J., Bhatia, A. K., Coffey, I. H., Barnsley, R., and Keenan, F. P., 1997, Astron. Astrophys., 324, 381

Pieksma, M., Bannister, M. E., Wu, W., and Havener, C. C., 1997, Phys. Rev. A , 55, 3526

Pike, C. D., et al., 1996, Astrophys. J., 464, 487

Pindzola, M. S., and Robicheaux, F. J., 2000, Phys. Rev. A , 61, 052707

Pindzola, M. S., Griffin, D. C. Bottcher, C., Crandall, D. H., Phaneuf, R. A., and Gregory, D. C., 1984, Phys. Rev. A , 29, 1749

Pindzola, M. S., Griffin, D. C., and Bottcher, C., 1986a, Phys. Rev. A , 33, 3787

Pindzola, M. S., Griffin, D. C., and Bottcher, C., 1986b, Phys. Rev. A , 34, 3668

Pindzola, M. S., Moores, D. L., and Griffin, D. C., 1989, Phys. Rev. A , 40, 4941

Pindzola, M. S., Badnell, N. R., and Griffin, D. C., 1990, Phys. Rev. A , 42, 282

Pindzola, M. S., Griffin, D., Bottcher, C., Buie, M., and Gregory, D., 1991, Phys. Scr., T37, 35

Pindzola, M. S., Griffin, D. C., and Macek, J. H., 1995, Phys. Rev. A , 51, 2186

Pindzola M. S., Robicheaux F., Badnell N. R. and Gorczyca T. W., 1997, Phys. Rev. A , 56 1994

Pindzola, M. S., Mitnik, D. M., Shaw, J. A., Griffin, D. C., Badnell, N. R., Summers, H. P., and Schultz, D. R., 1998, Phys. Scr., 57, 514

Pindzola, M. S., Colgan, J., Robicheaux, F., and Griffin, D. C., 2000, Phys. Rev. A , 62, 042705

Podobedova, L. I., Musgrove, A., Kelleher, D. E., Reader, J., Wiese, W. L., Coursey, J. S. and Olsen, K., 2003, http://physics.nist.gov/PhysRefData/Chandra/index.html,

Porquet, D., and Dubau, J., 2000, Astron. Astrophys. Suppl. Ser., 143, 495

Pradhan, A. K., 1983, Astrophys. J., 270, 339

Pradhan, A. K., 1985, Astrophys. J., 288, 824

Pradhan, A. K., 1994, At. Data Nucl. Data Tables, 57, 297

Pradhan, A. K., 2000, Astrophys. J. Lett., 545, L165

Pradhan, A. K., and Gallagher, J. W., 1992, At. Data Nucl. Data Tables, 52, 227

Pradhan, A. K., and Shull, J. M., 1981, Astrophys. J., 249, 821

Pradhan, A. K., Chen, G. X., Delahaye, F., Nahar, S. N., and Oelgoetz, J., 2003, Mon. Not. R. Astron. Soc., 341, 1268

Quinet, P., 2000, Phys. Scr, 61, 45

Racah, G., 1942, Phys. Rev., 62, 438

Racah, G., 1943, Phys. Rev., 63, 367

Rachafi, S., et al., 1991, J. Phys. B, 24, 1037

Ramadan, H. H., and Hahn, Y., 1989, Phys. Rev. A , 39, 3350

Rasmussen, A.P., Behar, E., Kahn, S.M., den Herder, J.W., and van der Heyden, K., 2001, Astron. Astrophys., 365, L231

Raymond, J. C., and Smith, B., 1977, Astrophys. J. Suppl. Ser., 35, 419

Raymond, J. C., and Smith, B. W., 1986, Astrophys. J., 306, 762

Reilman, R. F. and Manson, S. T., 1978, Phys. Rev. A , 18, 2124

Reilman, R. F. and Manson, S. T., 1979, Astrophys. J. Suppl. Ser., 40, 815

Rejoub, R., Bannister, M. E., Havener, C. C., Savin, D. W., Verzani, C. J., Wang, J. G., and Stancil, P. C., 2004, Phys. Rev. A , 69, 052704

Retter, J. A., Gau, J. N., and Hahn, Y., 1978, Phys. Rev. A , 17, 998

Rinn, K., Gregory, D. C., Wang, L. J., Phaneuf, R. A., and Müller, A., 1987, Phys. Rev. A , 36, 595

Robicheaux, F., and Pindzola, M. S., 1997, Phys. Rev. Lett., 79, 2237

Roszman, L. J., 1979, Phys. Rev. A , 20, 673

Roszman, L. J., 1987a, Phys. Rev. A , 35, 2138

Roszman, L. J., 1987b, Phys. Rev. A , 35, 3368

Roszman, L.J., 1987c, Phys. Rev. A , 35, 2122

Roszman, L. J., 1989a, Phys. Scr., T28, 36

Roszman, L. J., 1989b, Phys. Rev. A , 39, 2073

Roszman, L. J., 1989c, Phys. Rev. A , 39, 913

Rothe, E. W., Marino, L. L., Neynaber, R. H., and Trujillo, S. M., 1962, Phys. Rev., 125, 582

Ruszkowski, M., Brüggen, M., and Begelman, M. C., 2004, Astrophys. J., 611, 158

Safranova, U., Vasiliev, A., and Smith, R., 2000, Can. J. Phys., 78, 12.

Safronova, U.I., Vasilyev, A.A., and Smith, R.K., 2001, Can. J. Phys., 78, 1055

Safronova, U. I. and Urnov, A. M., 1980, J. Phys. B, 13, 869

Saghiri, A. A., et al., 1999, Phys. Rev. A , 60, 3350

Saha, B. C., 1995, Phys. Rev. A , 51, 5021

Sako, M., Kahn, S. M., Paerels, F., and Liedahl, D. A., 2000, Atrophys. J. Lett., 543, L115

Sampson, D. H., 1982, J. Phys. B, 15, 2087

Sampson, D. H. and Golden, L. B., 1979, J. Phys. B, 12, L785

Sampson, D. H. and Golden, L. B., 1981, J. Phys. B, 14, 903

Sampson, D. H., and Parks, A. D., 1974, Astrophys. J. Suppl. Ser., 28, 323

Sampson, D.H., Goett, S.J., and Clark, R.E.H., 1983, At. Data Nucl. Data Tables, 29, 467

Sampson, D. H., Weaver, G. M., Goett, S. J., Zhang, H., and Clark, R. E. H., 1986, At. Data Nucl. Data Tables, 35, 223

Sampson, D. H., Zhang, H. L., and Fontes, C. J., 1990, At. Data Nucl. Data Tables, 44, 209

Sampson, D. H., Zhang, H. L., and Fontes, C. J., 1991, At. Data Nucl. Data Tables, 48, 25

Sampson, D. H., Zhang, H. L., and Fontes, C. J., 1994, At. Data Nucl. Data Tables, 57, 97

Savin, D. W., 1999d, Astrophys. J., 523, 855

Savin, D. W., 2000, Astrophys. J., 533, 106

Savin, D. W., 2005, in "X-Ray Diagnostics of Astrophysical Plasmas" (XDAP 2000), ed. R. Smith (American Institute of Physics, New York, 2005),

Savin, D. W., and Laming, J. M., 2002, Astrophys. J., 566, 1166

Savin, D. W., Gardner, L. D., Reisenfeld, D. B., Young, A. R., and Kohl, J. L., 1995, Phys. Rev. A , 51, 2162

Savin, D. W., et al., 1997, Astrophys. J. Lett., 489, L115

Savin, D. W., et al., 1999a, Astrophys. J. Suppl. Ser., 123, 687

Savin, D. W., et al., 2002a, Astrophys. J., 576, 1098

Savin, D. W., et al., 2002b, Astrophys. J. Suppl. Ser., 138, 337

Savin, D. W., et al., 2003b, Astrophys. J. Suppl. Ser., 147, 421

Savin, D. W., Krstic, P. S.,Haiman, Z., and Stancil,P. C., 2004a, Astrophys. J. Lett., 606, L167

Schattenburg, M. and Canizares, C., 1986, Astrophys. J., 301, 579.

Schiff, B., Pekeris, C. L., and Accad, Y., 1971, Phys. Rev. A , 4, 885

Schippers, S., 1999, Phys. Scr., T80, 158

Schippers, S., Bartsch, T., Brandau, C., Gwinner, G., Linkemann, J., Müller, A., Saghiri, A. A.,and Wolf, A., 1998, J. Phys. B, 31, 4873

Schippers, S., Schnell, M., Brandau, C., Kieslich, S., Müller, A., and Wolf, A., 2004, Astron. Astrophys., 421, 1185

Schmidt, M., Beiersdorfer, P., Chen, H., Thorn, D. B., Träbert, E., and Behar, E., 2004, Astrophys. J., 604, 562

Schultz, M., Justiniano, E., Schuch, R., Mokler, P. H., and Reusch, S., 1987, Phys. Rev. Lett., 58, 1734

Seaton, M. J., 1958, Rev. Mod. Phys., 30, 979

Seaton, M. J., 1959, Mon. Not. R. Astron. Soc., 119, 81

Seaton, M. J., 1962, in ‘Atomic and Molecular Processes’. D. R. Bates, Ed. Library of Congress Catalog Card Number 62-13122. (Academic Press: New York), p.375,

Seaton, M., 1987, J. Phys. B, 20, 6363

Seaton, M. J. and Storey, P. J., 1976, in ‘Atomic Process and Applications,’ P. Burke and B. Moisewitch, eds. (North Holland: New York),

Seely, J. F., Feldman, U., Safronova, U. I., 1986, Astrophys. J., 304, 838

Seely, J. F., Feldman, U., and Doschek, G. A., 1987, Astrophys. J., 319, 541

Shapiro, J., and Breit, G., 1959, Phys. Rev., 113, 179

Shapiro, P. R. and Moore, R. T., 1976, Astrophys. J., 207, 460

Shevelko, V. P., Urnov, A. M., Vainshtein, L. A., and Müller, A., 1983, Mon. Not. R. Astron. Soc., 203, 45P

Shevelko, V. P., Tawara, H., Scheuermann, F., Fabian, B., Müller, A., and Salzborn, E., 2005, J. Phys. B, 38, 525

Shevelko, V. P., Tawara, H., Tolstikhina, I. Yu., Scheuermann, F., Fabian, B., Mller, A., and Salzborn, E., 2006, J. Phys. B, 39 1499

Shirai, T., Funatake, Y., Mori, K., Sugar, J., Wiese, W. L., and Nakai, Y., 1990, J. Phys. Chem. Ref. Data, 19, 127

Shirai, T., Sugar, J., Musgrove, A., et al., 2000, J. Phys. Chem. Ref. Data, Monograph 8

Shklovsky, J. S., 1968, Interscience Monographs and Texts in Physics and Astronomy, London: Wiley, 1968.,

Shore, B.W., 1969, Astrophys. J., 158, 1205

Shull, J. M., and van Steenberg, M., 1982a, Astrophys. J. Suppl. Ser., 48, 95

Shull, J. M., and van Steenberg, M., 1982b, Astrophys. J. Suppl. Ser., 49, 351

Silver, E. H., and Kahn,S. M., 1993, ‘UV and X-ray Spectroscopy of Laboratory and Astrophysical Plasmas’ Proceedings from the 10th International Colloquium held at Berkeley, California, 3-5 February 1992, (Cambridge: Cambridge University Press), —c1993, edited by Silver, Eric H.; Kahn, Steven M. ISBN 052143470X,

Smith, R., 2005, AIP Conf. Proc. 774: ‘X-ray Diagnostics of Astrophysical Plasmas: Theory, Experiment, and Observation’, 774, ,

Smith, B. W., Mann, J. B., Cowan, R. D., and Raymond, J. C., 1985, Astrophys. J., 298, 898

Smith, A. J., Bitter, M.,Hsuan, H., Hill, K. W., von Goeler, S., Timberlake, J., Beiersdorfer, P., and Osterheld, A., 1993, Phys. Rev. A , 47, 3073

Smith, A. J.,Beiersdorfer, P., Decaux, V., Widmann, K., Reed, K. J., and Chen, M. H., 1996, Phys. Rev. A , 54, 462

Smith, S. J., Chutjian,A., Greenwood, J. B., and Tayal, S. S., 2000a, Astrophys. J., 541, 501

Smith, A. J., Beiersdorfer, P., Reed, K. J., Osterheld, A. L., Decaux, V., Widmann, K., and Chen, M. H., 2000b, Phys. Rev. A , 62, 012704

Smith, R.K., Brickhouse, N.S., Liedahl, D.A., and Raymond, J.C., 2001, Astrophys. J. Lett., 556, L91

Smith, A. C. H., et al., 2003, Nucl. Instrum. Methods B, 205, 421

Stancil, P. C., 2001, ASP Conf. Ser. 247: Spectroscopic Challenges of Photoionized Plasmas, 247, 3

Stancil, P. C., Zygelman, B., Clarke, N. J., and Cooper, D. L., 1997, Phys. Rev. A , 55, 1064

Stancil, P. C., et al., 1998a, J. Phys. B, 31, 3647

Stancil, P. C., et al., 1998b, Astrophys. J., 502, 1006

Stancil, P. C., Turner, A. R., Cooper, D. L., Schultz, D. R., Rakovic, M. J., Fritsch, W., and Zygelman, B., 2001, J. Phys. B, 34, 2481

Steigman, G., 1975, Astrophys. J., 199, 336

Steigman, G., Werner, M. W., and Geldon, F. M., 1971, Astrophys. J., 168, 373

Stenke, M., et al., 1999, J. Phys. B, 32, 3627

Stenke, M., Hathiramani, D., Hofmann, G., Steidl, M., Salzborn, E., Volpel, R., and Shevelko, V. P., 1995a, Nucl. Instrum. Methods B, 98, 138

Stenke, M., Aichele, K., Hathiramani, D., Hofmann, G., Steidl, M., Salzborn, E., and Volpel, R., 1995b, Nucl. Instrum. Methods B, 98, 573

Stephan, K., et al., 1980, J. Chem Phys., 73, 3763

Stolterfoht, N., 1987, Phys. Rep., 146, 315

Storey, P. J., 1981, Mon. Not. R. Astron. Soc., 195, 27P

Storey, P. J., and Zeippen, C. J., 2000, Mon. Not. R. Astron. Soc., 312, 813

Storey, P. J., Mason, H. E., and Saraph, H. E., 1996, Astron. Astrophys., 309, 677

Stratton, B. C., Moos, H. W., and Finkenthal, M., 1984, Astrophys. J. Lett., 279, L31

Sugar, J., Corliss, C., 1979, J. Phys. Chem. Ref. Data, 8, 865

Sugar, J., and Corliss, C., 1985, ‘Atomic energy levels of the iron-period elements: Potassium through Nickel’, Washington: American Chemical Society.,

Summers, H. P., 1972, Mon. Not. R. Astron. Soc., 158, 255

Summers, H. P., 1974, Mon. Not. R. Astron. Soc., 169, 663

Summers, H. P., et al., 2006, Plasma Physics and Controlled Fusion, 48, 263

Suraud et al., 1991, J. Phys. B, 24 2543

Sutherland , R.S.and Dopita, M.A., 1993, Astrophys. J. Suppl. Ser., 88, 253

Sylwester J., Lemen J.R., Bentley R.D., Fludra A., Zolcinski M.-C., 1998, Astrophys. J. Suppl. Ser., 501, 397

Tanaka, K., 1986, Pub. Astron. Soc. Japan, 38, 225

Tanis, J. A. et al., 1981, Phys. Rev. Lett., 47, 828

Tarter, C. B., 1971, Astrophys. J., 168, 313

Tarter, C. B., and Salpeter, E. E., 1969, Astrophys. J., 156, 953

Tarter, C. B., Tucker, W. H., and Salpeter, E. E., 1969, Astrophys. J., 156, 943

Tawara, H., Okuno, K., Fehrenbach, C. W., Verzani, C., Stockli, M. P., Depaola, B. D., Richard, P., and Stancil, P. C., 2001, Phys. Rev. A , 63, 062701

Tayal, S. S., 1999, J. Phys. B, 32, 5311

Teng, H., 2000, J. Phys. B, 33, L553-L562.

Teng, H., Knopp, H., Ricz, S., Schippers, S., Berrington, K. A., Müller, A., 2000, Phys. Rev. A , 61, 060704

Terao, M., and Burke, P. G., 1990, J. Phys. B, 23, 1815

Thompson, J. S. and Gregory, D. C., 1994, Phys. Rev. A , 50, 1377

Tisone, G. C., and Branscomb, L. M., 1968, Phys. Rev., 170, 169

Tondello, G., and McWhirter, R. W. P., 1971, J. Phys. B, 4, 715

Träbert, E., 2002, Can. J. Phys., 80, 1481

Trefftz, E., 1963, Royal Society of London Proceedings Series A, 271, 379

Tucker, W. H., and Koren, M., 1971, Astrophys. J., 168, 283

Vainshtein, L., and Safranova, U., 1978, At. Data Nucl. Data Tables, 21, 49.

Van Regemorter, H., 1962, Astrophys. J., 136, 906

Verner, D. A. Barthel, P. D. and Tytler, D., 1994, Astron. Astrophys. Suppl. Ser., 108, 287,

Verner, D. A., Verner, E. M. and Ferland, G. J., 1996, At. Data Nucl. Data Tables, 64, 1,

Verner, D.A.and Ferland , G.J., 1996, Astrophys. J. Suppl. Ser., 103, 467

Verner, D.A., and Yakovlev, D.G., 1995, Astron. Astrophys. Suppl. Ser., 109, 125

Volonte, S., Lion, J.,Faucher, P., and Dubau, J., 1987, Astron. Astrophys., 182, 167

Voronov, G.S., 1997, At. Data Nucl. Data Tables, 65, 1

Walker, D. W., 1974, J. Phys. B, 7, 97

Walker, A. B. C., and Rugge, H. R., 1970, Astron. Astrophys., 5, 4

Wang, L. J., Rinn, K., and Gregory, D. C., 1988, J. Phys. B, 21, 2117

Wang, J.-S., Griem, H. R., Hess, R., and Rowan, W. L., 1988, Phys. Rev. A , 38, 4761

Wang, J. G., Stancil, P. C., Turner, A. R., and Cooper, D. L., 2003, Phys. Rev. A , 67, 012710

Wargelin, B. J., Beiersdorfer, P., and Kahn, S. M., 1993, Phys. Rev. Lett., 71, 2196

Wargelin, B. J., Kahn, S. M., and Beiersdorfer, P., 2001, Phys. Rev. A , 63, 022710

Watson, W. D. and Christensen, R. B., 1979, Astrophys. J., 231, 627

Wetzel, R. C. et al., 1987, Phys. Rev. A , 35, 559

Whiteford, A. D., Badnell, N. R., Ballance, C. P., O'Mullane, M. G., Summers, H. P., and Thomas, A. L., 2001, J. Phys. B, 34, 3179

Whiteford, A. D., Badnell, N. R., Ballance, C. P., Loch, S. D., O'Mullane, M. G., and Summers, H. P., 2002, J. Phys. B, 35, 3729

Widing, K. G., and Sandlin, G. D., 1968, Astrophys. J., 152, 545

Widing, K. G., Doyle, J. G., Dufton, P. L., and Kingston, E. A., 1982, Astrophys. J., 257, 913

Wiese, W.L. Smith, M.W. and Glennon, B.M., 1966, Natl Stand. Ref. Data Ser., Natl Bur. Stand. (U.S.), NSRDS-NBS 4, Vol. I ,

Wiese, W.L., Fuhr, J., and Deters, J., 1996, J. Phys. Chem. Ref. Data, Monograph 7

Wilson, S. M., McLaughlin, T. K., McCullough, R. W., and Gilbody, H. B., 1990a, J. Phys. B, 23, 1315

Wilson, S. M., McLaughlin, T. K., McCullough, R. W., and Gilbody, H. B., 1990b, J. Phys. B, 23, 2969

Woitke, O., Djuric, N., Dunn, G. H., Bannister, M. E., Smith, A. C. H., Wallbank, B., Badnell, N. R., and Pindzola, M. S., 1998, Phys. Rev. A , 58 4512

Wojdowski, P. S., Liedahl, D. A., and Sako, M., 2001, Astrophys. J., 547, 973

Wong, K. L., et al., 1993, Phys. Rev. A , 48, 2850.

Woodruff, P. R., Hublet, M.-C., and Harrison, M. F. A., 1978, J. Phys. B, 11, L305

Woods, D. T., Shull, J. M., and Sarazin, C. L., 1981, Astrophys. J., 249, 399

Younger, S. M., 1980a, Phys. Rev. A , 22, 111

Younger, S. M., 1980b, Phys. Rev. A , 22, 1425

Younger, S. M., 1981a, Phys. Rev. A , 23, 1138

Younger, S. M., 1981b, Phys. Rev. A , 24, 1272

Younger, S. M., 1982a, Phys. Rev. A , 25, 3396

Younger, S. M., 1982b, Phys. Rev. A , 26, 3177

Younger, S., 1983, J. Quant. Spec. Radiat. Transf., 29, 67

Young, P. R., Del Zanna, G., Landi, E., Dere, K. P., Mason, H. E., and Landini, M., 2003, Astrophys. J. Suppl. Ser., 144, 135

Zatsarinny, O., Gorczyca, T. W., Korista, K. T., Badnell, N. R., and Savin, D. W., 2003, Astron. Astrophys., 412, 587

Zatsarinny, O., Gorczyca, T. W., Korista, K., Badnell, N. R., and Savin, D. W., 2004a, Astron. Astrophys., 426, 699

Zatsarinny, O., Gorczyca, T. W., Korista, K. T., Badnell, N. R., and Savin, D. W., 2004b, Astron. Astrophys., 417, 1173

Zatsarinny, O., Gorczyca, T. W., Korista, K. T., Fu, J., Badnell, N. R., Mitthumsiri, W., and Savin, D. W., 2005a, Astron. Astrophys., 440, 1203

Zatsarinny, O., Gorczyca, T. W., Korista, K. T., Fu, J., Badnell, N. R., Mitthumsiri, W., and Savin, D. W., 2005b, Astron. Astrophys., 438, 743

Zatsarinny, O., Gorczyca, T. W., Fu, J., Korista, K. T., Badnell, N. R., and Savin, D. W., 2006, Astron. Astrophys., 447, 379

Zeijlmans, P. A., van Emmichoven, Bannister, M. E., Gregory, D. C., Havener, C. C., Phaneuf, R. A., Bell, E., Guo, W., X. Q. Thompson, J. S., and Sataka, M., 1993, Phys. Rev. A , 47, 2888

Zhang, H., 1996, Astron. Astrophys. Suppl. Ser., 119, 523

Zhang, H., and Sampson, D., 1987, Astrophys. J. Supp. Ser., 63, 487

Zhang, H., and Sampson, D., 1989, At. Data Nucl. Data Tables, 43, 1

Zhang, H. L., and Sampson, D. H., 1992, At. Data Nucl. Data Tables, 52, 143

Zhang, H. L., and Sampson, D. H., 1994a, At. Data Nucl. Data Tables, 56, 41

Zhang, H. L., and Sampson, D. H., 1994b, At. Data Nucl. Data Tables, 58, 255

Zhang, H. L., and Sampson, D. H., 1996, At. Data Nucl. Data Tables, 63, 275

Zhang, H., et al., 1989, At. Data Nucl. Data Tables, 41,1

Zhang, H. L., Sampson, D. H., and Fontes, C. J., 1990, At. Data Nucl. Data Tables, 44, 31

Zhang, Y., Reddy, C.B., Smith, R. S. Golden, D. E. Mueller, D. W., and Gregory, D. C., 1991, Phys. Rev. A , 44, 4368

Zhang, H. L., Graziani, M., and Pradhan, A. K., 1994, Astron. Astrophys., 283, 319

Ziegler, D. L., Newman,J. H., Goeller, L. N., Smith, K. A., and Stebbings, R. F., 1982, Planet. Space Sci., 30, 1269

Zirin, H., 1988, “Astrophysics of the Sun”. Cambridge and New York, Cambridge University Press, 1988, 440

Zong, W., Schuch, R., Lindroth, E., Gao, H., Dewitt, D. R., Asp, S., and Danared, H., 1997, Phys. Rev. A , 56, 386

Zygelman, B., Stancil, P. C., Clarke, N. J., and Cooper, D. L., 1997, Phys. Rev. A , 56, 457